This ATM presents the final thermal analysis and test data on the ALSEP Prototype "A" Central Station, with the primary purpose of improving the Central Station analytical model for use in future pretest and flight steady-state temperature predictions in a simulated or real environment.

ALSEP PROTOTYPE "A" CENTRAL STATION

FINAL THERMAL ANALYSIS AND TEST RESULTS

Prepared by: P. A. Johnson

Approved by: J. McNaughton

Approved by: M. Katz

TABLE OF CONTENTS

TABLE OF CONTENTS (Cont.)

TABLE OF CONTENTS (Cont.)

ILLUSTRATIONS

TABLES

APPENDICES

1.0 INTRODUCTION

This document describes the final thermal analysis and presents test results on the ALSEP Prototype "A" Central Station (C/S). The primary reason for conducting the analysis was to improve C/S temperature predictions for equilibrium operating conditions. The analysis centers on a C/S thermal model which is basically equivalent to the Reference 1 model but which includes the formerly neglected heat transfer listed below:

1. Heat conduction through wiring within the C/S.
2. Heat conduction and radiation along cables between the C/S and deployed experimental packages.
3. Conduction between the primary structure and sunshield.
4. Heat input to the structure from resistors.
5. Radiation from cutouts in radiator plate insulation masks.

Refined test temperatures, obtained through improved data reduction, were correlated with the predicted values.

Analytically-predicted temperatures for both the "simulated" test moon and a "real" moon are compared and correlated with Prototype "A" C/S test values. By varying heat transfer resistance paths, the influence of various sections of the C/S on each other was evaluated.

General descriptions of the thermal model and analysis techniques are contained in Sections 4 and 5, while Sections 3 and 6 present analysis and test results and conclusions.

2.0 OBJECTIVES

The capability for accurate prediction of C/S equilibrium temperatures for any operating condition on the lunar surface was the principal analysis objective. Efforts were directed toward improved correlation between predicted and Prototype "A" test temperatures for lunar "noon" and "night" through the following actions:

1. Refined evaluation of "critical" heat transfer resistance paths.

2. Inclusion of heat transfer paths formerly neglected.

3. Improved reduction of test data.

Due to the nature of the physical model of the C/S, a relatively high degree of uncertainty was inherent in some "critical" resistances and heat inputs which could have a significant effect on C/S temperatures if their values were much different from analysis values. Consequently, tradeoffs were conducted to show the variation in temperatures caused by variation in these critical parameters.

A final objective was to predict temperatures for a "real" lunar environment and compare them with values for the test's "simulated" lunar environment in the Bendix 20' x 27' thermal vacuum chamber.

3.0 SUMMARY OF RESULTS AND CONCLUSIONS

3.1 Analytical and Test Results

The prototype model of the ALSEP Central Station was subjected to an accelerated lunar day to night cycle, one lunation, with the lunar surface temperature ranging from +250° F to -300°F during the Proto A test program. The test program included a lunar morning ALSEP System turn-on followed by thermal stabilization at both simulated lunar noon and lunar night environmental conditions.

Figure 1 illustrates the temperature swing of the Central Station radiator plate temperature for the accelerated lunar cycle and depicts the major events which occurred during the cycle; i. e., pre-test ambient IST, lunar morning, lunar noon, lunar night and post test ambient IST.

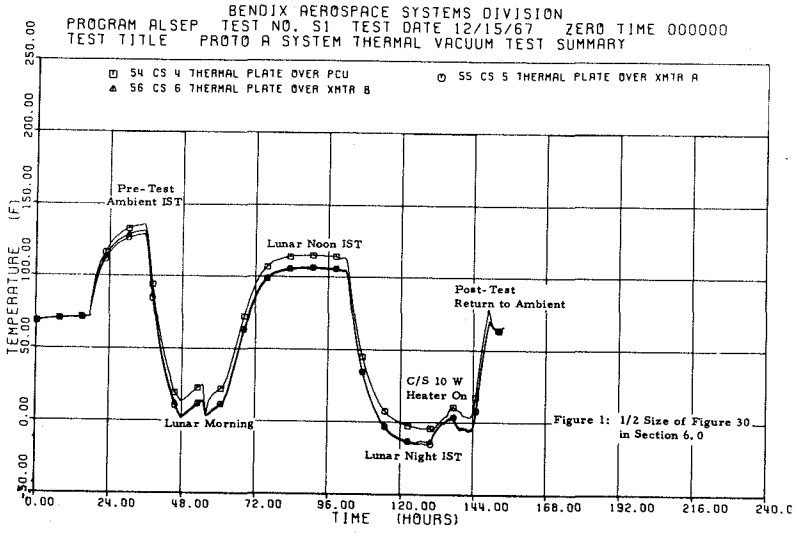

Figure 1: 1/2 Size of Figure 30 in Section 6.0

The analytical predictions and subsequent post test correlation with chamber test results were performed for equilibrium conditions for both the lunar noon and lunar night cases.

The overall test results from the Proto A thermal vacuum tests revealed favorable temperature distributions on all central station components, thermal plate, sunshield and primary structure surfaces. As indicated in Table 1 and Figures 2 to 6, excellent temperature correlation was obtained with the pretest predicted values. All component temperatures inside the Central Station were within the operating limits established prior to the Proto A test.

Table 1 lists the best analytical temperature predictions and compares them with Prototype "A" C/S test results, while Table 2 compares temperature predictions for the test "simulated" and "real" lunar surfaces. Temperature distribution over the C/S is illustrated by the following figures:

Figure No.	C/S Component
2	Radiator Baseplate - Noon
3	Radiator Baseplate - Night
4	Electronic Components - Noon
5	Electronic Components - Night
6	Structure & Sunshield - Noon & Night

Discrepancies between predicted and test values ranged from $0^{\circ}F$ to $24^{\circ}F$ and averaged $7^{\circ}F$ and $5^{\circ}F$, respectively, for the radiator plate (nodes 101 - 114) for lunar noon and lunar night. Note that radiator temperatures are about $28^{\circ}F$ higher for the real lunar noon surface. Test, predicted, and design temperature swings were $120^{\circ}F$, $132^{\circ}F$, and $125^{\circ}F$.

Figures 20 through 24 in Section 6 depict the effect of "critical" resistance paths and heat inputs on various C/S temperatures. These tradeoffs showed the radiator plate to be relatively unaffected by primary structure and sunshield temperatures. However, electronics heat dissipation and thermal conductance of the side curtains and insulation masks strongly influence radiator temperatures.

Figures 29 through 38 in Section 6 exhibit temperature histories during the simulated lunar cycle for various C/S components and for sections of the cryowall and lunar surface simulator.

TABLE 1

ANALYSIS AND TEST TEMPERATURES
FOR PROTOTYPE "A" CENTRAL STATION

Thermal Analyzer Node No.	Node Description	Temperatures (°F)			
		Lunar Noon		Lunar Night	
		Analysis	Test (4)	Analysis	Test (4)
27	Side Curtain, External Surface	57		-234	
28	"	97		-231	
29	"	100		-230	
30	"	107		-238	
31	Sunshield, Top Surface	38	41	-249	-230
32	"	81		-242	
33	"	81		-243	
34	Sunshield, Bottom Surface	60		-246	
35	Side Curtain, Internal Surface	59		-233	
36	"	96		-231	
37	P. C. U.	125	129 (5)	- 8	11 (5)
38	P. D. U.	114	118 (5)	- 19	- 1 (5)
39	Analog Multiplex Converter	113	108 (5)	- 20	- 16 (5)
40	Passive Seismometer	114		- 19	
41	Command Receiver	110	111 (5)	- 24	- 9 (5)
42	Data Processor	110	105 (5)	- 23	- 19 (5)
43	Command Decoder	111	102 (5)	- 23	- 20 (5)
44	Timer	110		- 24	
45	Diplexer Switch	111		- 23	
46	Diplexer Filter	110		- 25	
47	Transmitter A	127	121 (5)	- 18	3 (5)
48	Transmitter B	118		- 10	
49	Primary Structure	207		-101	
50	"	161	185	-149	-141
51	"	168	179	-154	-159
52	"	170	165	-147	-156
53	"	213	232	-143	-144
54	Thermal Bag, Internal Surface	130		- 31	
55	Thermal Bag, External Surface	194		-125	
56	Primary Structure Insulation	141		- 62	

TABLE 1 (CONT.)

Thermal Analyzer Node No.	Node Description	Temperatures (°F)			
		Lunar Noon		Lunar Night	
		Analysis	Test (4)	Analysis	Test (4)
57	Primary Structure Insulation	134		-110	
58	"	136		-113	
59	"	131		- 98	
60	Environment for Cable Heat Leak	221		-300	
97	Space (Cryowall Curtain)	-203		-231	
98	Space (Cryowall Door)	-212		-239	
99	Lunar Surface	241 (1)	250 (2)	-300	-300
100	Space (Cryowall Arch)	-248		-260	
101	Radiator Baseplate	114	114	- 19	-5
102	"	111	106	- 21	- 13
103	"	110	102	- 22	- 17
104	"	111	98	- 21	- 22
105	"	119	109	- 14	- 11
106	"	114	109	- 18	- 11
107	"	113	103	- 20	- 18
108	"	113		- 20	
109	"	109	107	- 25	- 13
110	"	109	102	- 24	- 17
111	"	109	98	- 25	- 22
112	"	112		- 22	
113	"	118	106	- 17	- 15
114	"	112	100	- 22	- 22
115	Radiator Baseplate Insulation	55		-154	
116	"	67		-146	
117	Specular Reflector	93		-195	
118	"	93		-192	
119	Side Curtain, Internal Surface	96		-231	
120	Sunshield, Bottom Surface	91		-242	
121	Side Curtain, Internal Surface	62		-233	
122	"	62		-233	
123	Sunshield, Bottom Surface	89		-241	
124	Side Curtain, Internal Surface	108		-238	
125	"	101		-229	
126	"	96		-230	
128	Radiator Plate for Radiosity Network	110		- 21	
130	"	108		- 25	
132	Gap Between Reflector and Curtain	101		-175	

TABLE 1 (CONT.)

Thermal Analyzer Node No.	Node Description	Temperatures (°F)			
		Lunar Noon		Lunar Night	
		Analysis	Test (4)	Analysis	Test (4)
140	Lunar Surface	265 (3)	275	N/A	N/A
141	"	260 (3)	270	"	"
142	"	238 (3)	248	"	"
143	"	263 (3)	272	"	"
144	"	256 (3)	265	"	"
145	"	238 (3)	248	"	"
146	!	270 (3)	280	"	"
147	"	254 (3)	263	"	"
148	"	241 (3)	250	"	"
149	"	290 (3)	300	"	"
150	"	285 (3)	295	"	"
151	"	265 (3)	275	"	"
152	"	290 (3)	300	"	"

NOTES:
1) This is the average lunar surface test temperature corrected for "non-black" properties of the test surface with the method in Section 5.3.
2) This is the average temperature of the entire test lunar surface, uncorrected for non-black surface properties.
3) This value is corrected for "non-black" properties of test lunar surface.
4) Test values are from the Digital Acquisition System (DAS) measurements, unless specified otherwise.
5) Average of several Telemetry measurements.

NA - Not Applicable

TABLE 2

ANALYSIS TEMPERATURES FOR PROTOTYPE "A" CENTRAL STATION IN VACUUM CHAMBER TEST AND REAL LUNAR ENVIRONMENTS

Thermal Analyzer Node No.	Temperatures (°F)			
	Lunar Noon		Lunar Night	
	Chamber	Real Moon	Chamber	Real Moon
27	57	136	-234	-280
28	97	134	-233	-276
29	100	139	-228	-274
30	107	143	-239	-285
31	38	38	-248	-328
32	81	87	-242	-291
33	81	41	-244	-379
34	60	86	-246	-324
35	59	135	-232	-280
36	96	135	-230	-275
37	125	151	- 8	- 14
38	114	140	- 19	- 25
39	113	139	- 20	- 26
40	114	141	- 19	- 25
41	110	138	- 24	- 30
42	110	138	- 23	- 29
43	111	139	- 23	- 29
44	110	138	- 24	- 30
45	111	140	- 23	- 29
46	110	138	- 25	- 31
47	127	155	- 18	- 23
48	118	147	- 10	- 16
49	207	185	-101	-122
50	161	143	-149	-172
51	168	147	-154	-177
52	170	145	-147	-170
53	213	159	-143	-168
54	130	144	- 31	- 39
55	194	157	-125	-144
56	141	153	- 62	- 78
57	134	142	-110	-131
58	136	144	-113	-133
59	131	141	- 98	-117

TABLE 2 (CONT.)

Thermal Analyzer Node No.	Temperatures (°F)			
	Lunar Noon		Lunar Night	
	Chamber	Real Moon	Chamber	Real Moon
60	221	227	-300	-340
75	NA	162	NA	-189
76	"	164	"	-181
77	"	-25	"	- 25
78	"	-22	"	- 28
79	"	- 4	"	- 46
80	"	22	"	- 72
81	"	54	"	-104
82	"	84	"	-134
83	"	114	"	-164
84	"	144	"	-194
85	"	174	"	-224
86	"	204	"	-254
87	"	234	"	-284
88	"	160	"	-170
89	"	-23	"	- 27
90	"	- 1	"	- 49
91	"	27	"	- 77
92	"	60	"	-109
93	"	90	"	-138
94	"	116	"	-161
95	"	137	"	-178
96	"	153	"	-188
97	-203	-460	-231	-460
98	-212	-460	-239	-460
99	241	250	-300	-300
100	-248	-460	-260	-460
101	114	140	- 19	- 25
102	111	138	- 21	- 27
103	110	137	- 22	- 28
104	111	138	- 21	- 28
105	119	145	- 14	- 20
106	114	141	- 18	- 24
107	113	139	- 20	- 26
108	113	140	- 20	- 26

TABLE 2 (CONT.)

Thermal Analyzer Node No.	Temperatures (°F)			
	Lunar Noon		Lunar Night	
	Chamber	Real Moon	Chamber	Real Moon
109	109	138	- 25	- 31
110	109	138	- 24	- 30
111	109	138	- 25	- 31
112	112	141	- 22	- 28
113	118	147	- 17	- 23
114	112	140	- 22	- 28
115	55	76	-154	-168
116	67	115	-146	-156
117	93	135	-195	-218
118	93	140	-192	-212
119	96	132	-228	-275
120	91	35	-239	-379
121	62	133	-229	-279
122	62	139	-228	-279
123	89	100	-237	-290
124	108	146	-235	-285
125	101	142	-219	-273
126	96	135	-219	-274
128	110	136	- 22	- 28
130	108	137	- 26	- 32
132	101	163	-175	-190

NOTES: Nodes 75 to 96 are moon nodes along with node 99. Their function is to simulate the real moon under the C/S as described in Section 6.5.

TABLE 2 (CONT.)

Thermal Analyzer Node No.	Temperatures (^{o}F)			
	Lunar Noon		Lunar Night	
	Chamber	Real Moon	Chamber	Real Moon
109	109	138	- 25	- 31
110	109	138	- 24	- 30
111	109	138	- 25	- 31
112	112	141	- 22	- 28
113	118	147	- 17	- 23
114	112	140	- 22	- 28
115	55	76	-154	-168
116	67	115	-146	-156
117	93	135	-195	-218
118	93	140	-192	-212
119	96	132	-228	-275
120	91	35	-239	-379
121	62	133	-229	-279
122	62	139	-228	-279
123	89	100	-237	-290
124	108	146	-235	-285
125	101	142	-219	-273
126	96	135	-219	-274
128	110	136	- 22	- 28
130	108	137	- 26	- 32
132	101	163	-175	-190

NOTES: Nodes 75 to 96 are moon nodes along with node 99. Their function is to simulate the real moon under the C/S as described in Section 6.5.

$T_{Ave_{Meas}}$ = 105

$T_{Ave_{Pred}}$ = 112 (14 nodes)

DAS Measurements

xxx = Measured
(xxx) = Predicted

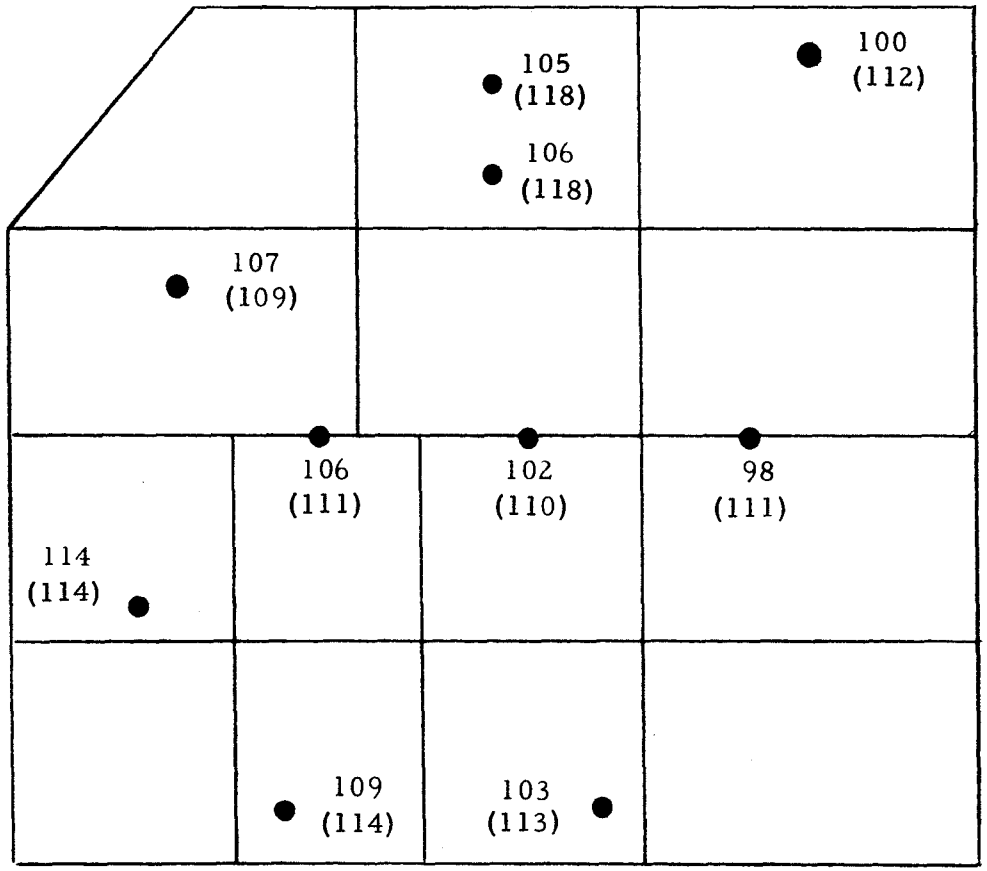

Figure 2 ALSEP Prototype "A" System Test; Measured vs Predicted Radiator Temperatures for Lunar Noon (^{o}F)

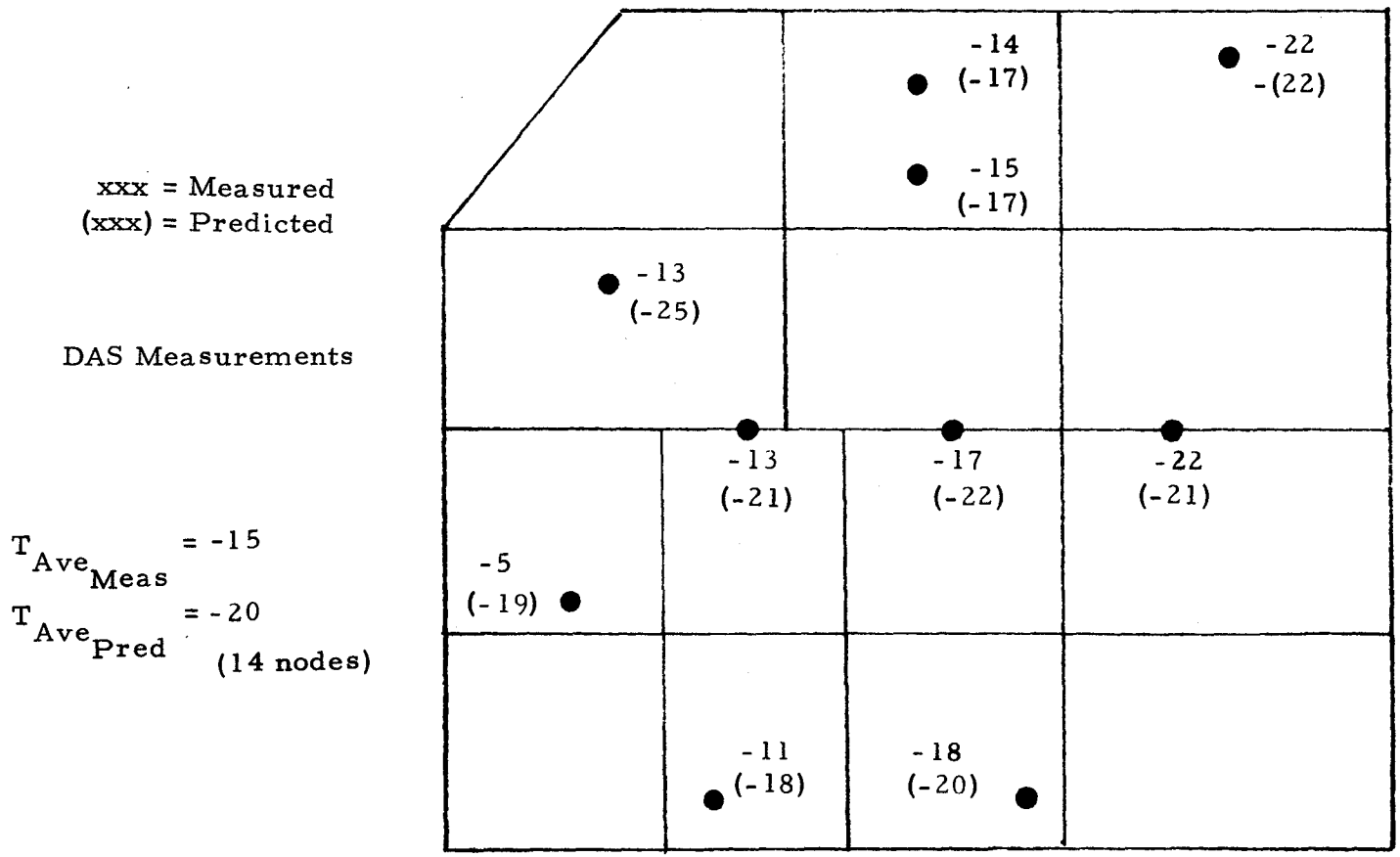

Figure 3 ALSEP Prototype "A" System Test; Measured vs Predicted Radiator Temperatures for Lunar Night (°F)

XXX Measured
(XXX) Predicted

Note: Most "measured" values are average of several test data.

Telemetry Measurements

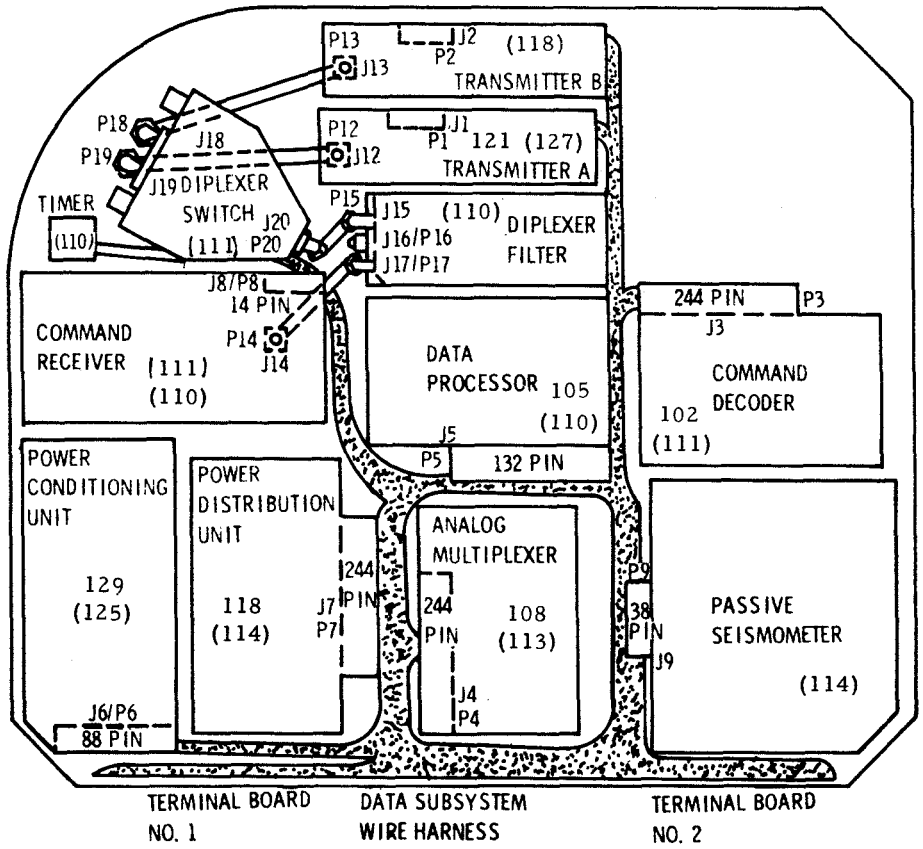

Figure 4 ALSEP Prototype "A" System Test; Measured vs Predicted Electronics Temperatures for Lunar Noon (°F)

XXX Measured
(XXX) Predicted

Note: Most "measured" values are average of several test data.

Telemetry Measurements

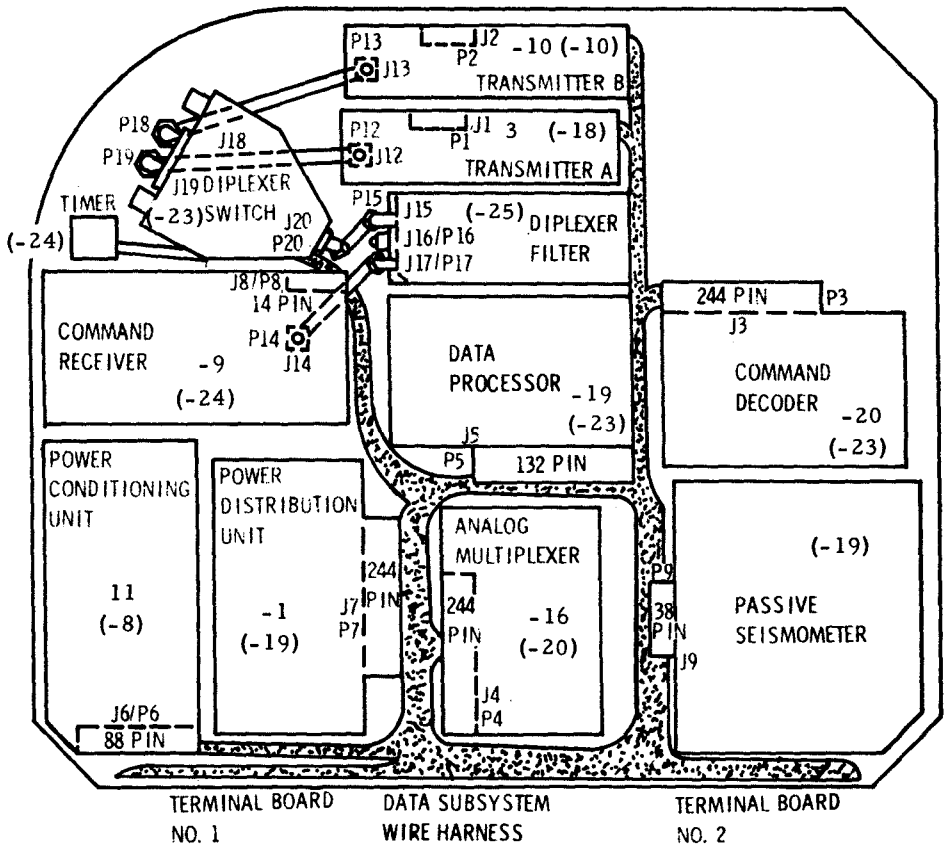

Figure 5 ALSEP Prototype "A" System Test; Measured vs Predicted Electronics Temperatures for Lunar Night (°F)

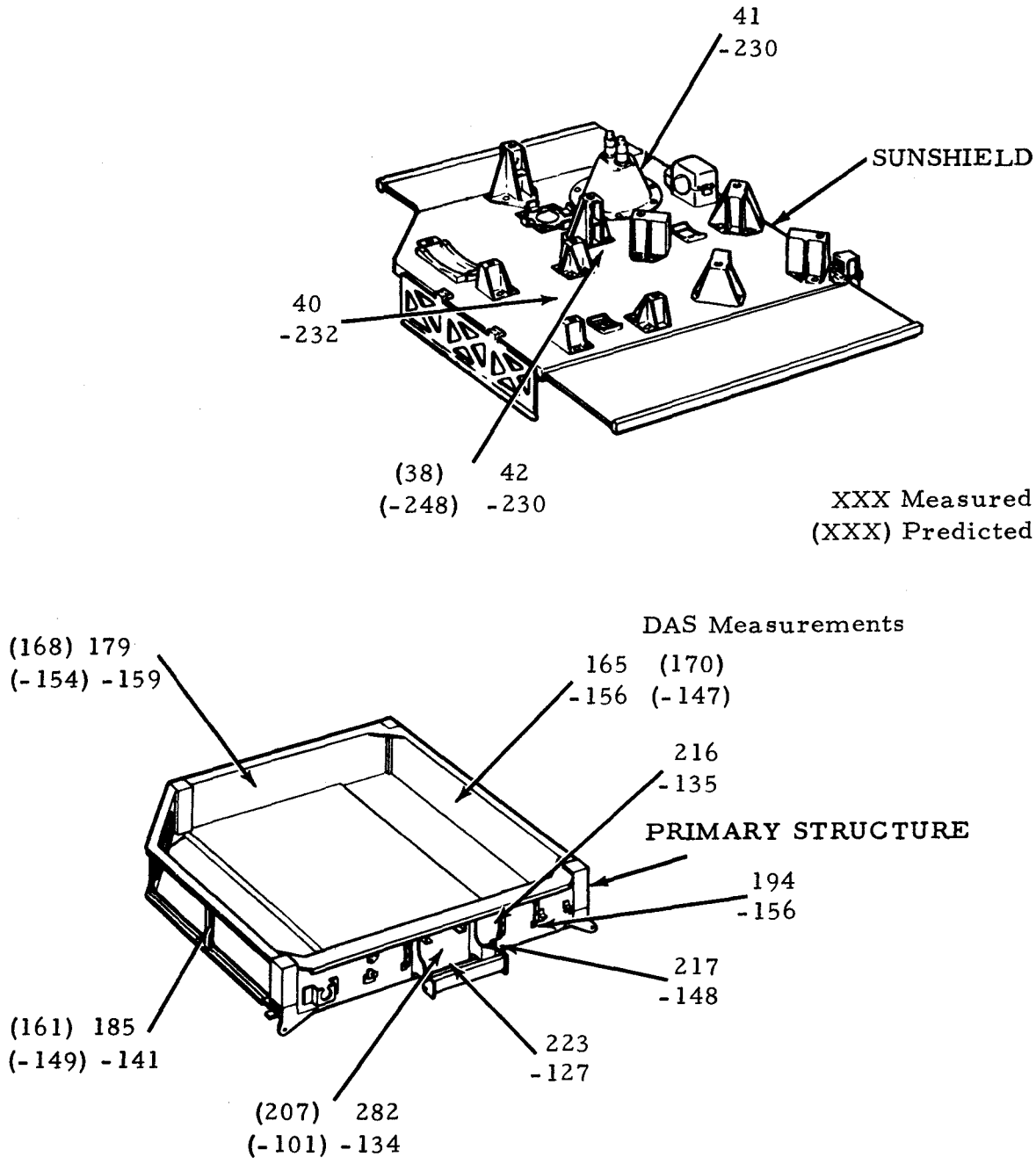

Figure 6 ALSEP Prototype "A" System Test; Measured vs Predicted Sunshield and Primary Structure Temperatures for Lunar Noon and Night (^{o}F)

3.2 Improvement in Analytical Temperature Predictions

Overall, the attempt to improve analytical C/S temperature predictions is considered successful, as shown by the following brief comparison of test values (^{o} F) to predictions from Reference 1 and from this report.

Description	Noon			Night		
	Ref. 1	Final Report	Test	Ref. 1	Final Report	Test
Radiator Plate, Average	120	112	104	-11	-20	-15
Sunshield	46	38	41	-289	-248	-230
Primary Structure Sides, Average	141	166	176	-224	-151	-152
Primary Structure Bottom	193	213	232	-221	-143	-144

Reasons for these improvements are outlined below:

1. Radiator Plate - Improvements resulted from the following:

   a. A reduction of nearly 2.5 watts in electronics heat dissipation data, which occurred after a revised calibration on the P.C.U. and other central station components was obtained from the Qual SA power calibration test.

   b. Consideration of cutouts in the insulation masks.

   c. Use of in-chamber cryowall test temperatures, which affected only the night condition.

   d. Decreased resistance through side curtains, which affected only the noon condition.

Night temperature correlation was not improved as the radiation average temperature was lowered 9° F rather than the desired 5° F. However, a one watt error in analysis heat dissipation at the radiator plate would account for the 4° F discrepancy.

2. Sunshield - Use of actual cryowall test temperatures, which were considerably higher than the -300° F used in Reference 1, caused the improved "night" correlation. Detailed information on these test temperatures was not available until after Reference 1 was published. The noon temperature prediction, controlled by solar heating, decreased since the analysis sunshield area was reduced.

3. Primary Structure Sides - A number of changes caused the improved correlation here.

   a. Addition of resistor heat dissipation. The result is an obvious temperature increase.

   b. Division of the test lunar surface into isothermal nodes for the "noon" condition. Thus, the "hot" nodes adjacent to the structure had a greater effect than the cooler nodes at a distance, with an overall effect of increased structure temperatures.

   c. Use of test cryowall temperatures.

   d. Increased structure radiation resistance values to moon and space. This resulted from a reduction in radiation area, which in turn was due to side curtain overhang, cables, connectors, brackets, etc. See Appendix 2, Section 8.0 for details.

It should be noted that the structure average test temperatures do not include data on the front side where the resistors are located. Measurements were taken at resistor locations and are not considered representative of the overall surface temperature.

4. Primary Structure Bottom - Good correlation, which is actually better than shown in the table for reasons to be stated, occurred when the test moon temperature under the structure was used in the analysis instead of the average -250° F.

Refinements made in the Reference 1 model to obtain the current model and their individual effects on C/S temperatures are summarized in Table 3. Values are only approximate since it is not possible to completely isolate the various effects. Refinement effects are interrelated because they are dependent on temperature. The intention of Table 3 is to present an order-of-magnitude influence of each refinement on C/S temperatures.

TABLE 3

EFFECT OF REFINEMENTS ON CENTRAL

STATION TEMPERATURES

Refinement	Temp. Change (°F)* Noon	Night	C/S Component Affected
Reduced Electronics Heat Dissipation	-3	-8	Radiator Plate - Avg.
Insulation Mask Cutouts	-4	-6	" " "
Decreased Side Curtain Resistance	-1	0	" " "
Cryowall Test Temperatures	0	5	" " "
" " "	0	8	Structure Sides - Avg.
" " "	0	2	Structure Bottom
" " "	3	35	Sunshield
Resistor Heat Dissipation	5	60	Structure Sides - Avg.
" " "	3	85	Structure Bottom
Lunar Surface Test Temperatures	11	0	Structure Sides - Avg.
Lunar Surface Test Temperatures	39	0	Structure Bottom
Cables from C/S to Experiments	0	-5	Structure Sides - Avg.
" " " " "	0	-3	Structure Bottom

TABLE 3 (CONT.)

EFFECT OF REFINEMENTS ON CENTRAL

STATION TEMPERATURES

Refinement	Temp. Change (^{o}F)* Noon	Night	C/S Component Affected
Increased Radiation Resistance from Structure to Moon & Space	3	7	Structure Sides - Avg.
" " " " "	0	3	Structure Bottom
Decreased Conduction Resistance between Structure Sides & Bottom	8	3	Structure Sides - Avg.
" " " "	-22	-9	Structure Bottom
Decreased Sunshield Area	-6	6	Sunshield
C/S Internal Wiring	Negligible Effect		
Heat Transfer between Structure & Sunshield	"	"	

*Positive and negative figures indicate increases and decreases, respectively, in analysis temperatures.

3.3 Capability of Analytical Model

The thermal model developed in this analysis is considered capable of predicting steady-state temperatures for vacuum chamber testing within accuracies listed below:

C/S Component	Temperature Accuracy
Radiator Baseplate	± 10° F (Noon & Night)
Primary Structure	± 20° F (Noon & Night)
Sunshield	± 5° F (Noon)
	± 20° F (Night)

These accuracies are applicable providing that (1) differences between model and actual heat dissipations at the radiator and structure are less than ± 10%; (2) the side curtains, insulation masks, and thermal paint are properly installed; and (3) there is no significant deterioration of radiation properties for the reflector and other surfaces during operation.

3.4 Discrepancies Between Predicted and Test Results

Reasons for differences in predicted and test temperatures for the various C/S Sections are listed below:

3.4.1 Primary Structure

1. The analysis treats each structure side as a node, which means that large areas are assumed isothermal.

2. Test measurements were not taken at the middle of the side nodes. When predicted values were adjusted to the thermocouple locations, better correlation was achieved. For example, adjusted "noon" and "night" values for node 50 were 171° F and -139°F, respectively, which are 10° F and 6° F improvements in correlation.

3. The test measurement on the structure bottom was centered. However, since heat flow from the center to the outside edge is not constant due to radiation to or from the entire surface, the analysis assumes the single node is located halfway between the center and outside edge for each conduction path to the sides. This is discussed in detail in Appendix 2, Section 6. Consequently, the analysis and test temperatures are at different locations on the bottom surface. As heat always flows from the bottom to the sides, the bottom center will have a higher temperature than the analysis node. An adjustment in the analysis to account for the location difference gives noon and night temperatures of 232° F and -140° F for the structure bottom, which agree very well with test figures.

4. Resistor heat dissipation was assumed to occur at the center of node 49, whereas the heat was actually distributed unevenly over this primary structure surface. Because the exact heat distribution for the test is unknown and because the model would be further complicated, this non-uniformity of heat dissipation was ignored. Since the resistor heat output is effectively isolated from the structure in the Qual SA model, temperature gradients around the primary structure will be significantly reduced, and correlation should be improved.

5. Non-uniform test temperatures over the vacuum chamber "lunar" surface and cryowalls made it extremely difficult to establish accurate radiation resistance paths. To prevent prohibitive complexity in the thermal model, average temperatures and form factors were used which probably affected temperature accuracy, especially for the structure and sunshield.

3.4.2 Radiator Baseplate

Thermal conductance of the side curtains and insulation masks can have a marked effect on radiator temperatures, as shown by the trade-off studies in Section 6. Estimated values of thermal conductivity, not test figures, were used in conjunction with design thicknesses to obtain conductance. No allowance has been made for variation of conductivity with temperature, which might be significant because of the wide range of operating temperatures. As the insulation is composed of layers of silk

and/or aluminized mylar, overall thickness of installed sections can vary significantly from design specifications. The final analysis model used a constant conductance figure which gave good overall correlation for noon and night conditions. However, if thermal conductivity of the masks and curtains varies markedly from noon to night, as does the thermal bag conductivity, significant improvement in temperature correlation might be achieved.

Though we consider electronic component heat dissipation figures in the analysis to be fairly accurate, even a small error in data or data reduction is enough to affect radiator plate temperature correlation — especially for the night condition where one watt makes a 3^{o} F difference in plate temperature.

3.4.3 Sunshield

Non-uniform temperatures over the test chamber cryowalls introduced correlation problems similar to those discussed for the primary structure.

3.4.4 Electronic Components

The subject of temperature correlation on the electronic components has been neglected so far. One cannot expect analysis temperatures to match with test values since the analysis assumes each component is at constant temperature, whereas test measurements were generally taken on each component's outside case and base. However, analytical predictions fell within the range of test values, and the analysis simulation of electronics is considered adequate. Measured temperatures in Figures 3 and 4 for the electronics are really averages of several measurements on each component. Table 8 in Section 6 shows a breakdown of this temperature data.

Many of the aforementioned analysis problems should be minimized and accuracy of temperature predictions improved by 1) the resistor location redesign and 2) operation in the actual lunar/space environment.

Two sets of Prototype "A" test data were recorded: DAS and Telemetry. Where differences occurred in the two data types, DAS was considered the more accurate.

3.5 "Real" Lunar Surface Analysis Results

As stated previously, lunar noon analysis results predict a 28°F higher average radiator plate temperature for the real lunar surface environment than for the Prototype "A" test condition. This difference is due primarily to the higher radiation heat transfer between the plate and lunar surface and to the lower radiation from the plate to space for actual moon operation. Even though the vacuum chamber cryowall arch had a -248°F average "noon" temperature, the 28°F difference would not be significantly altered if the arch had been at the -300°F test goal or at the -460°F of real space.

For lunar night, the thermal model predicts a 7°F lower average radiator plate temperature for the real lunar environment than for the test condition. Figure 7, which plots predicted average radiator "night" temperature versus space (cryowall) temperature, helps to explain this difference. As shown by the figure, the spread between the real moon and chamber test predictions is 2°F at each "space" temperature and can be attributed to the lower structure temperatures during real moon operation. This allows increased heat loss through the bag, cables, and support posts which, in turn, permits the plate to dissipate the remaining heat at a lower average temperature.

Also note the 3°F radiator temperature drop when going from the actual vacuum chamber space test temperature of -260°F to the -300°F test goal. An additional 2°F temperature drop occurs when -460°F replaces -300°F as the space temperature. Consequently, the 7°F difference can be allocated as follows:

1. The lower structure temperature of the real moon model accounts for 2°F.

2. Failure to achieve the -300°F cryowall temperature during testing is responsible for 3°F.

3. The remaining 2°F results from the difference between the test goal and actual space temperatures.

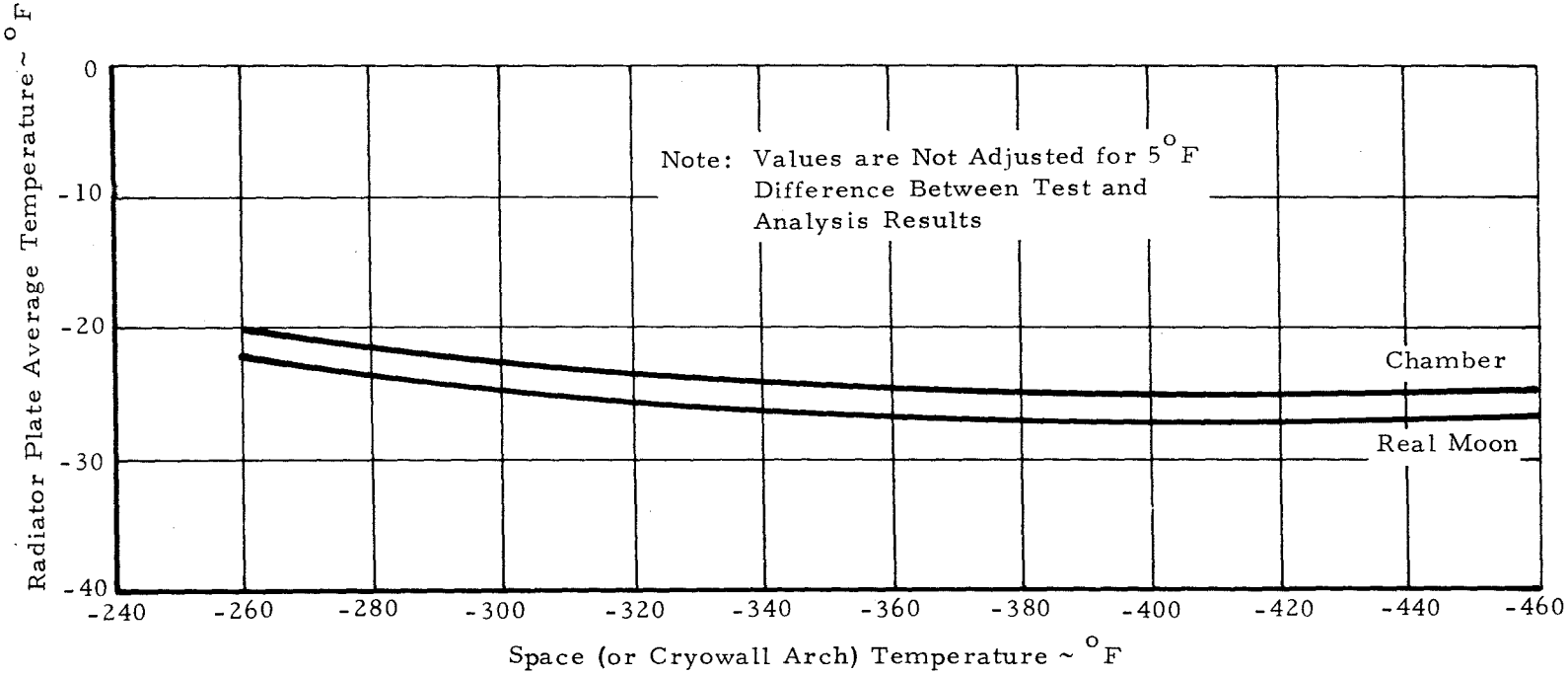

Figure 7 Predicted Radiator Plate Average Temperature vs Space (or Cryowall Arch) Temperature for Lunar Night

3.6 Design Improvements for Qual SA Model

Based on test results obtained from the Proto A Test Program, several design improvements have been incorporated into the Qual SA and subsequent ALSEP Flight Central Station models. The improvements were initiated due to several electrical and thermal system performance changes between the Proto A and Qual SA models. The system performance changes include:

1. Higher RTG input power
2. Higher experiment night time loads
3. Wider PCU regulator range
4. Increase in C/S component day time thermal dissipation
5. Reduction in C/S component night time thermal dissipation

The overall effect of the above changes results in a thermal dissipation swing for Qual SA and the Flight model of up to 42 watts during lunar day and 32 watts during lunar night. This compares to the measured dissipation for Proto A of approximately 32 ± 1 watts for both lunar day and night.

To accommodate the wider range in Central Station internal thermal dissipation for the Qual SA model, three modifications to the existing design have been proposed. They include:

1. The Central Station awnings and attached side curtains were revised to increase the radiator view factor to space.
2. The Central Station radiator masks were resized from six to seven inches to optimize the thermal plate temperature swing.
3. Additional backup commandable heaters of 5 and 10 watts were added to the thermal plate to provide contingency power for lunar night.

The verification of the thermal/electrical performance of the central station design with the above improvements included will be accomplished as part of the Qual SA Acceptance and Mission Simulation Test Program.

4.0 THERMAL MODEL

Figures 8, 9, and 10 illustrate the deployed assembly and primary components of the C/S. For details concerning physical characteristics and functions of these components, refer to Appendix 1.

4.1 Nodal Designation

The C/S components are divided into isothermal "nodes", as identified in Figures 11 through 16. When correlating predicted and test results, the test lunar surface and cryowalls (space) were also divided into nodes, as shown in Figures 17 and 18, since the desired uniform temperatures over these surfaces were not obtained during testing.

4.2 Resistance Paths

Nodes are connected by conduction and radiation resistance paths to form a network analogous to an electrical circuit, where voltage and current are replaced by temperature and heat flux, respectively. Section 5 describes general techniques used to evaluate resistances, and Appendix 2 presents calculation details on various "critical" resistances. For a brief summary of resistance paths, see Table 4, or refer to Appendix 3 for a complete listing of paths.

4.3 Thermal Analyzer Computer Program

Data on nodes and resistances are input to a "Thermal Analyzer" computer program (described in Ref. 2) along with information on solar, electronic, and resistor heating. The program, which employs a finite difference technique, performs successive energy balances on each node to establish node temperatures until a "steady-state" condition is achieved, which is when the net heat flow at each node is zero.

In regard to the manner of supplying data to the program, the resistance reciprocal or conductance is input for radiation paths while resistance is input for conduction paths.

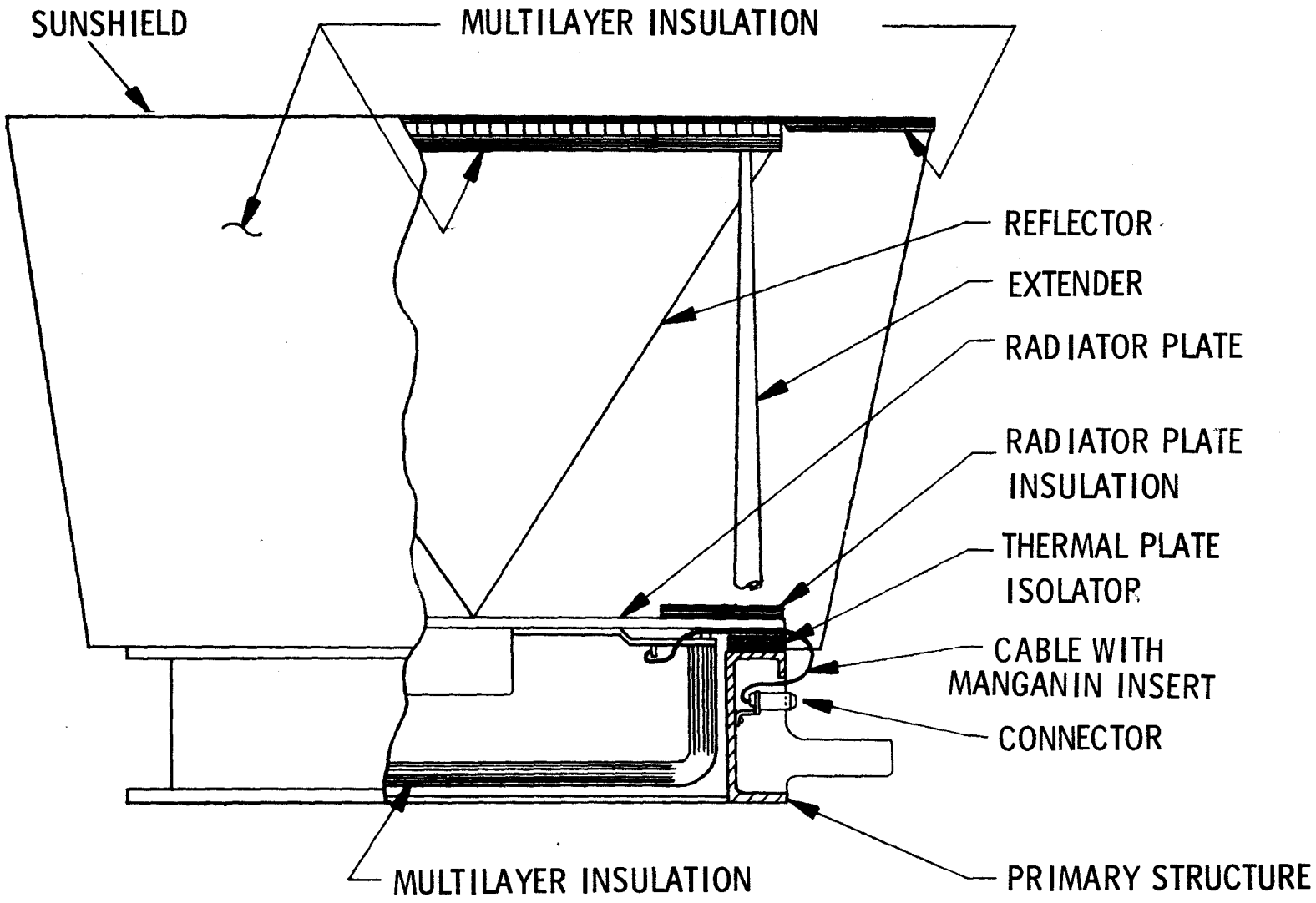

Figure 8 Central Station Assembly

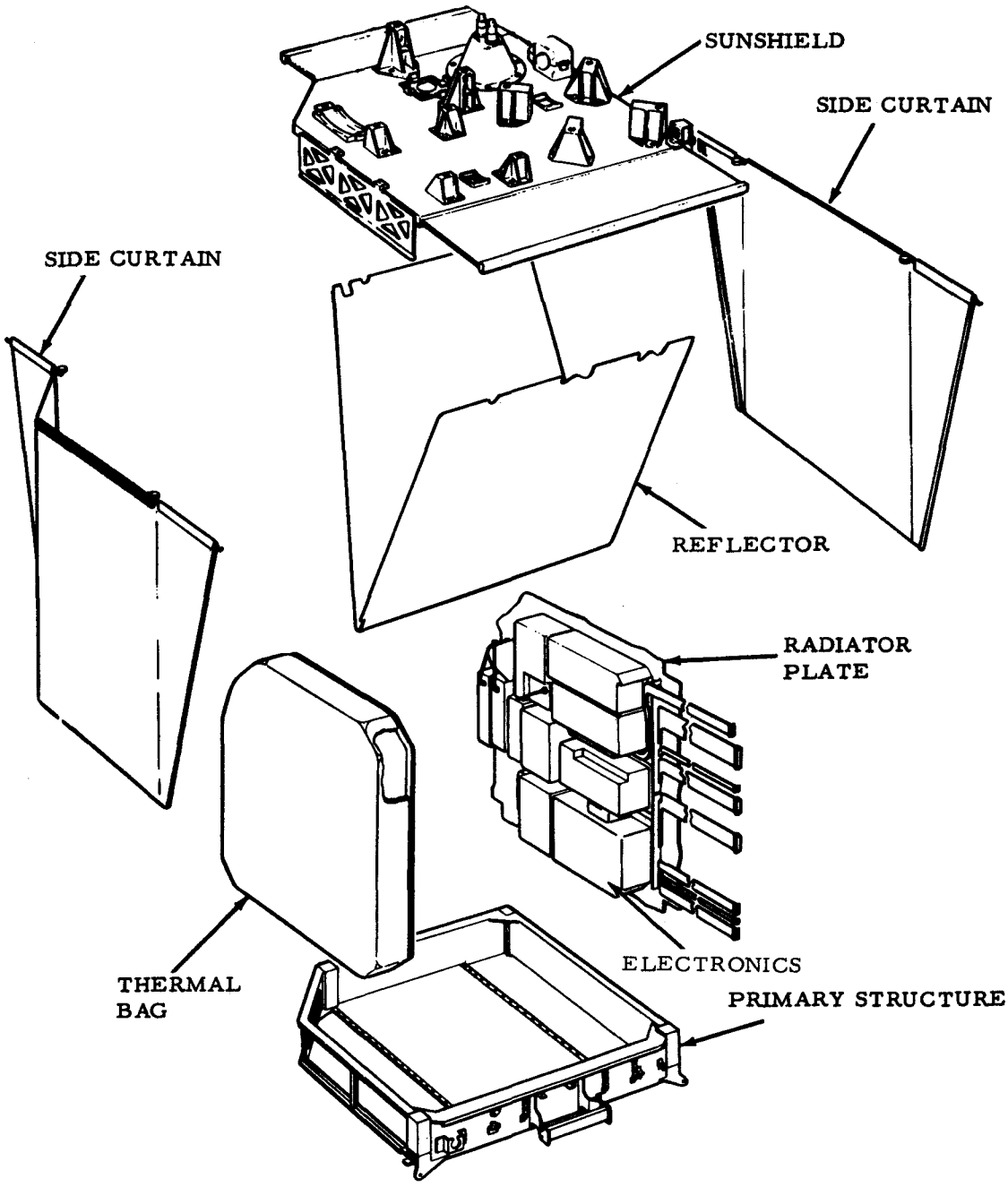

Figure 9 Primary Components of Central Station Thermal Control System

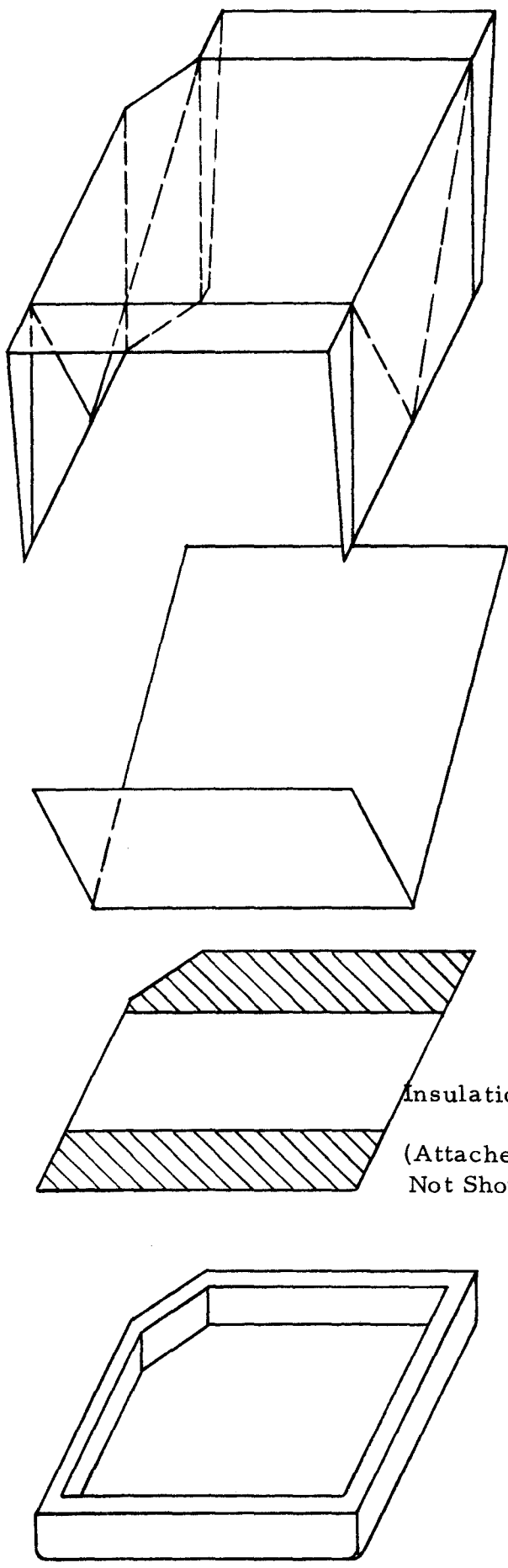

Figure 10 Exploded Schematic View of ALSEP Central Station Thermal Control System

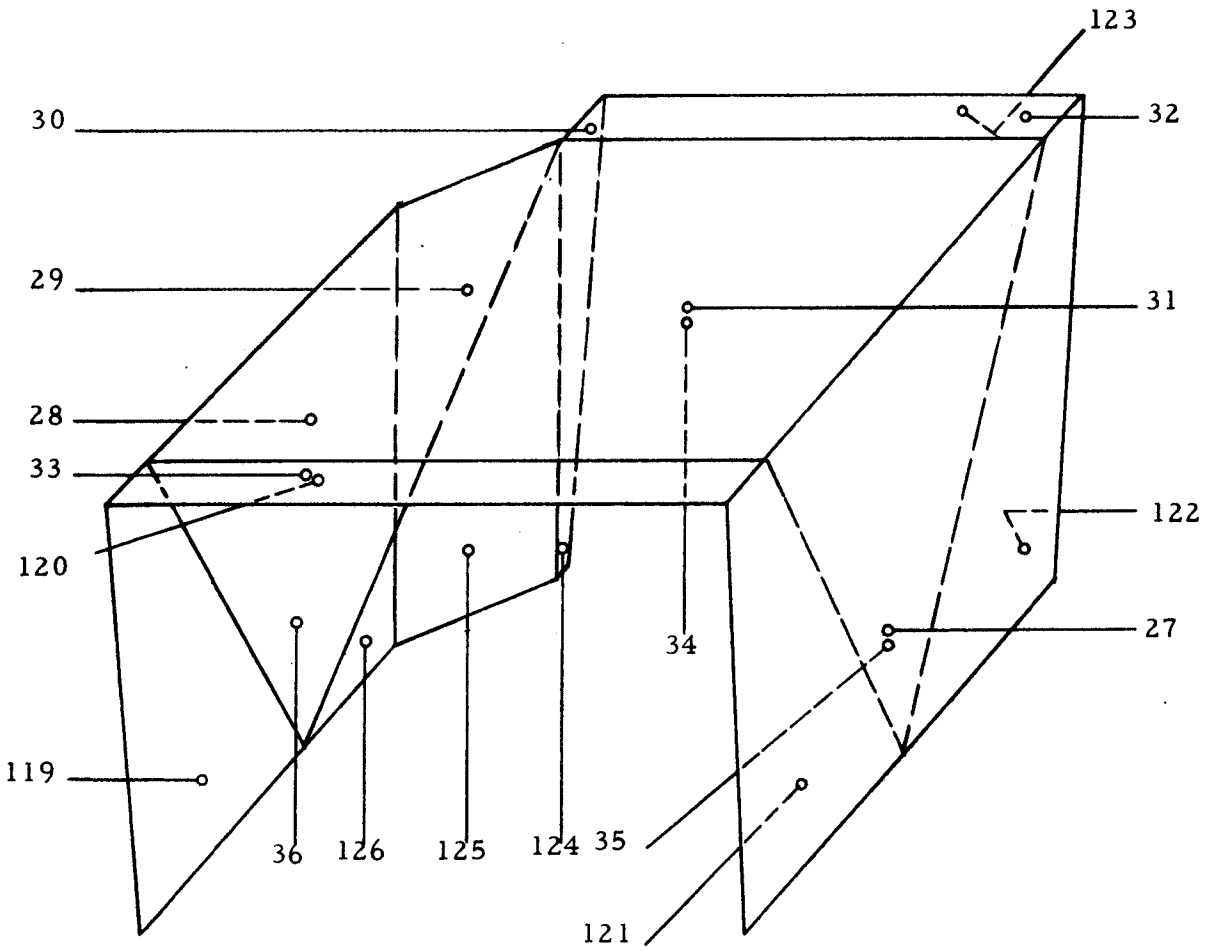

Figure 11 Sunshield and Side Curtain Assembly Nodal Designation

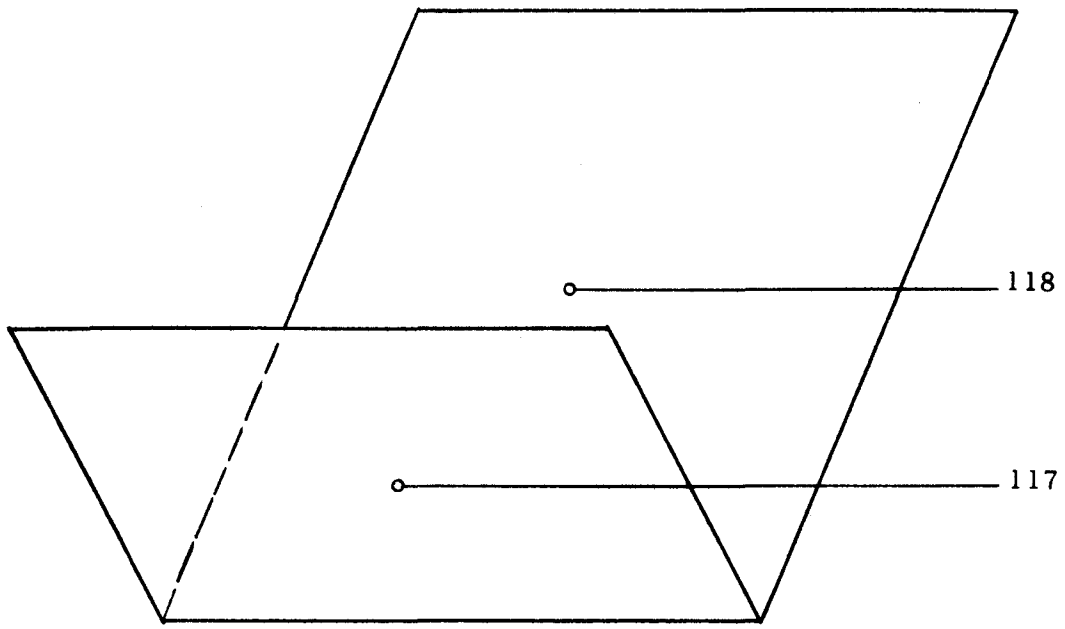

Figure 12 Reflector Assembly Nodal Designation

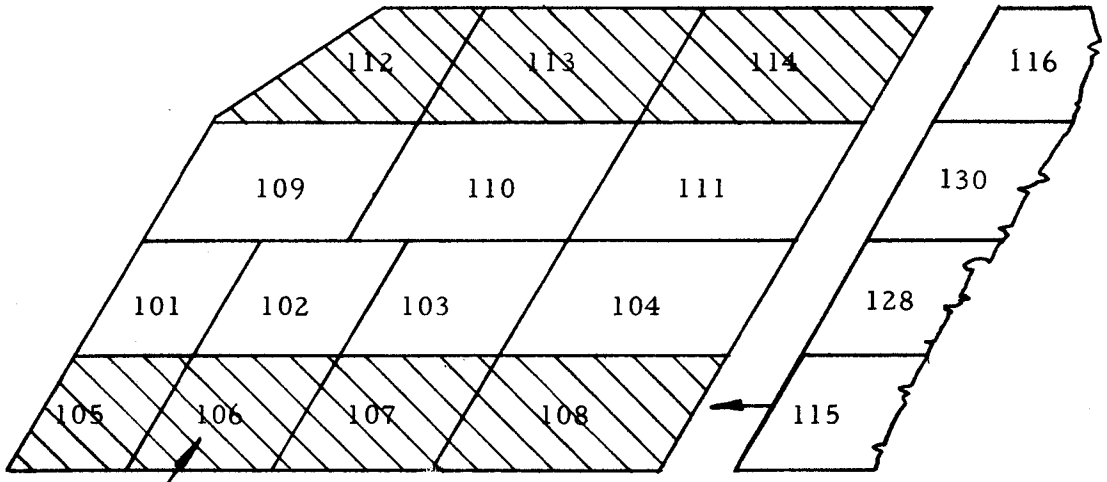

Indicates position of radiator insulation denoted by nodes 115 and 116. Attached electronic components identified on separate diagram.

Nodes 128 and 130 are part of the radiosity network and are attached to nodes 101-104 and to 109-111, respectively, by negligible resistances.

Figure 13 Radiator-Baseplate Assembly Nodal Designation

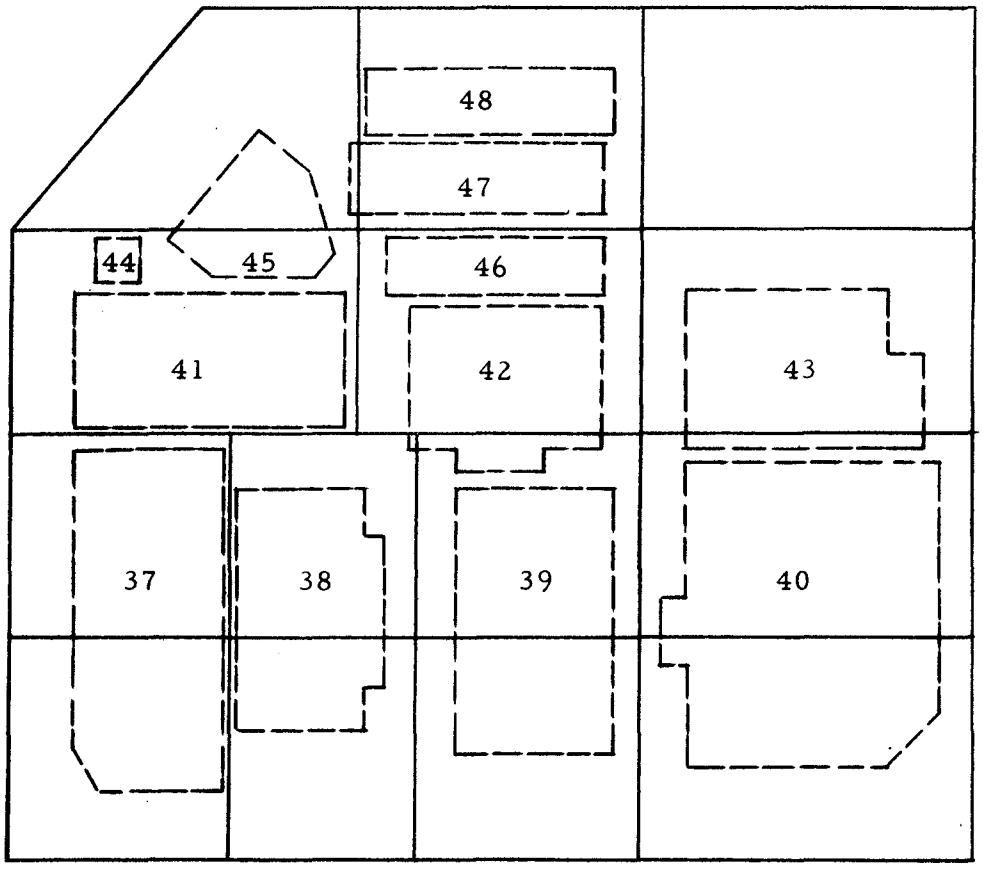

Top View

Figure 14 Radiator Baseplate Assembly with Electronic Components Nodal Designation

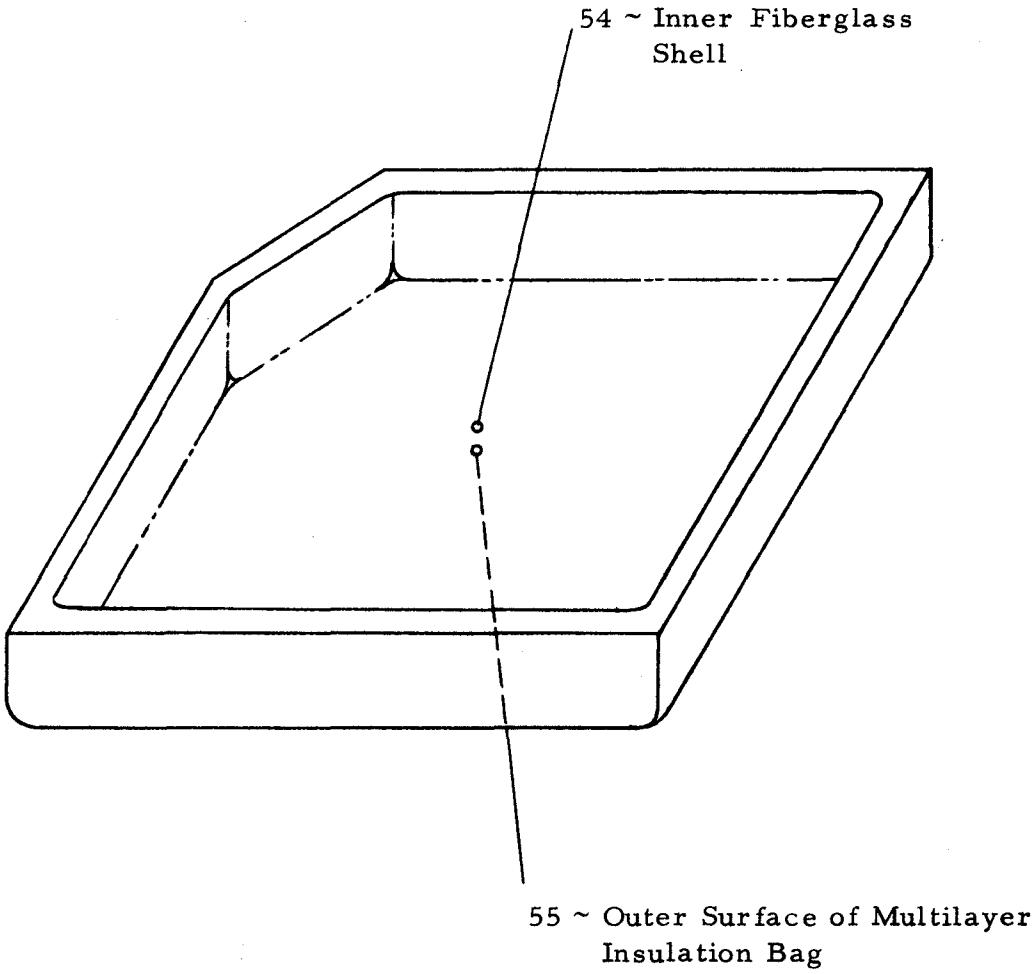

Figure 15 Thermal Bag Assembly Nodal Designation

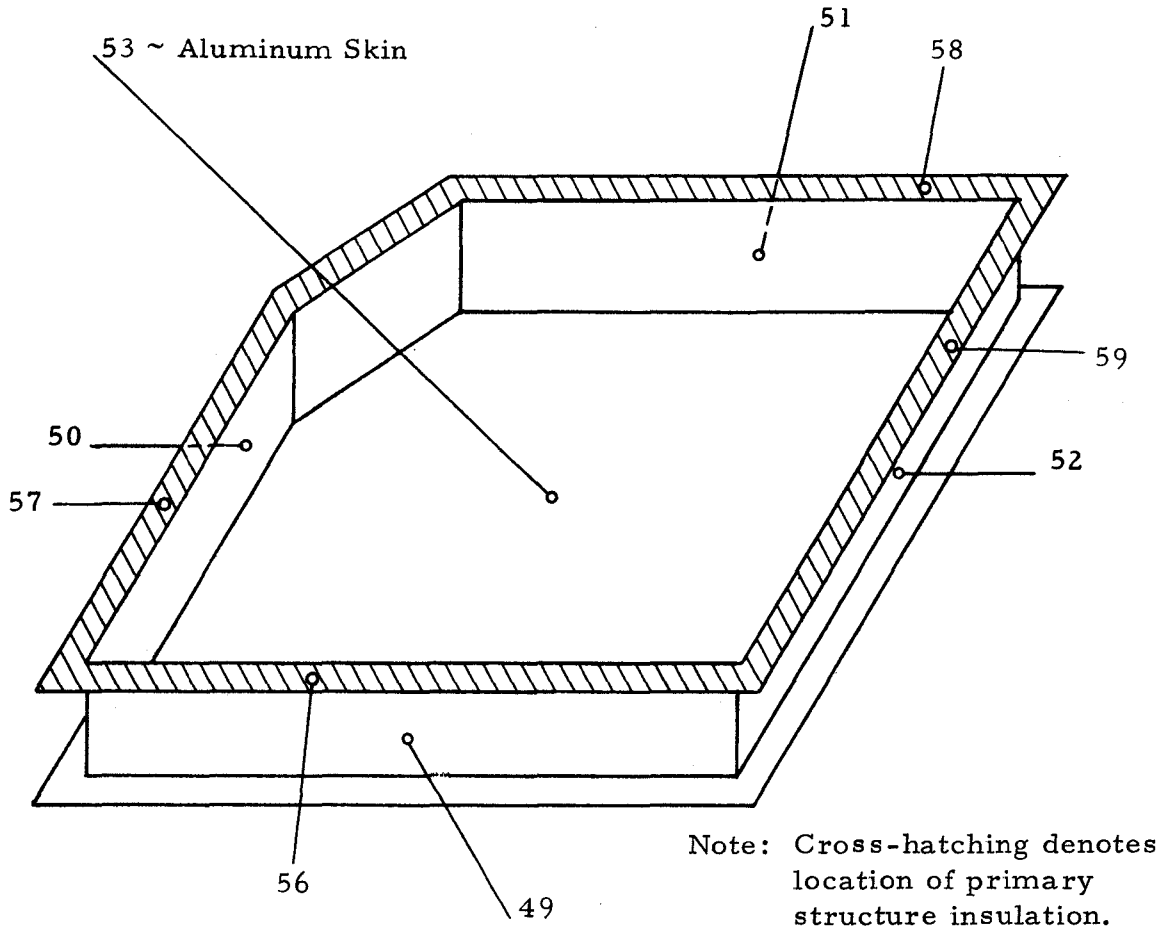

Figure 16 Primary Structure Assembly Nodal Designation

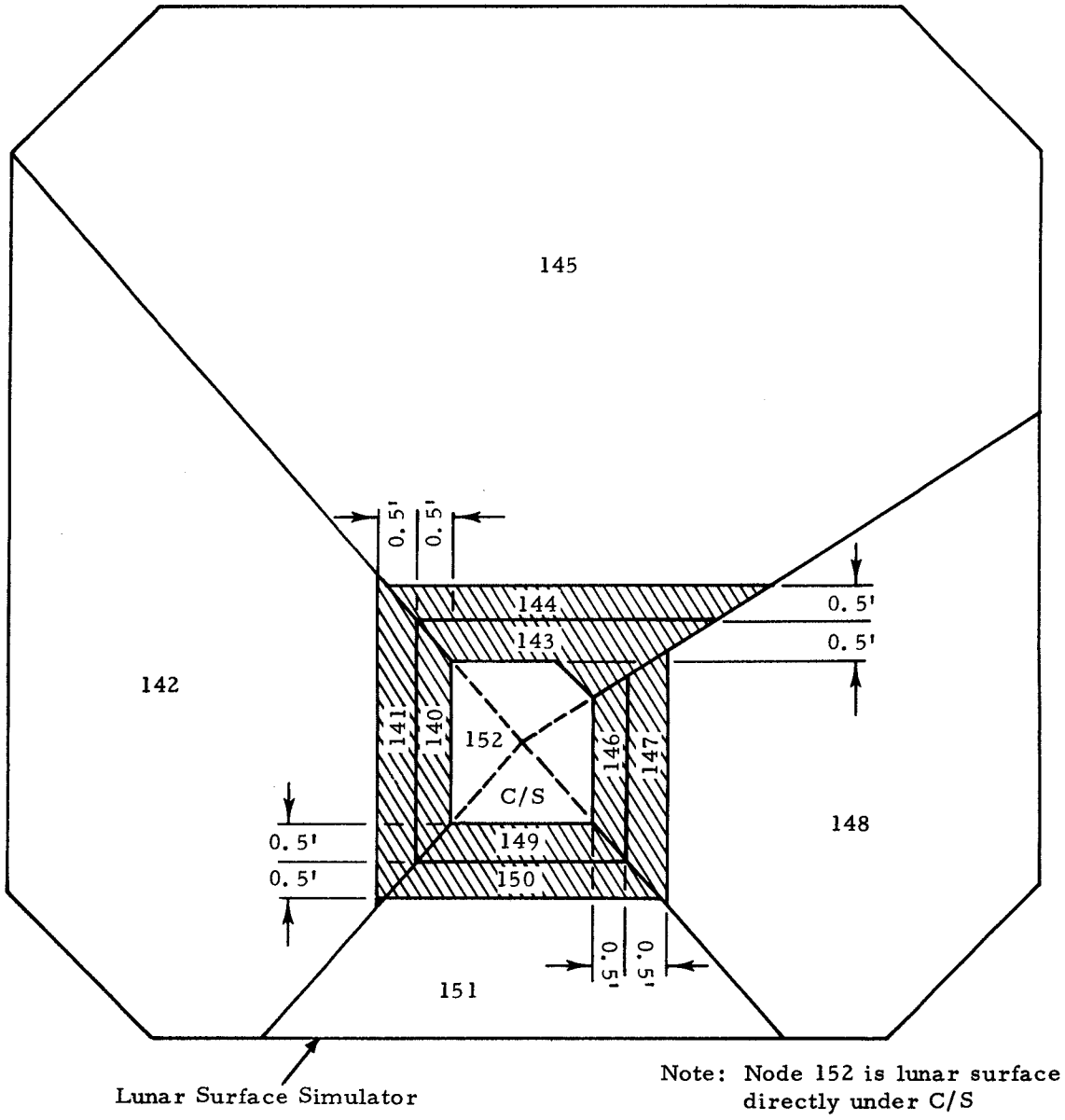

Figure 17 Nodal Division of Prototype "A" Test Lunar Noon Surface Simulator

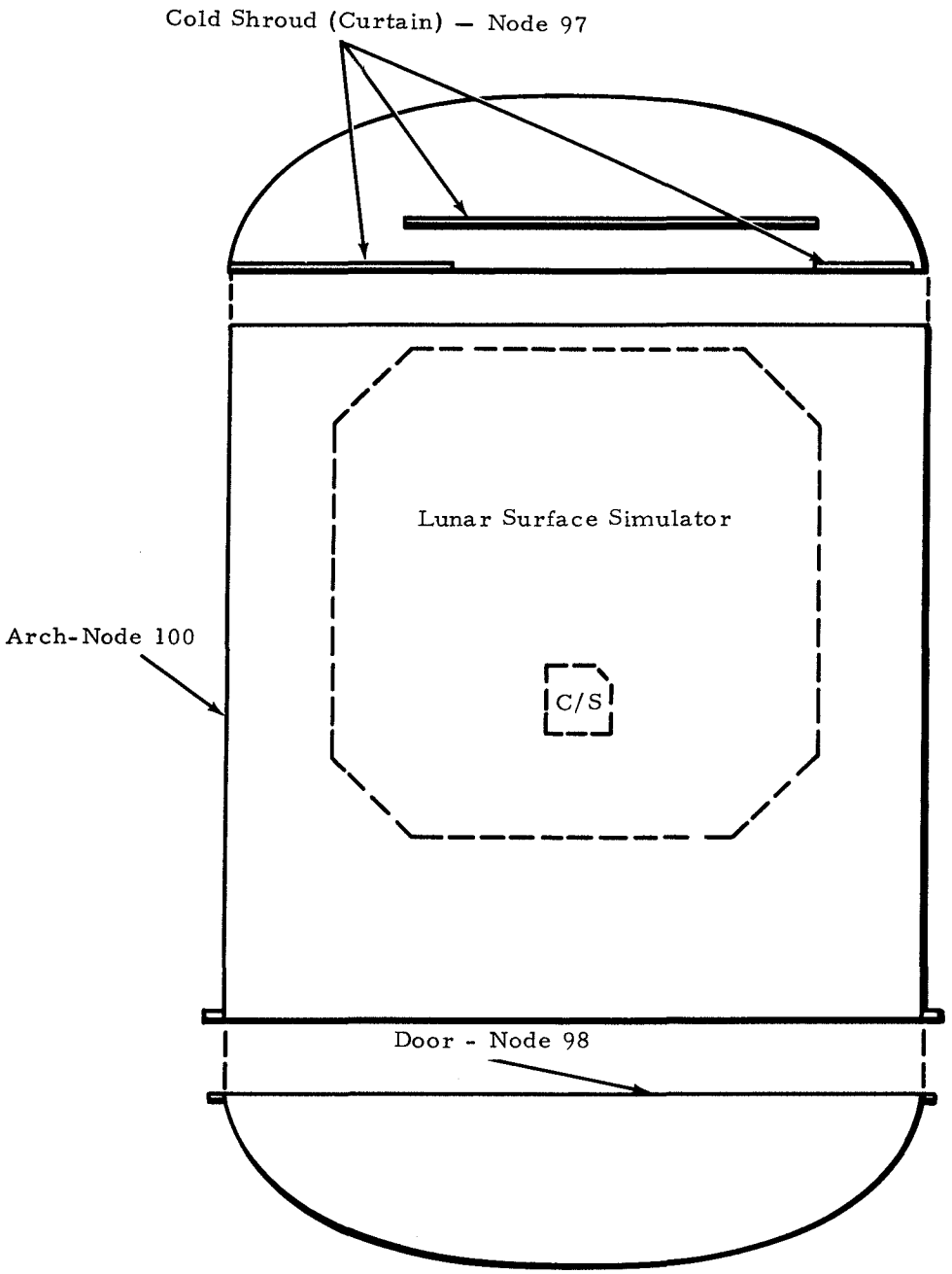

Figure 18 Division of Prototype "A" Test Chamber Cryowalls into Space Nodes

TABLE 4

SUMMARY OF RADIATION AND CONDUCTION RESISTANCE PATHS

Paths	Description	Mode of Heat Trans.	Section With Analysis Method*
1-27	Electronics to Radiator	Conduction	5.2.2
31-52	Radiator Node Connections	Conduction	5.2.1
53-59	Insulation Mask Resistance	Conduction	5.2.1
61-64	Structure to Radiator via Posts	Conduction and Radiation	5.1.2.2, 5.2
65-68	Structure Insulation Resistance	Conduction	5.2.1
69-83	Structure to Radiator	Radiation	5.1.2.3
86-97	Electronics to Thermal Bag	Radiation	5.1.2.2
98-111	Radiator to Thermal Bag	Radiation	5.1.2.2
112-116	Structure to Thermal Bag	Radiation	5.1.2.2
117	Thermal Bag Insulation Resistance	Conduction	5.2.1
118-121	Structure Node Connections	Conduction	5.2.1
122-125	Structure to Sunshield	Conduction	5.2.1
126-146	Structure to Moon and Space	Radiation	5.1.2.1
147	Structure to Moon	Conduction	5.2.1
149-152	Structure Sides to Bottom	Conduction	5.2.1
153-164	Side Curtain and Sunshield Insulation Resistance	Conduction	5.2.1
166-174	Side Curtains to Moon and Space	Radiation	5.1.2.1

TABLE 4 (CONT.)

Paths	Description	Mode of Heat Trans.	Section With Analysis Method*
175-179	Sunshield to Space	Radiation	5.1.2.1
180-194	Enclosure Behind Reflectors	Radiation	5.1.2.3
200-299	Radiosity Node Network	Radiation	5.1.1
350-412	Cable Resistances	Conduction	5.2
413	Cable Resistance	Conduction and Radiation	5.2 5.1.2.1
416-421	Cable Resistance	Conduction	5.2
422	Cable Resistance	Conduction and Radiation	5.2 5.1.2.1

* Detailed calculations for resistance paths are presented in Appendix 2.

5.0 ANALYSIS METHODS

Various methods for establishing heat flow resistance paths are described below. Some of the analysis techniques were discussed in Reference 1 but are outlined again for easier understanding of this section.

5.1 Radiation

5.1.1 Radiosity Network

The standard Oppenheim radiation or "radiosity" network method is described in Reference 3 and Appendix 4 but will be outlined briefly here. A radiation path between two nodes consists of two surface resistors and a space resistor. While the network assumes each node is at "black body" potential, a surface resistor accounts for the non-black properties of a node. The space resistance allows for that portion of radiant energy exchanged "directly" between two nodes. A dummy or "radiosity" node connects the surface and space resistors, as illustrated below in a three node system.

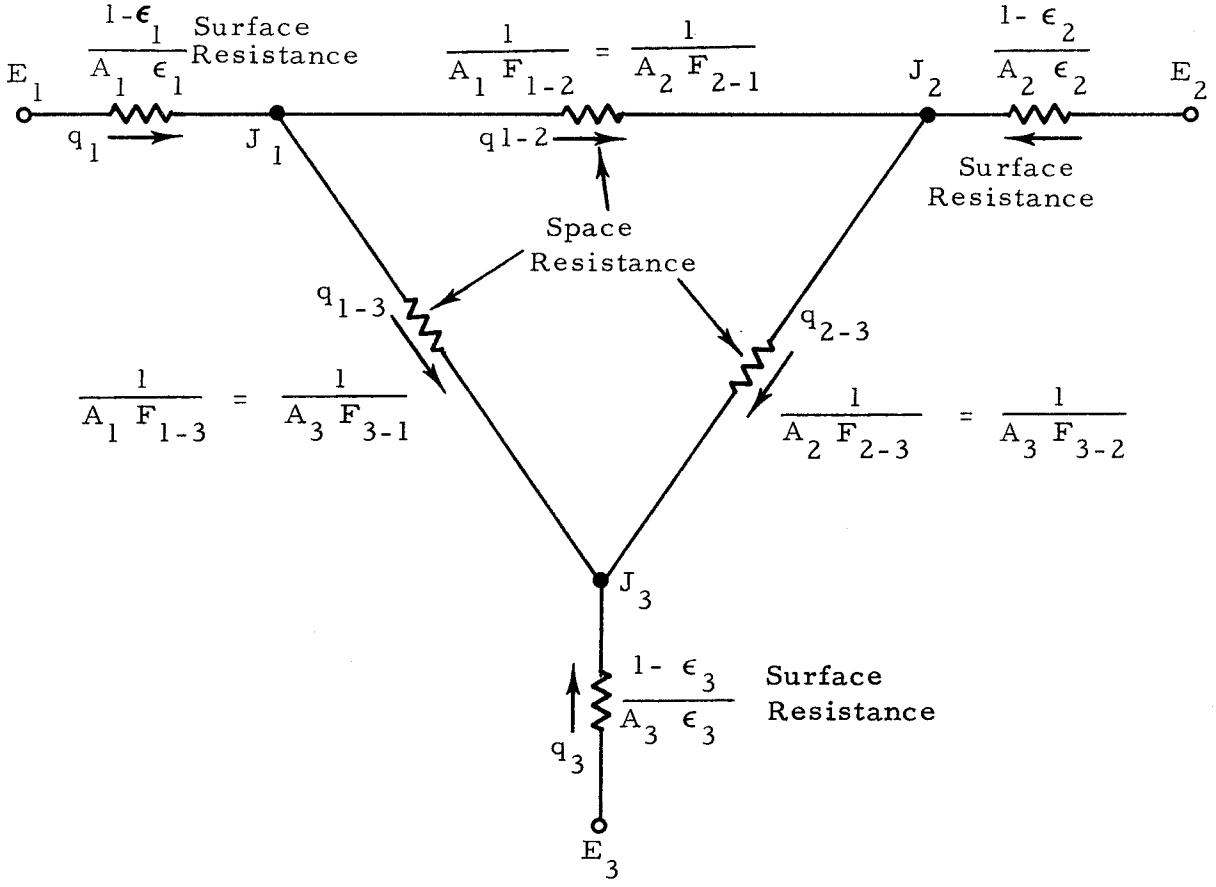

q = heat transfer rate

E = black body emissive power of surface = σT^4

J = diffuse flux density leaving surface (diffuse radiosity)

T = absolute surface temperature

σ = Stefan-Boltzman Constant

A = radiator surface area

ϵ = surface emissivity

F_{m-n} = form factor from surface m to surface n

Subscripts

1 = surface 1

2 = surface 2

3 = surface 3

The diffuse radiosity J includes both emitted and reflected radiation.

A radiosity network is processed by the thermal analyzer as follows. Surface and space resistance data is input along with the actual nodes which have energy potentials or emissive powers E_1, E_2, ... E_n. Since resistances must be joined by a node, "radiosity" nodes, which have energy potentials J_1, J_2, ... J_n, are input. The program assumes that J, as well as E, is represented by σT^4, so that temperatures calculated for radiosity nodes are meaningless. Since all solutions are for steady-state conditions and all energy is accounted for, the method is theoretically exact.

A radiosity network was used to represent each of the two enclosures formed by the radiator baseplate, side curtain interior surfaces, specular relector, moon, and space. Consequently, each network contains only one reflector and can be easily analyzed. The Oppenheim network was modified as outlined in Reference 4 in order to handle the reflector.

Basically, the modification involves one more term in the radiosity expression which represents specular reflection. Form factors between

"diffuse" nodes include "images" of diffuse nodes in the reflector. For example, with a single reflector, the form factor from node 1 to node 2 consists of the normal factor plus the specular reflectance times the form factor between node 1 and the image of node 2 seen in the reflector. Figure 19 shows typical construction of surface images in the specular reflector.

For a three-node system, where two nodes (1 and 2) are diffuse and the other is specular-diffuse, the "modified" radiosity network is as follows:

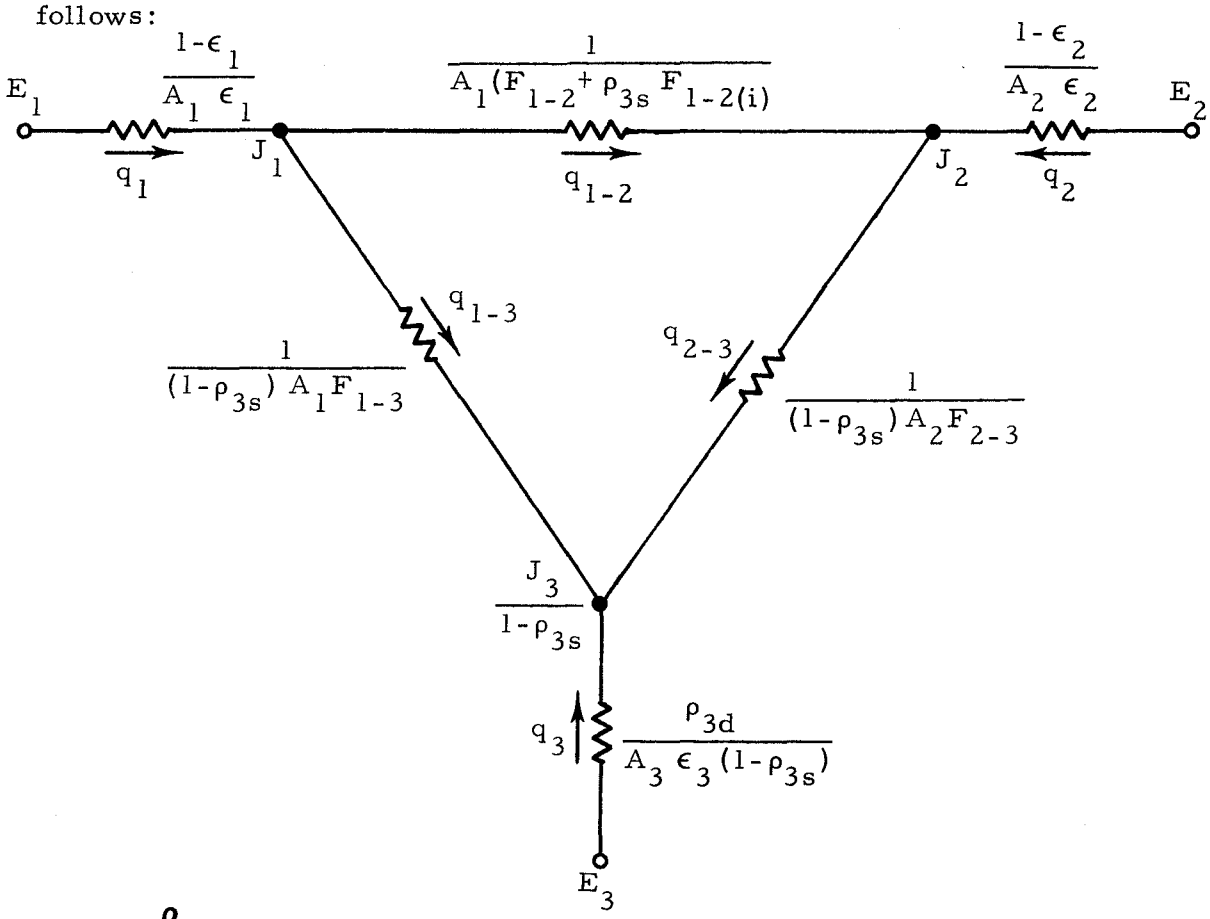

ρ_{3d} = diffuse reflection

ρ_{3s} = specular reflection

$F_{1-2(i)}$ = Form factor between node 1 and image of node 2 in reflector.

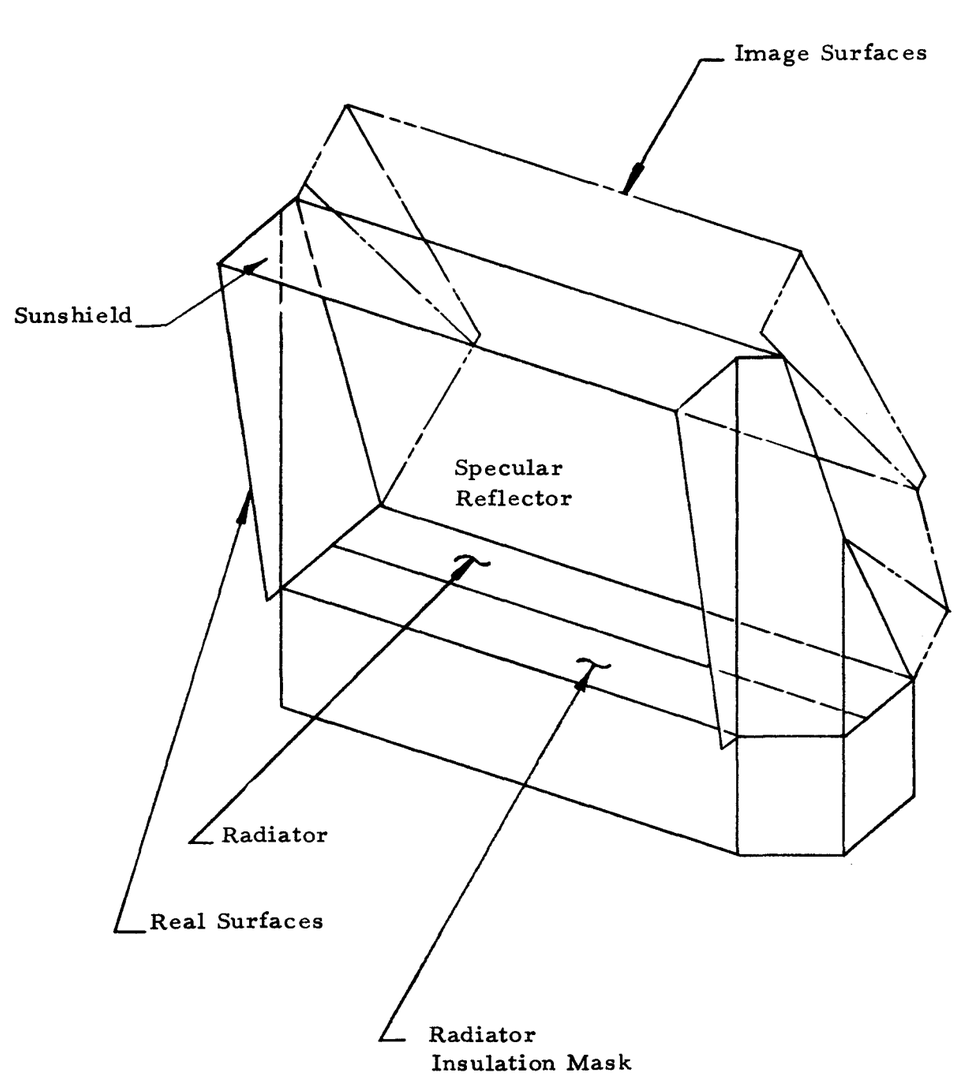

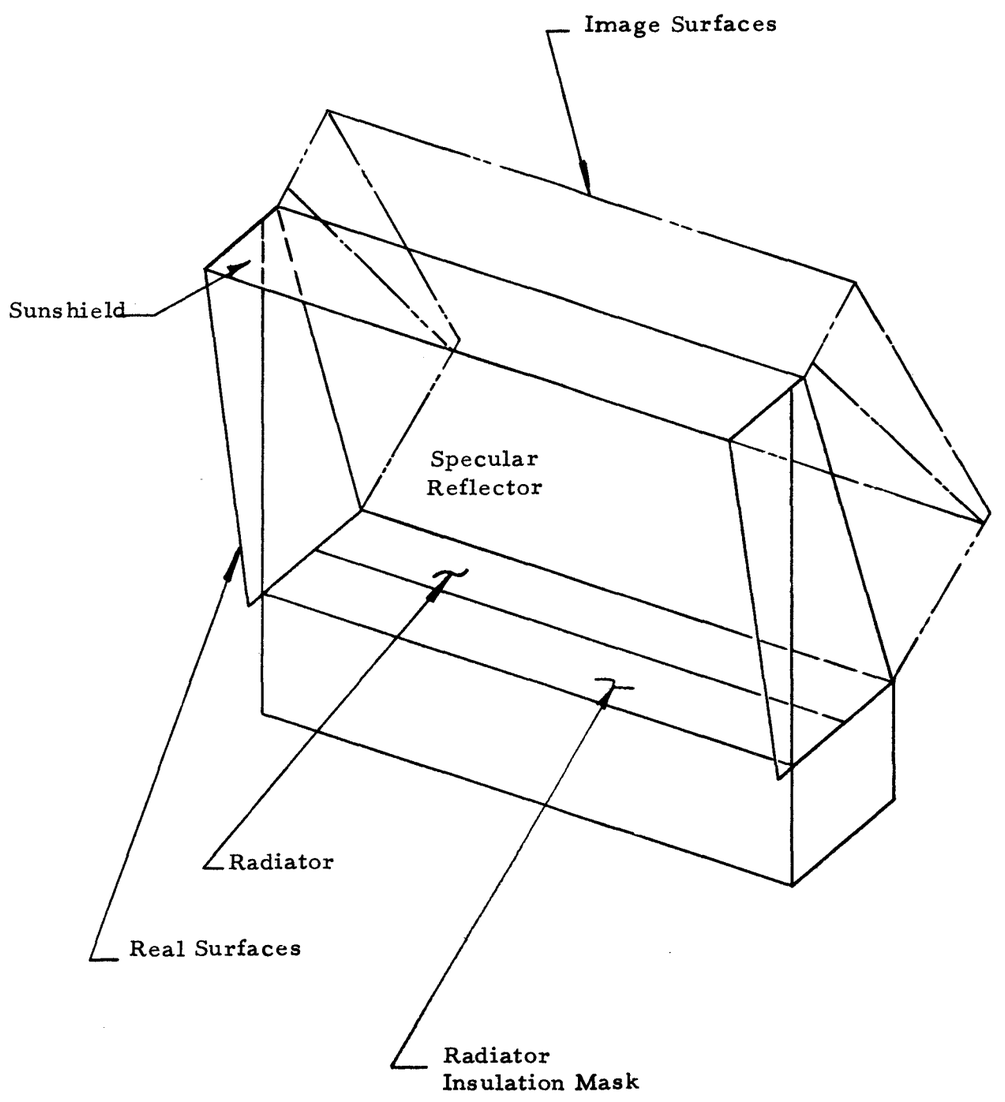

Figure 19 Typical Surface Image Construction

A specular-diffuse node in this problem is one which emits diffusely and reflects both diffusely and specularly.

5.1.2 Interchange Factor Networks

For those radiation heat transfer networks which do not involve specular reflection it is more convenient to use a single resistance based on interchange factors (Script F's) in place of surface and space resistances. When interchange factors are used, the 3-node radiosity network reduces to

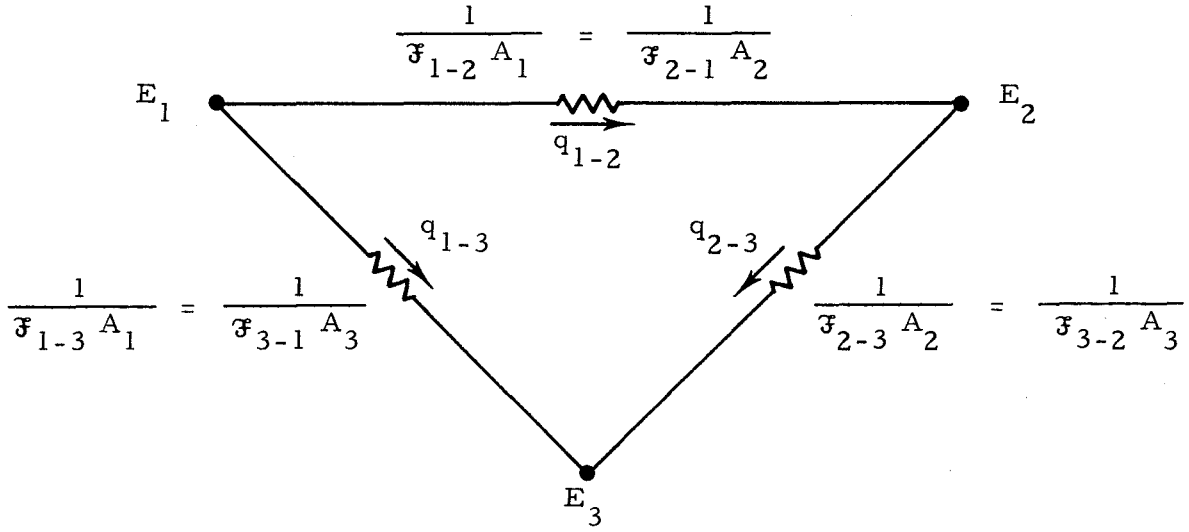

$\mathcal{F}_{m-n}$ = radiation interchange factor.

Interchange factors include reflected as well as direct radiation between surfaces and are therefore a function of form factors, emissivity, and reflectivity.

Following sections discuss various methods used to obtain interchange factors and specify where these factors were applied.

5.1.2.1 Factors Between a Surface, Moon, and Space

Moon and space were assumed to have emissivities of one, so that the three node radiosity network can be reduced to the following:

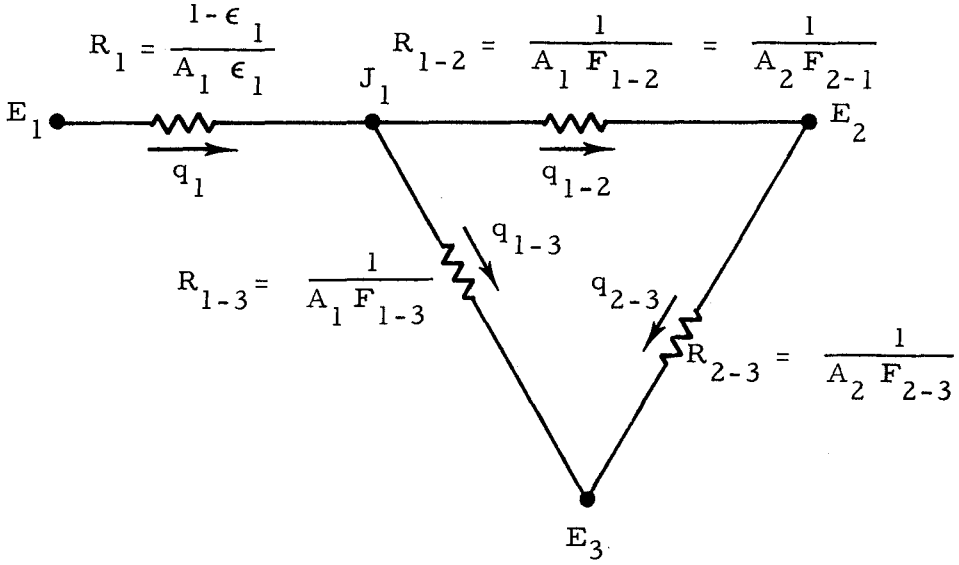

where $E_2 = J_2$, $E_3 = J_3$, $q_2 = q_3 = 0$, and $\epsilon_1 \neq 0$. Assume that $F_{1-2} + F_{1-3} = 1$, $A_2 >>> A_1$, and $A_3 >>> A_1$. The heat transfer relations are as follows:

$$q_1 = \frac{E_1 - J_1}{R_1} = q_{1-2} + q_{1-3}$$

$$q_{1-2} = \frac{J_1 - E_2}{R_{1-2}} = \mathcal{F}_{1-2} A_1 (E_1 - E_2)$$

$$q_{1-3} = \frac{J_1 - E_3}{R_{1-3}} = \mathcal{F}_{1-3} A_1 (E_1 - E_3)$$

$$q_{2-3} = \frac{E_2 - E_3}{R_{2-3}} = \mathcal{F}_{2-3} A_1 (E_2 - E_3)$$

$$q_2 = 0 = q_{2-3} + q_{2-1} = q_{2-3} - q_{1-2}$$

The above equations can be combined and solved to give

$$\mathcal{F}_{1-2} = F_{1-2}\ \epsilon_1 \qquad R_{\text{total }(1-2)} = \frac{1}{F_{1-2}\ \epsilon_1}$$

$$\mathcal{F}_{1-3} = F_{1-3}\ \epsilon_1 \qquad R_{\text{total }(1-3)} = \frac{1}{F_{1-3}\ \epsilon_1}$$

This method was used to obtain resistance paths from moon and space to the primary structure, sunshield top, and side curtains. Appendix 2 presents calculation details for resistances from the curtains to moon and space.

5.1.2.2 Factors in a Two-Surface Network

For this case, it is assumed that all heat exchange occurs between two surfaces. Thus $q_1 = q_{1-2} = q_2$, and the radiosity network is as below:

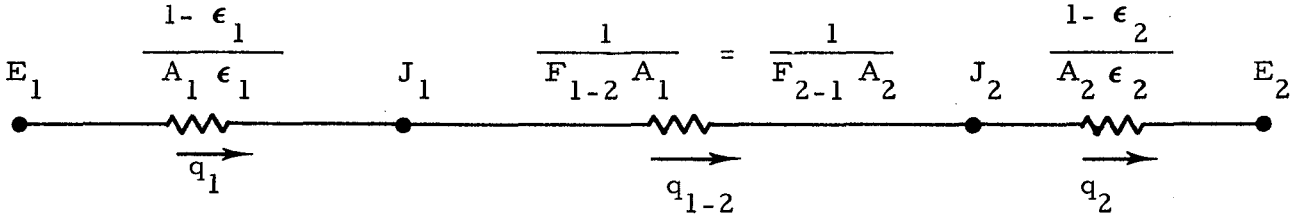

The equivalent interchange factor network is

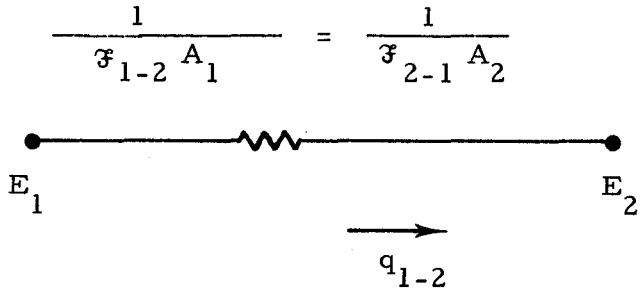

Therefore, $$\frac{1}{\mathcal{F}_{1-2} A_1} = \frac{1-\epsilon_1}{A_1 \epsilon_1} + \frac{1}{F_{1-2} A_1} + \frac{1-\epsilon_2}{A_2 \epsilon_2}$$

$$\mathcal{F}_{1-2} = \frac{1}{\frac{1}{F_{1-2}} + \frac{1}{\epsilon_1} - 1 + \frac{A_1}{A_2}\left(\frac{1}{\epsilon_2} - 1\right)} \qquad (5.1)$$

Since $q_{1-2} = \frac{E_1 - E_2}{R_{total\ (1-2)}}$ and $R_{total\ (1-2)} = \frac{1}{\mathcal{F}_{1-2} A_1}$,

$$R_{total\ (1-2)} = \frac{1}{A_1}\left[\frac{1}{F_{1-2}} + \frac{1}{\epsilon_1} - 1 + \frac{A_1}{A_2}\left(\frac{1}{\epsilon_2} - 1\right)\right] \qquad (5.2)$$

where $R_{total\ (1-2)}$ = total resistance between surfaces 1 and 2

Since the basic assumption is that all heat flow is between surfaces 1 and 2, F_{1-2} and F_{2-1} have values of 1.0. This means that $A_1 = A_2$, and equations 5.1 and 5.2 reduce to

$$\mathcal{F}_{1-2} = \frac{1}{\frac{1}{\epsilon_1} + \frac{1}{\epsilon_2} - 1} \qquad (5.3)$$

$$R_{total\ (1-2)} = \frac{1}{A_1}\left(\frac{1}{\epsilon_1} + \frac{1}{\epsilon_2} - 1\right) \qquad (5.4)$$

If $F_{1-2} < 1$ and $F_{2-1} < 1$, equations 5.1 and 5.2 are not exact since all heat exchange does not occur between nodes 1 and 2. However, the equations are good approximations providing the form factors are not greatly different from one.

The above equations were used to evaluate resistance paths between the thermal bag and following components: 1) electronics, 2) thermal plate, and 3) primary structure. Refer to Appendix 2 for representative resistance calculations between the thermal bag and structure.

5.1.2.3 Factors for Multiple-Surface Systems

A general method, outlined in Reference 5, is computerized and used when the previous simplified techniques are not applicable - usually when many surfaces are involved in a network. The computer program (ABSORP) supplied interchange factors for (1) the region bounded by the reflector backsides, sunshield bottom, and side curtains and (2) the network involving the primary structure insulation and radiator plate.

5.1.3 Evaluation of Radiation Resistances

The following information is required to evaluate radiation resistance paths:

1. Thermal emissivity
2. Diffuse reflectance
3. Specular reflectance (if applicable)
4. Solar absorptivity
5. Surface area
6. Form factors.

Items 1 through 4 are physical properties which are specified by design and are summarized in Table 5. Surface area is obtained from design specifications. Form factors are geometric factors based on the "views" between surfaces and were obtained with 1) Reference 6, a general computer program which supplies form factors when surface geometries and spacing are input or 2) Reference 7, which has graphs of form factors for simple geometries. The computer program can handle complex configurations since it employs a finite difference approach and allows for "blockage" or "shadowing" effects.

5.2 Conduction

Heat conduction is assumed to obey the following relation:

TABLE 5

RADIATION PROPERTIES OF CENTRAL STATION SURFACES

Nodes	Surface	α *	ϵ	Surface Finish
101-104 & 109-111	Radiator Top Surface	.2	.90	S13-G White Paint
101-114	Radiator Bottom Surface	NA	.05	Aluminized
115&116	Radiator Insulation	NA	.10	Aluminized Mylar
117&118	Specular Reflector	NA	.05	Specular ρ = .90 Diffuse ρ = .05
27-30	Side Curtain Exterior	.15	.5	SiO Over Aluminized Mylar
35, 36, 119, 121, 122, 124-126	Side Curtain Interior	NA	.1	Aluminized Mylar
31-33	Sunshield Top	.2	.9	S13-G White Paint Undegraded α
34, 120, 123	Sunshield Bottom	NA	.1	Aluminized Mylar
49-52	Primary Structure Exterior Except Bottom Skin	.2	.9	S13-G White Paint
49-53	Primary Structure Interior and Bottom Skin	NA	.1	Aluminized
55	Insulation Bag Exterior	NA	.5	
54	Insulation Bag Interior	NA	1.0	

*Solar absorptivity
NA Not Applicable

$$q_{1-2} = \frac{T_1 - T_2}{R}$$

T = node temperature

R = resistance between nodes

q = heat transfer rate

A resistance can represent more than one physical conduction path or a variety of materials and/or areas in a single path. Contact resistance can also be included in a general resistance term.

5.2.1 Conduction Resistances in Series

A sample resistance circuit is presented below for constant heat flow along a conduction path consisting of three materials and a single contact conductance.

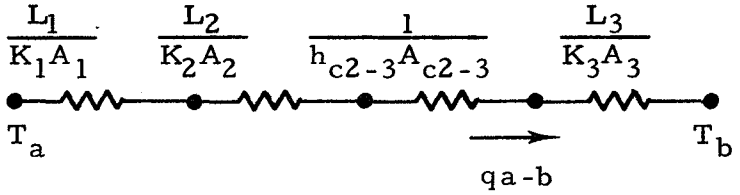

$$R_{Total\ (a-b)} = \frac{L_1}{K_1A_1} + \frac{L_2}{K_2A_2} + \frac{1}{h_{c2-3}A_{c2-3}} + \frac{L_3}{K_3A_3}$$

A = cross-sectional area normal to heat flow

K = material thermal conductivity

L = length over which A and K apply

h_{c2-3} = contact conductance between materials 2 and 3

A_{c2-3} = contact area between materials 2 and 3

T_a and T_b refer to temperatures at ends of path

Subscripts 1, 2, and 3 refer to materials 1, 2, and 3, respectively.

5.2.2 Conduction Resistances in Parallel

If three paths exist in parallel between nodes a and b, the equivalent circuit and total resistance equation are as follows:

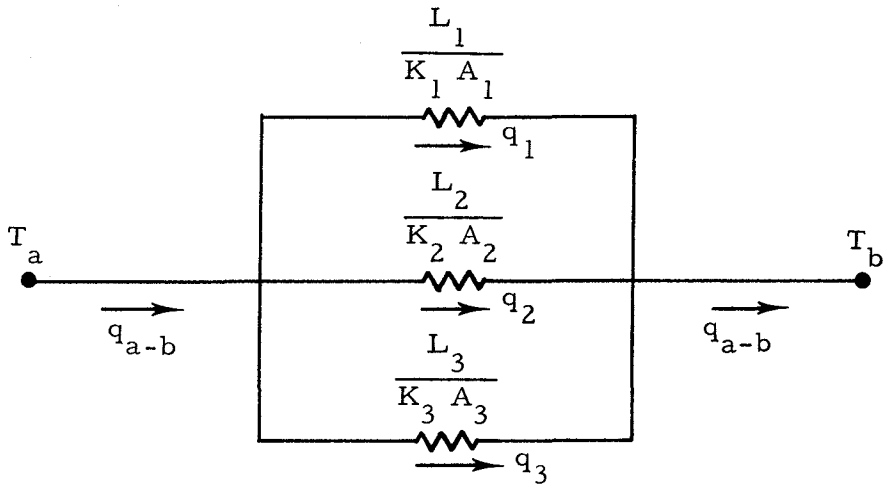

$$\frac{1}{R_{Total\ (a-b)}} = \frac{1}{\frac{L_1}{K_1 A_1}} + \frac{1}{\frac{L_2}{K_2 A_2}} + \frac{1}{\frac{L_3}{K_3 A_3}}$$

The above resistance equations can be extended to any number of materials or paths. Examples of conduction resistance calculations are contained in Appendix 2.

5.2.3 Evaluation of Conduction Resistance Paths

Information required for evaluation of conduction resistances are 1) thermal conductivity or conductance, 2) path area normal to heat flow, 3) path length, and 4) contact conductances.

Item 1 is a physical property. Items 2 and 3 are obtained from design specifications, while item 4 is a function of design and assembly and is very difficult to evaluate. However, rough estimates are satisfactory in most cases; i.e., the analysis was relatively insensitive to contact conductance.

5.3 Heat Inputs

Three sources of heat input to the C/S exist:

1. Generated heat from electronics
2. Generated heat from heat dissipation resistors attached to outside front surface of the primary structure
3. Solar radiation (direct and reflected)

Heating values for the electronics and resistors are listed in Table 6.

Direct solar heat inputs to various areas of the C/S are listed in Table 7 and are calculated as follows:

$$Q = q_s A \alpha$$

Q = total heat absorbed by surface

A = projected surface area normal to impinging solar flux

α = surface solar absorptivity

q_s = normal intensity of impinging solar radiation = 442 Btu/ft^{2}hr

Reflected solar radiation or albedo is handled by assuming that the moon absorbs all incident solar radiation and emits as a black body ($\epsilon = 1.0$). If the solar absorptivity and thermal emissivity of a surface receiving radiation from the moon are different, some error exists. However, the error is not considered significant in view of the large amount of additional effort required for an exact treatment of albedo radiation.

For the Prototype A test, there was no solar heating, and the simulated moon surface had an emissivity less than 1. Consequently, an effective blackbody temperature was computed as specified below and used in the thermal analyzer for correlation with test results:

TABLE 6

HEAT DISSIPATION OF CENTRAL STATION
ELECTRONIC COMPONENTS AND RESISTORS

Node	Description	Computer Input Table	Heat Dissiptation (Watts) Day	Night)
37	PCU	4	14.5	15.0
38	PDU	5	1.8	1.8
39	Analog Multiplex Converter	6	1.4	1.4
40	Passive Seismic	7	4.4	4.4
41	Comm. Receiver	8	.7	.7
42	Data Processor	9	.5	.5
43	Comm. Decoder	10	1.3	1.3
44	Timer	-	-	-
45	Diplexer Switch	12	-	-
46	Diplexer Filter	-	-	-
47	Transmitter A	14	-	-
48	Transmitter B	14	6.9*	5.9*
49	Resistors	15	12.9	11.0
	Dust Detector	12	.2	.2
	Total Electronics	-	31.7	31.2

*Thermal Heat Dissipation

TABLE 7

LUNAR NOON SOLAR HEAT INPUTS

Node	Description	Computer Input Table	Heat Input Btu/hr
31	Sunshield	3	344.0
32	Sunshield Awning	2	65.4
33	Sunshield Awning	2	84.3

$$\sigma \epsilon_{SM} T_{SM}^4 = \sigma T_{eff}^4$$

ϵ_{SM} = emissivity of simulated test moon surface

T_{SM} = simulated moon temperature

T_{eff} = moon effective blackbody temperature

5.4 Heat Leak Through External Cables

External cables are divided into two groups described below:

5.4.1 Cables Between Terminal Boards and Primary Structure

These cables are approximately 8 inches in length, with about 5 inches completely outside the C/S and exposed to direct environmental influence from the moon and space. For the "noon" condition, this environmental influence can be of some significance though very difficult to evaluate without incorporating additional nodes and resistance paths into the program. Such effort was not warranted because of the anticipated small increase in accuracy. A modified approach was taken where the cable lengths were reduced to the three inches not exposed to moon and and space. Since the primary structure is hotter than internal nodes during "noon", the cable heat flow into the C/S was maximized and therefore conservative. This reduction in length allowed a higher heat flow than would the longer length with the environmental influences included. Analysis results showed the cable heat leak for the noon condition to be very small in relation to the other heat flows, so the approximation is satisfactory.

However, for the "night" condition cable heat leak is more significant, and the above simplification was considered too conservative. It happens that the radiant heat exchange rate between the cabling, moon and space is insignificant at night compared to the simple conduction along the wires. That is, the effective heat transfer coefficient between the cables and night environment is negligible - about 0.01 Btu/ft^{2}hr$^\circ$F as compared to the 0.5 value for lunar noon. Consequently, the entire 8 inches was used in the conduction resistance paths for the cables in a lunar night environment.

To minimize heat leak, most of these cables were made of Manganin, a material with a thermal conductivity approximately 1/15 the value for copper.

5.4.2 Cables Between Primary Structure and Deployed Experiments

A method for analyzing these cables, which considers moon and space environmental effects, is presented in Appendix 2.

6.0 DISCUSSION

6.1 Isolation of Central Station Components

From thermal considerations, the radiator plate is the most critical section of the Central Station since it dissipates nearly all heat from the electronics. The plate radiates heat to space both directly and indirectly via the reflector, side curtains, and sunshield awning. The main purpose of the sunshield, side curtains, thermal bag, and radiator plate insulation masks is to "isolate" the electronics from external direct heating and cooling effects of the lunar surface, sun, and space. Manganin wiring was used between cable connectors on the primary structure and the terminal boards inside the C/S to minimize heat leak.

Several regions of the C/S are essentially isolated from each other from a heat transfer standpoint because of large resistance heat flow paths. Combinations of C/S components in this category are listed below:

1. Primary structure and thermal plate
2. Sunshield and thermal plate
3. Side curtains and primary structure
4. Side curtains and sunshield.
5. Primary structure and sunshield.

A large change in primary structure temperature, for instance, produces little effect on the thermal plate.

6.2 Tradeoffs

As stated in Section 3, accurate values of heat inputs of aluminized mylar conductance are needed for meaningful analysis predictions. Consequently, tradeoffs were conducted to establish the sensitivity of C/S performance to the following parameters:

1. Electronics Heat Dissipation
2. Resistor Heat Dissipation at Primary Structure
3. Thermal Conductance of Insulation Masks
4. Thermal Conductance of Side Curtains

Figures 20 to 24 show the effect of the parameters on primary structure and thermal plate average temperatures. The structure is relatively unaffected by electronic heat dissipation or insulation conductance, while resistor heat has an insignificant effect on the radiator plate. This is due to the high resistance of the plate support posts and low radiation from the structure to the plate. Where parameters have little effect on each other, no curves are presented.

6.3 Simulated Lunar Surface for Prototype "A" Test

The Prototype "A" test lunar surface, simulated by a 14' x 14' platform, did not attain the desired uniform 250°F temperature for the lunar noon condition but exhibited the temperature distribution shown in Figure 25. This uneven distribution was considered in the evaluation of heat flow between the moon and primary structure but was otherwise unimportant in affecting C/S temperatures. For analysis purposes the surface was divided into isothermal nodes, as depicted in Figure 17, and resistance paths determined between each moon and applicable structure node. Section 8 of Appendix 2 contains details on the incorporation of these nodes into the analysis. Only a single moon node was used in resistance paths to other C/S components. For lunar night the desired uniform -300°F simulator temperature was realized, thus precluding any need for multiple moon nodes.

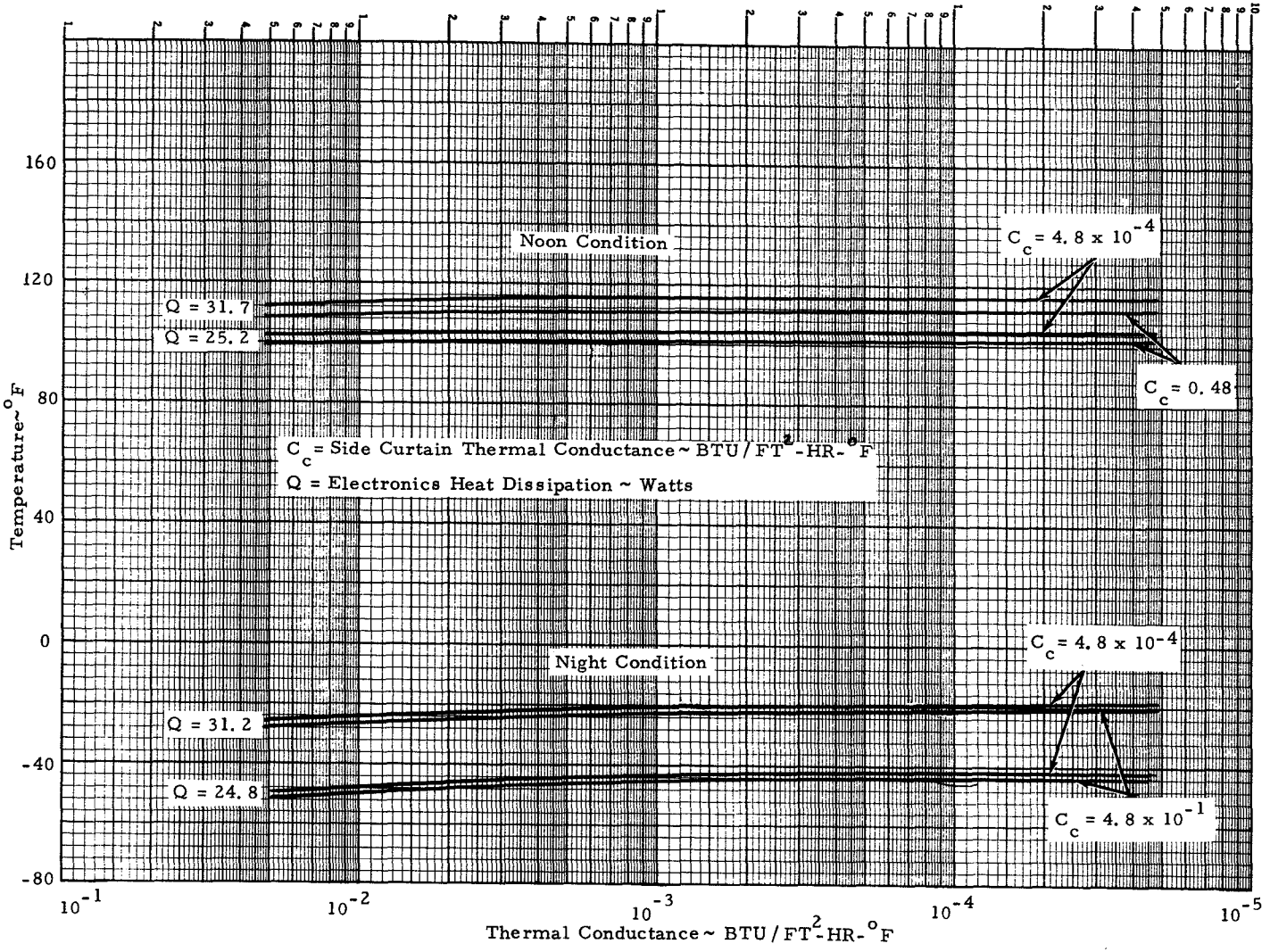

Figure 20 Radiator Baseplate Average Temperature vs Radiator Insulation Mask Thermal Conductance

Figure 21 Radiator Baseplate Average Temperature vs Side Curtain Thermal Conductance

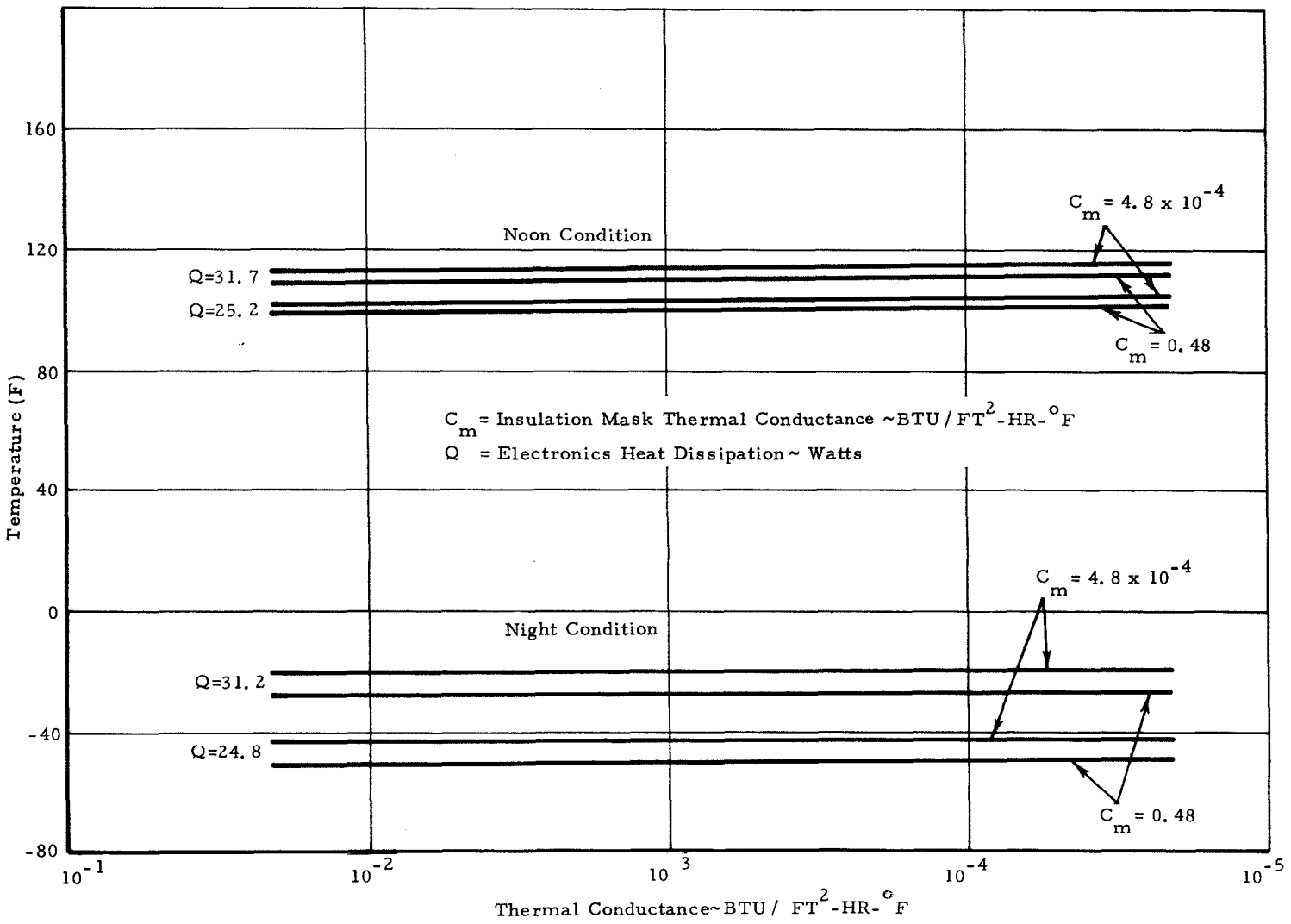

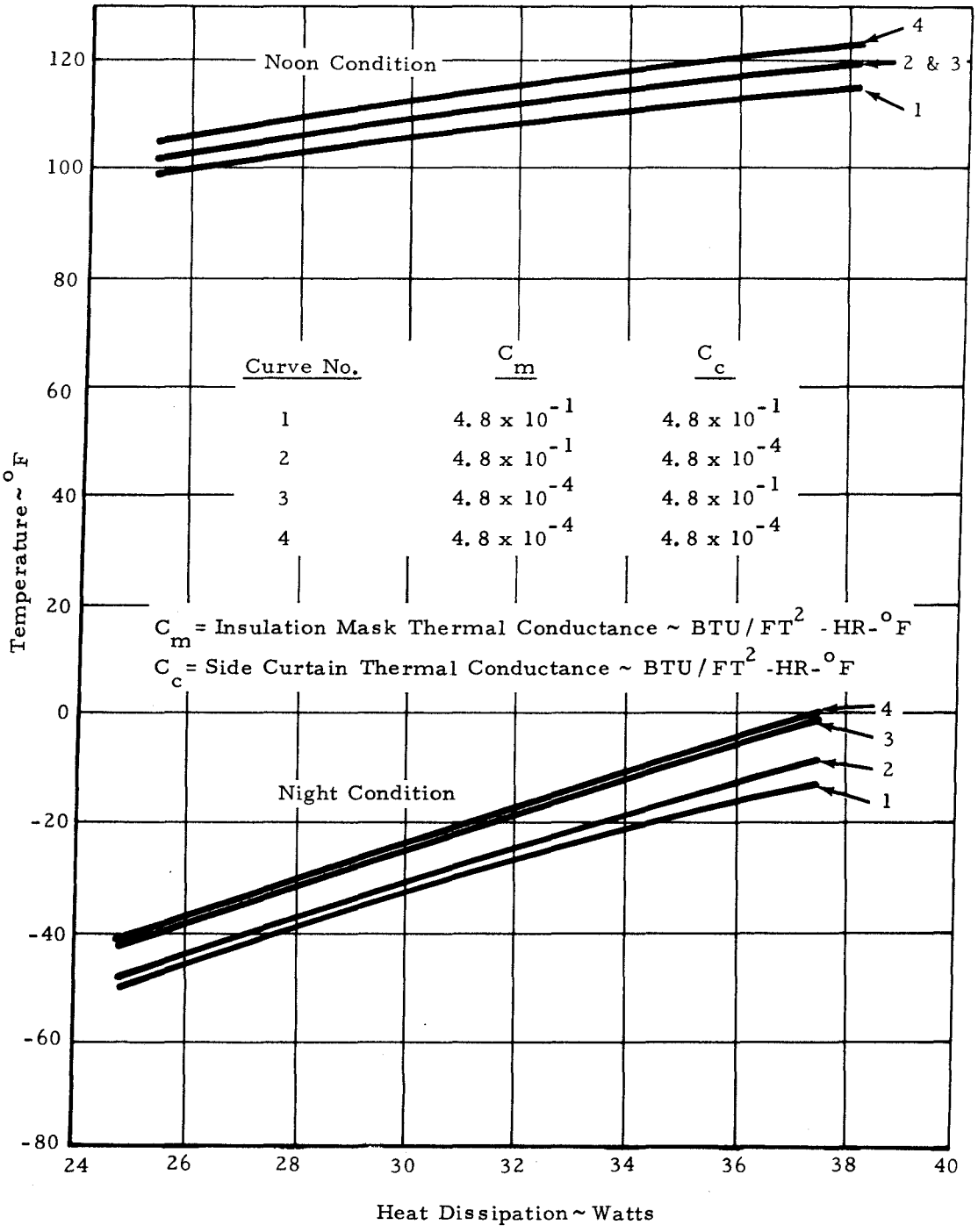

Figure 22 Radiator Baseplate Average Temperature vs Electronics Thermal Dissipation

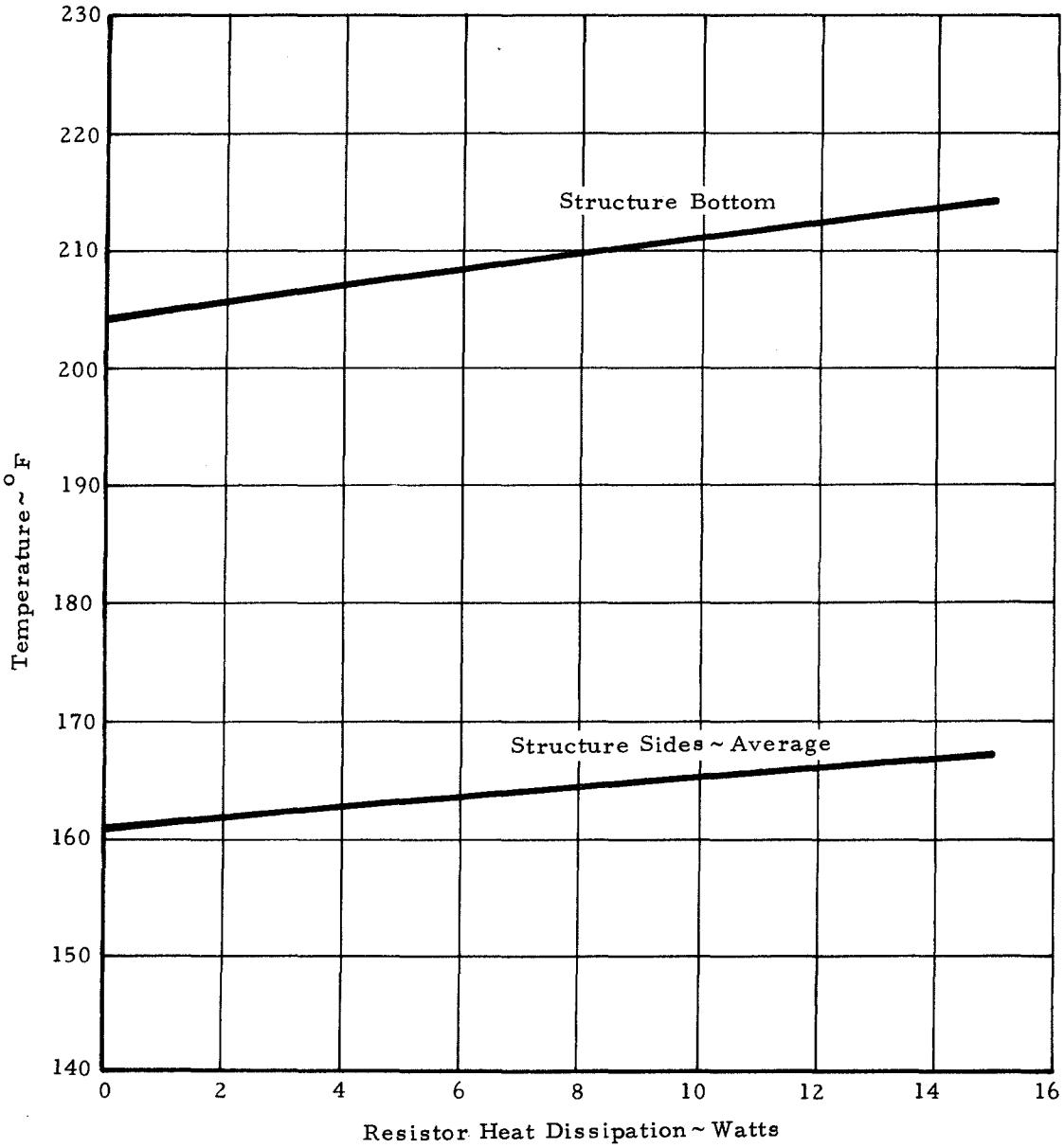

Figure 23 Primary Structure Temperature vs Resistor Heat Dissipation for Lunar Noon

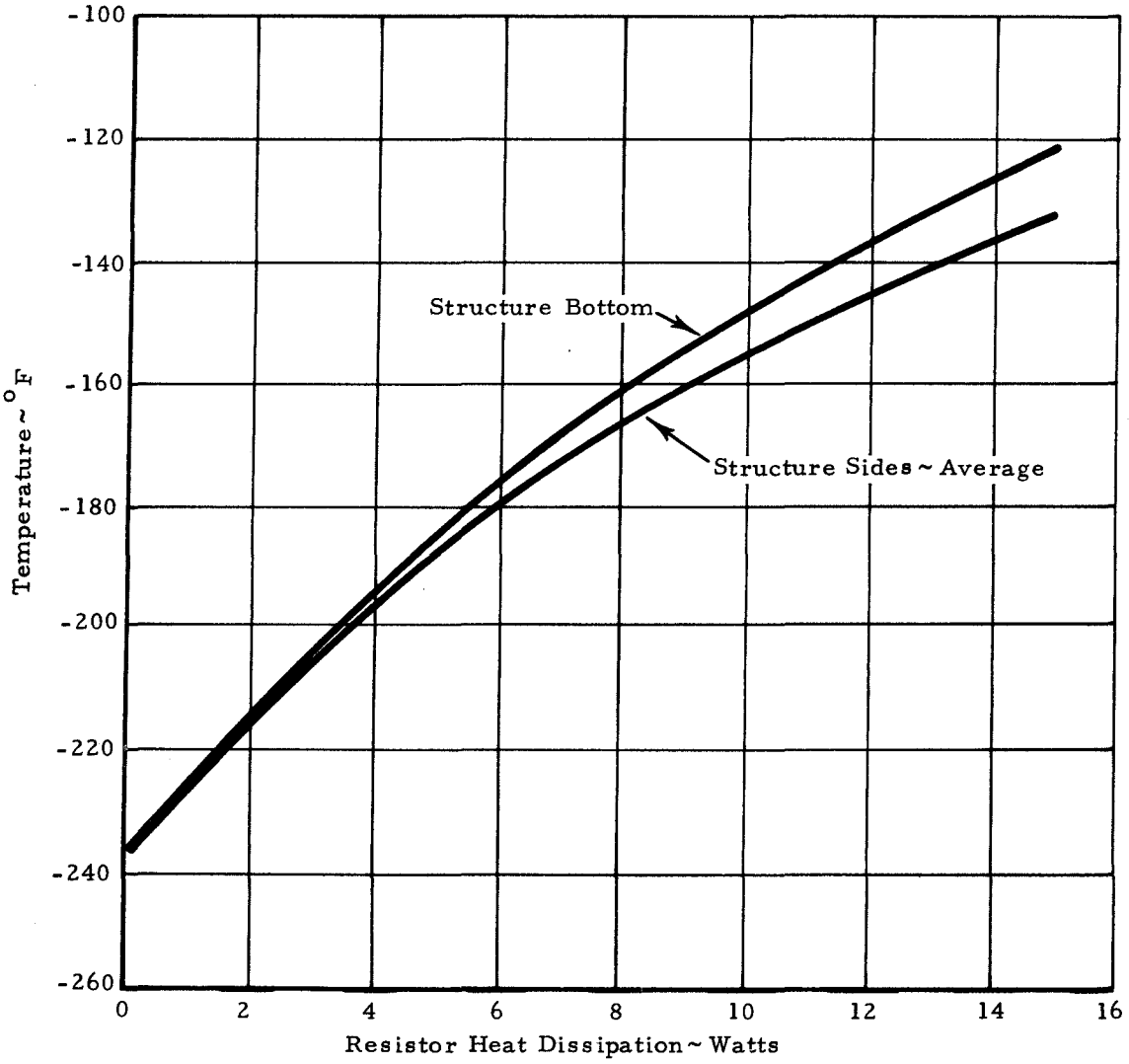

Figure 24 Primary Structure Temperature vs Resistor Heat Dissipation for Lunar Night

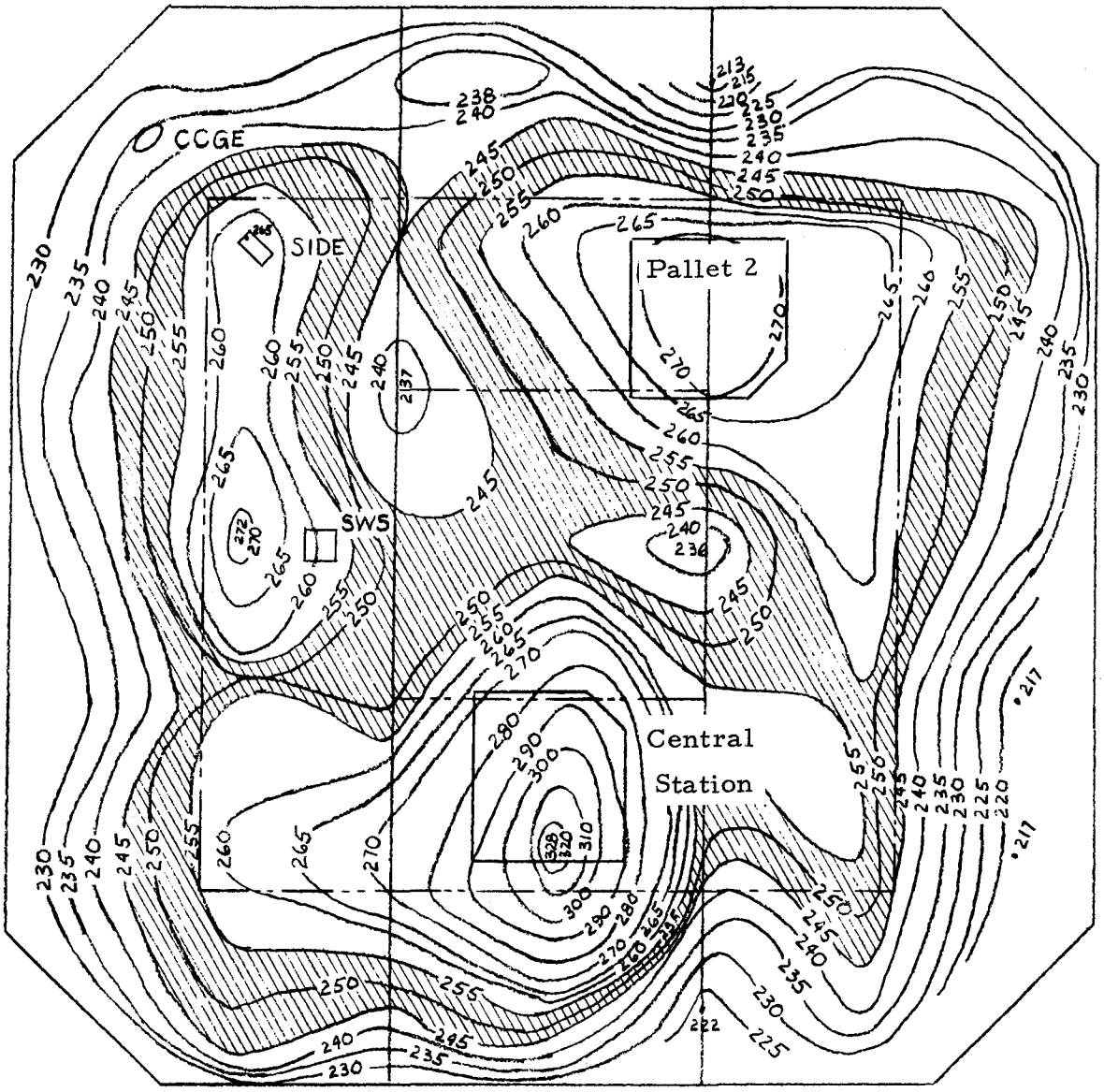

All Temperatures Are In °F

255
250
245
Area Where Temperatures Are Within Tolerance Specified By 9712-713

Figure 25 Prototype "A" Test Lunar Surface Simulator Temperature Distribution for Lunar Noon

6.4 Simulated Space for Prototype "A" Test

The vacuum chamber cryowalls, which simulated space during testing, exhibited the uneven temperature distribution illustrated in Figure 26. Space was divided into three isothermal nodes, as specified in Figure 18, in the evaluation of resistance paths for the thermal model. Further details on the use of space nodes in the analysis are contained in Sections 8, 9, and 10 of Appendix 2.

6.5 Simulated "Real" Moon

For analysis predictions of C/S performance in an actual lunar environemnt, we used a 500 ft. x 500 ft. "node" with an emissivity of 1.0 and at uniform temperatures of 250°F for noon and -300°F for night to simulate the "real" lunar surface. In addition, the following modification was employed. When the C/S is deployed, the section of lunar surface directly under the primary structure will not be at the temperature of the remaining lunar surface since it exchanges heat with the primary structure bottom while being blocked-off from solar heating and from heat exchange with space. This lunar section is therefore strongly influenced by subsurface strata and by the surrounding lunar surface.

Consequently, the moon in the vicinity of the C/S was divided horizontally and vertically into a series of nodes to account for this effect, as depicted in Figure 27. "Infinite" nodes, which are unaffected by the C/S and which are at fixed temperatures, are connected to "active" nodes which are located directly under the C/S. Active nodes are allowed to achieve equilibrium temperatures along with the C/S nodes in the thermal model. Construction of the "subsurface" model is described in detail in Reference 9.

6.6 Radiosity Nodes

Temperatures of radiosity nodes (nodes 1-26, 127, 129, and 131) have no significance and are therefore not presented in this report.

6.7 Central Station Heat Balance

Heat flow at the radiator baseplate and primary structure is specified in Figure 28 for the analysis temperatures in Table 1. For

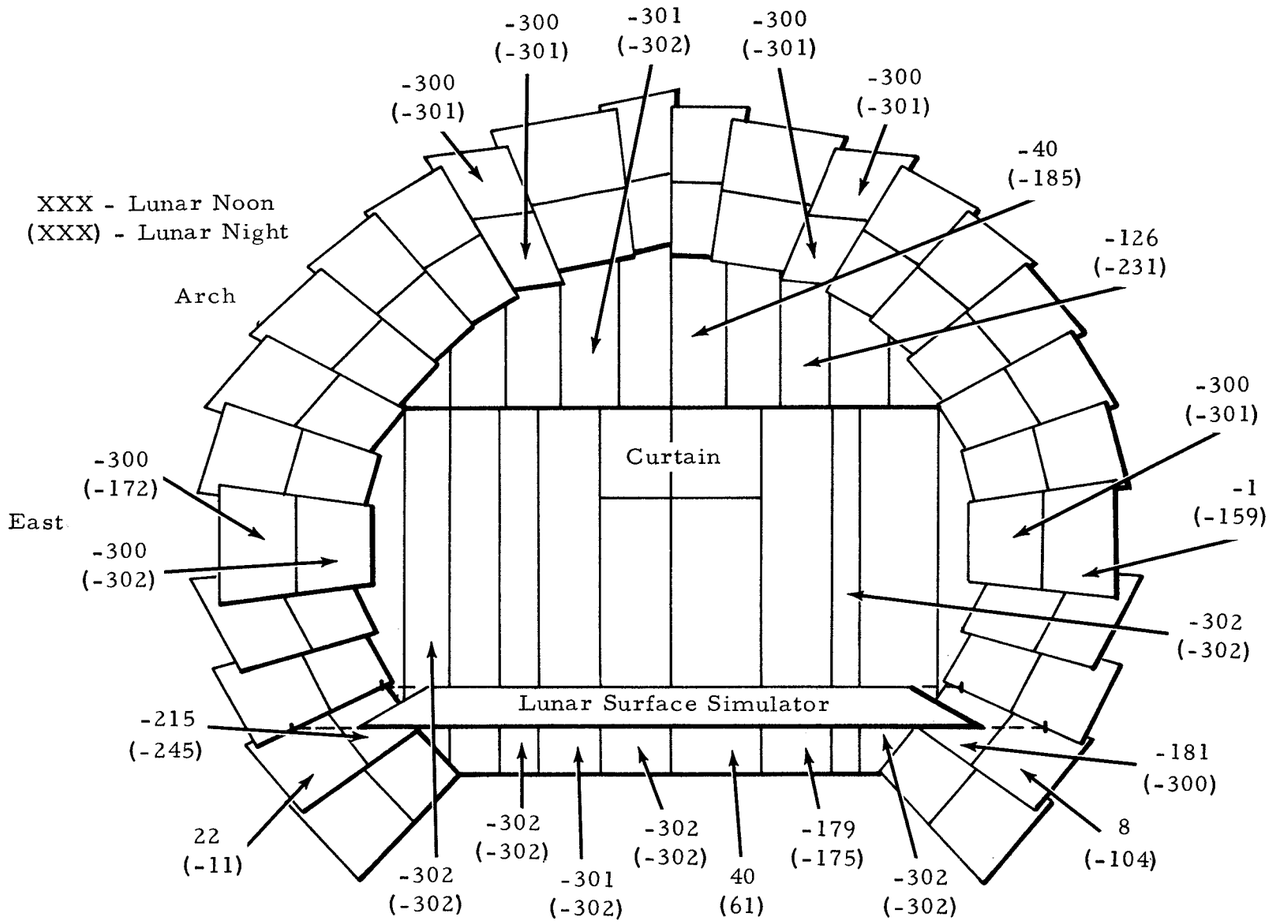

View of Cryowall Looking South

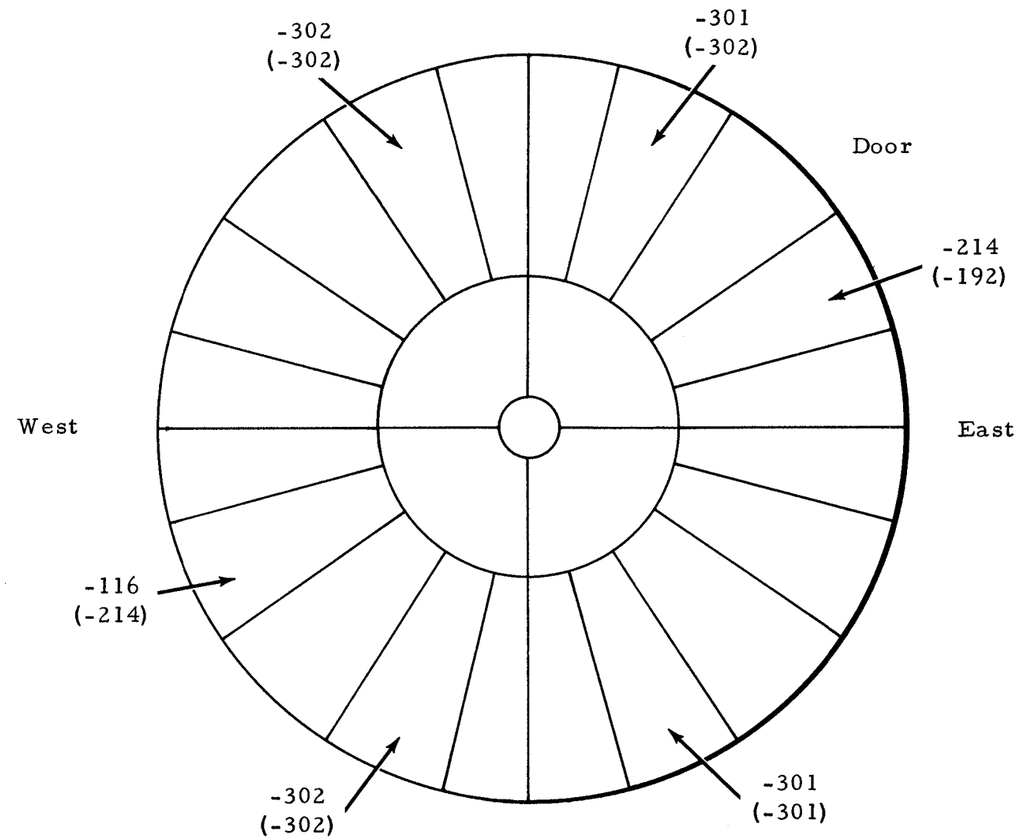

View of Cryowall Looking North

Figure 26 Prototype "A" Test Cryowall (Space)
Temperature Distribution ~ °F

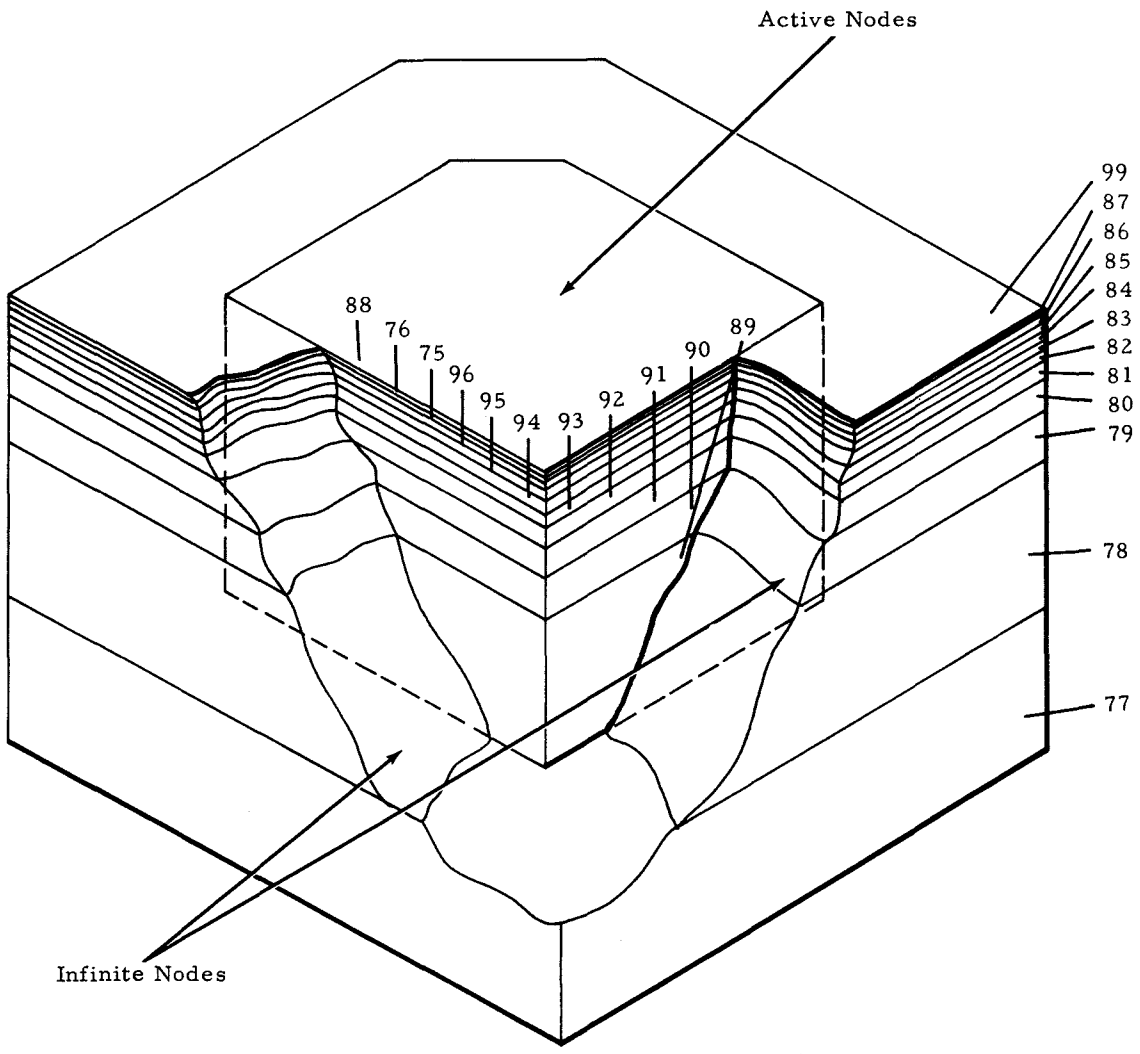

Figure 27 Lunar Subsurface Computer Model for Real Moon Analysis

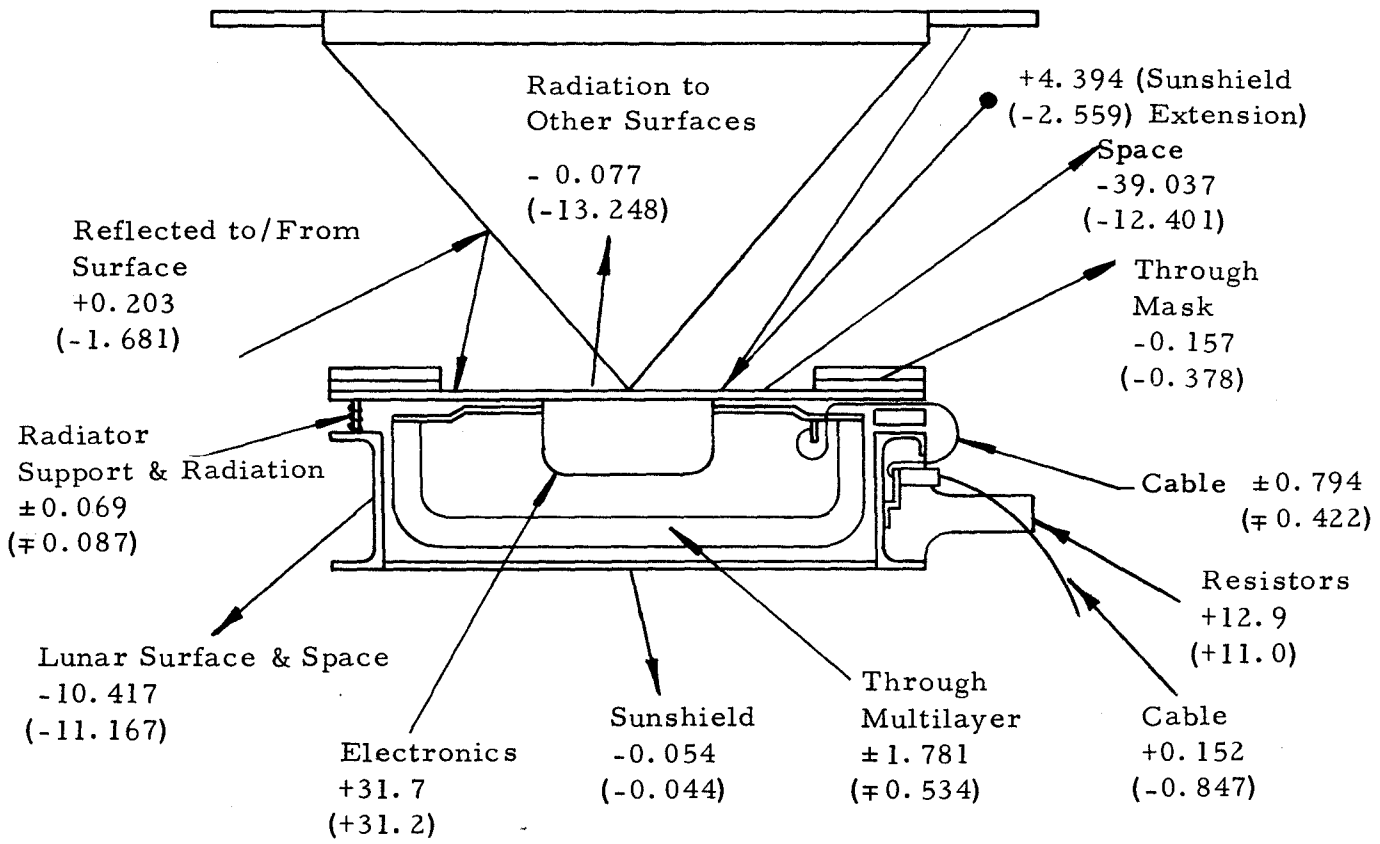

\+ Into Radiator or Structure
\- From Radiator or Structure
± Into Radiator, From Structure
∓ From Radiator, Into Structure

xxx Noon
(xxx) Night

Note: All values are in watts

Figure 28 Prototype "A" Central Station Heat Balance for Lunar Noon and Lunar Night

equilibrium conditions, the net heat flow at each surface must be zero. If the entire radiator plate is treated as a single surface, the "noon" heat flow or energy balance is:

$$\Sigma Q = 31.700 + .069 + .203 + 4.394 + .794 + 1.781 - .077 - 39.037 - .157 \approx 0$$

where ΣQ = summation of all heat to and from the surface.

Similarly, if the entire primary structure is handled as one surface,

$$\Sigma Q = 12.900 + 0.152 - 1.781 - 0.054 - 10.417 - 0.069 - 0.794 \approx 0$$

6.8 Prototype "A" Test Results

Figures 29 through 38 show DAS temperature measurements versus time for the sunshield, radiator baseplate, radiator baseplate support, primary structure, lunar surface simulator, and test chamber cryowalls. For these figures, the following table summarizes the significant test events.

Event	Time (hrs)
Ambient IST	20 to 40
Lunar Morning	58 to 65
Lunar Noon	80 to 104
Lunar Night	120 to 146
C/Slow. Heater On	132
Return to Ambient	152

Table 8 present Telemetry data for lunar noon and lunar night.

Figure 29

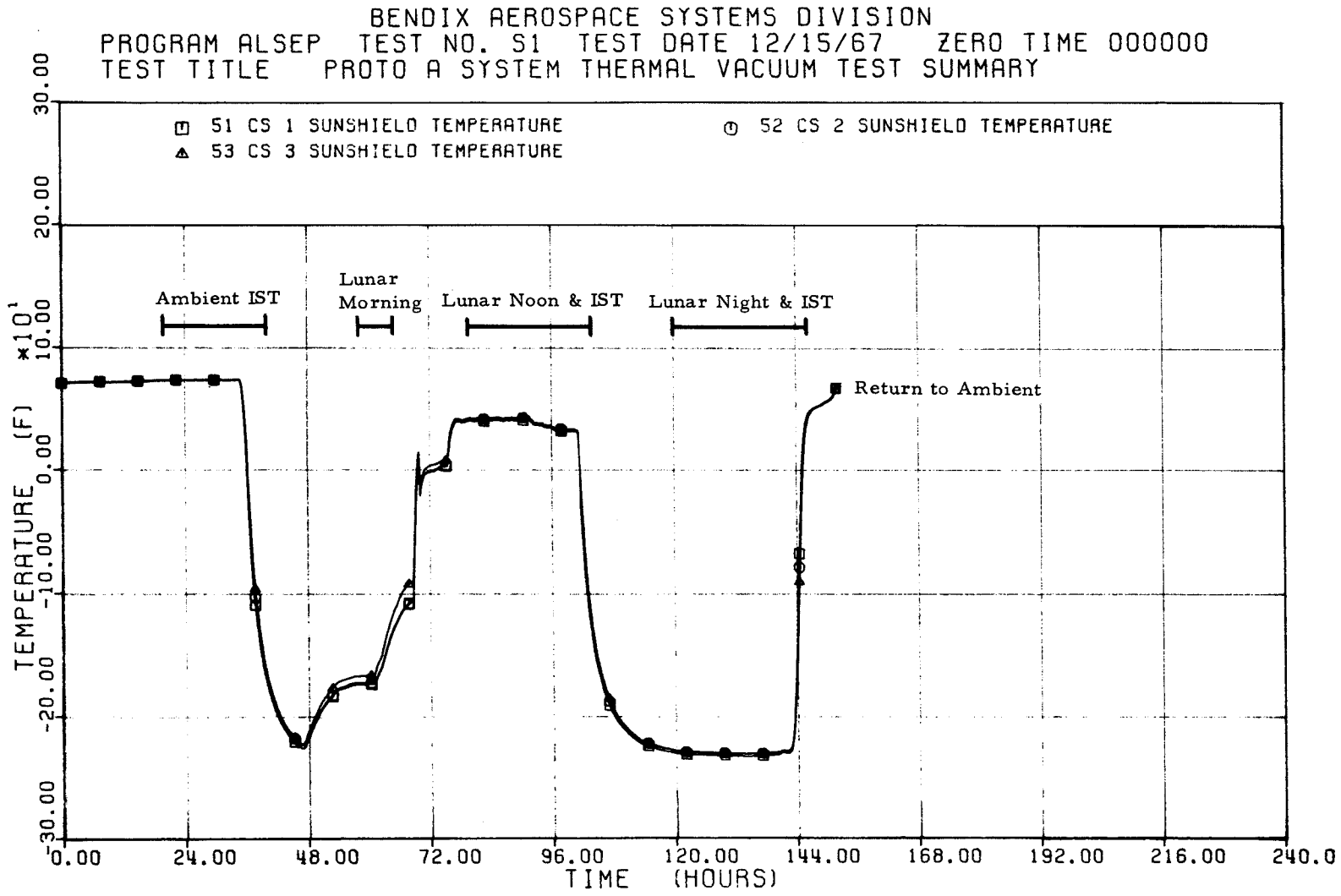
BENDIX AEROSPACE SYSTEMS DIVISION
PROGRAM ALSEP TEST NO. S1 TEST DATE 12/15/67 ZERO TIME 000000
TEST TITLE PROTO A SYSTEM THERMAL VACUUM TEST SUMMARY
51 CS 1 SUNSHIELD TEMPERATURE
52 CS 2 SUNSHIELD TEMPERATURE
53 CS 3 SUNSHIELD TEMPERATURE
Ambient IST
Lunar Morning
Lunar Noon & IST
Lunar Night & IST
Return to Ambient
TEMPERATURE (F) *10¹
30.00
20.00
10.00
0.00
-10.00
-20.00
-30.00
0.00
24.00
48.00
72.00
96.00
120.00
144.00
168.00
192.00
216.00
240.0
TIME (HOURS)

Figure 30

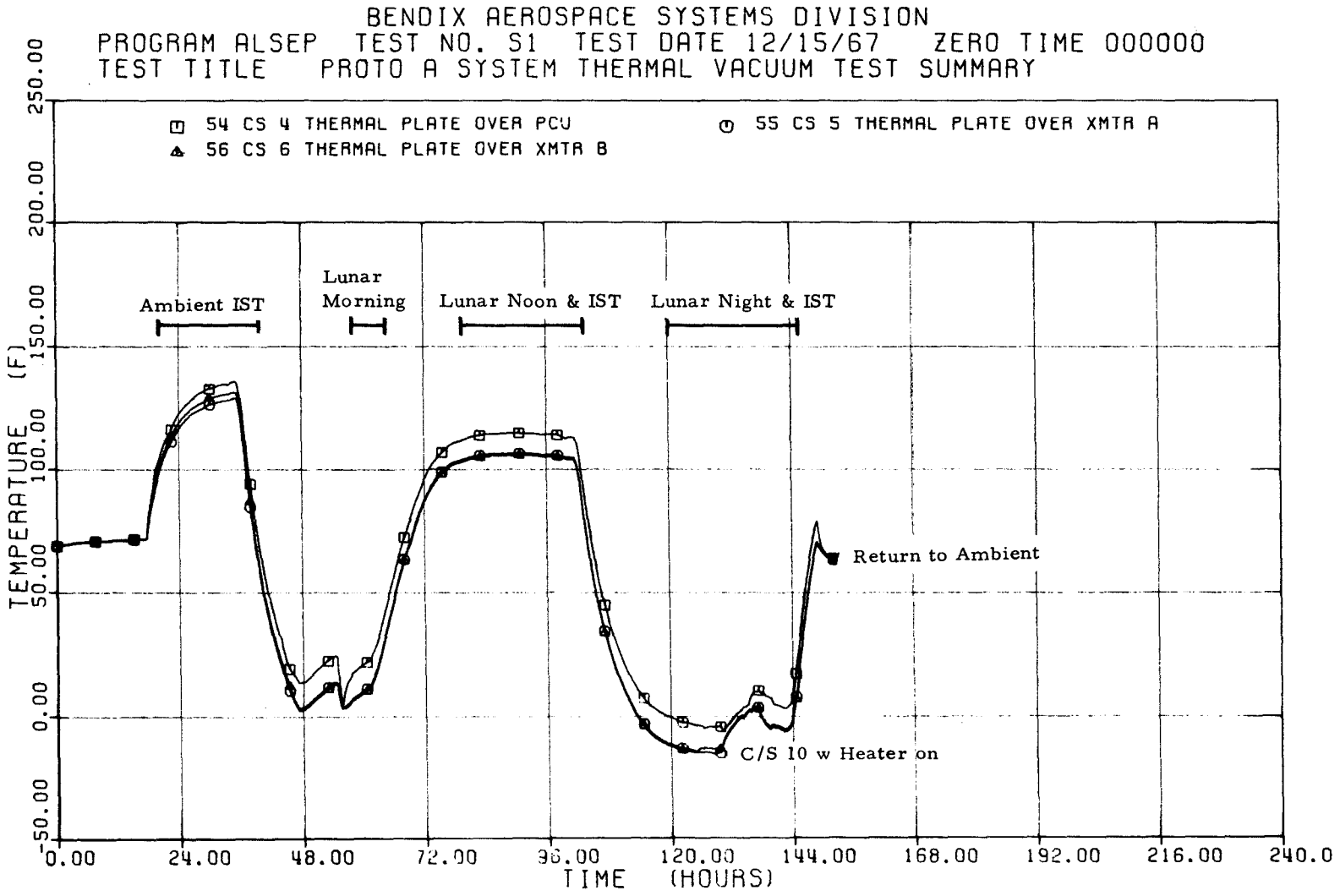
BENDIX AEROSPACE SYSTEMS DIVISION
PROGRAM ALSEP TEST NO. S1 TEST DATE 12/15/67 ZERO TIME 000000
TEST TITLE PROTO A SYSTEM THERMAL VACUUM TEST SUMMARY
54 CS 4 THERMAL PLATE OVER PCU
55 CS 5 THERMAL PLATE OVER XMTR A
56 CS 6 THERMAL PLATE OVER XMTR B
Ambient IST
Lunar Morning
Lunar Noon & IST
Lunar Night & IST
Return to Ambient
C/S 10 w Heater on
TEMPERATURE (F)
250.00
200.00
150.00
100.00
50.00
0.00
-50.00
0.00
24.00
48.00
72.00
96.00
120.00
144.00
168.00
192.00
216.00
240.0
TIME (HOURS)

Figure 31

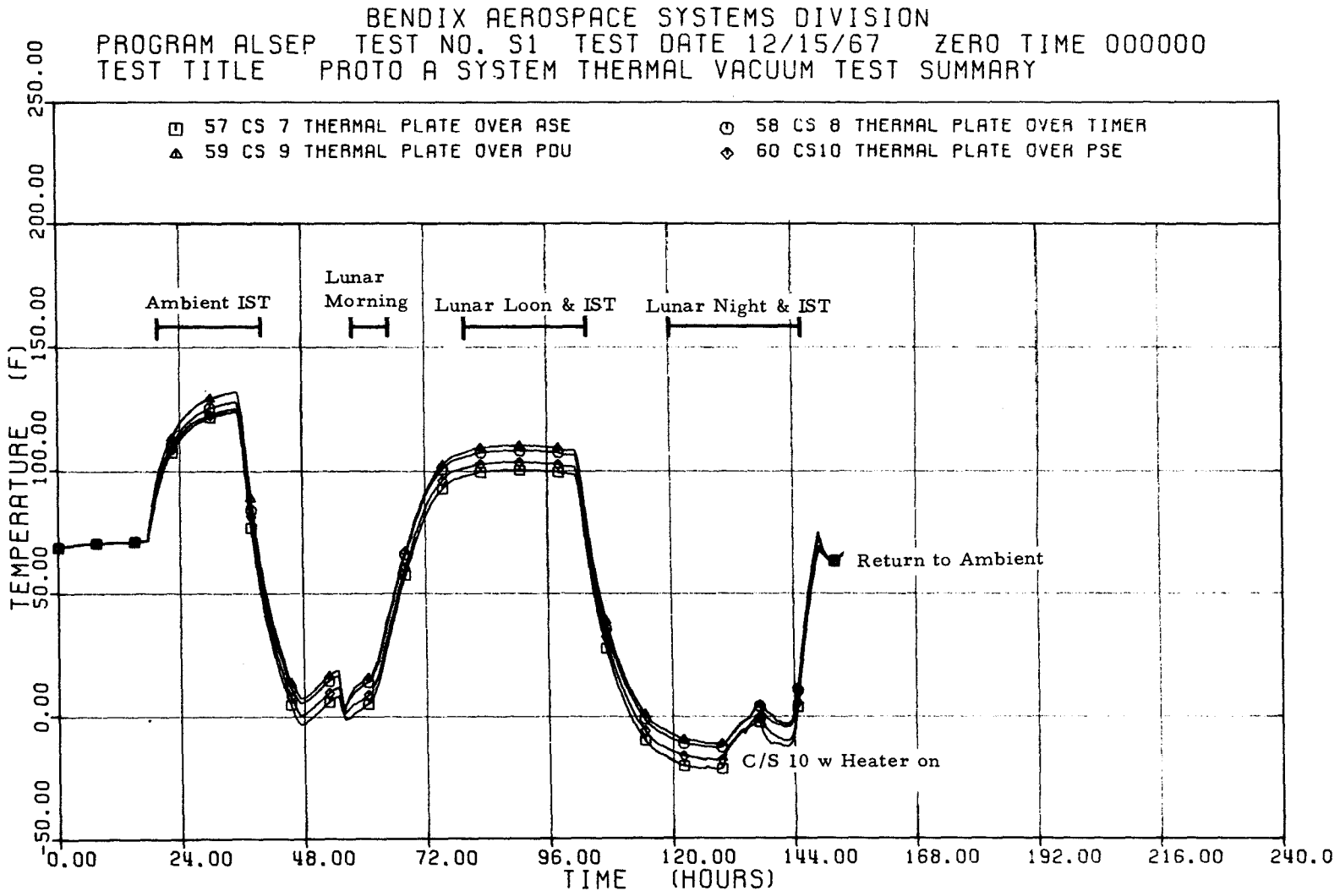
BENDIX AEROSPACE SYSTEMS DIVISION
PROGRAM ALSEP TEST NO. S1 TEST DATE 12/15/67 ZERO TIME 000000
TEST TITLE PROTO A SYSTEM THERMAL VACUUM TEST SUMMARY
57 CS 7 THERMAL PLATE OVER ASE
58 CS 8 THERMAL PLATE OVER TIMER
59 CS 9 THERMAL PLATE OVER PDU
60 CS10 THERMAL PLATE OVER PSE
Ambient IST
Lunar Morning
Lunar Loon & IST
Lunar Night & IST
Return to Ambient
C/S 10 w Heater on
TEMPERATURE (F)
250.00
200.00
150.00
100.00
50.00
0.00
-50.00
0.00
24.00
48.00
72.00
96.00
120.00
144.00
168.00
192.00
216.00
240.0
TIME (HOURS)

Figure 32

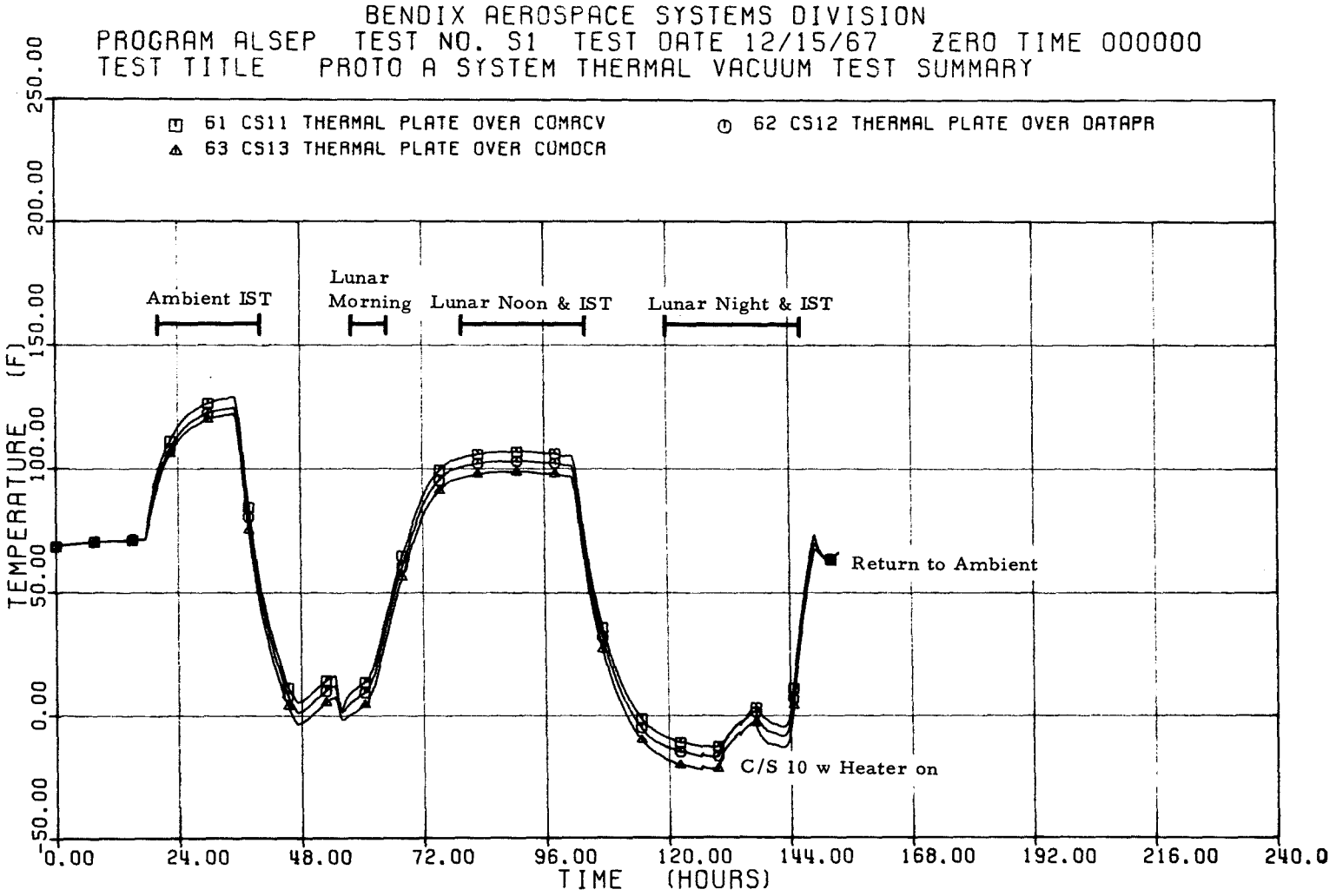
BENDIX AEROSPACE SYSTEMS DIVISION
PROGRAM ALSEP TEST NO. S1 TEST DATE 12/15/67 ZERO TIME 000000
TEST TITLE PROTO A SYSTEM THERMAL VACUUM TEST SUMMARY
61 CS11 THERMAL PLATE OVER COMRCV
62 CS12 THERMAL PLATE OVER DATAPR
63 CS13 THERMAL PLATE OVER COMOCR
Ambient IST
Lunar Morning
Lunar Noon & IST
Lunar Night & IST
Return to Ambient
C/S 10 w Heater on
TEMPERATURE (F)
250.00
200.00
150.00
100.00
50.00
0.00
-50.00
0.00
24.00
48.00
72.00
96.00
120.00
144.00
168.00
192.00
216.00
240.0
TIME (HOURS)

Figure 33

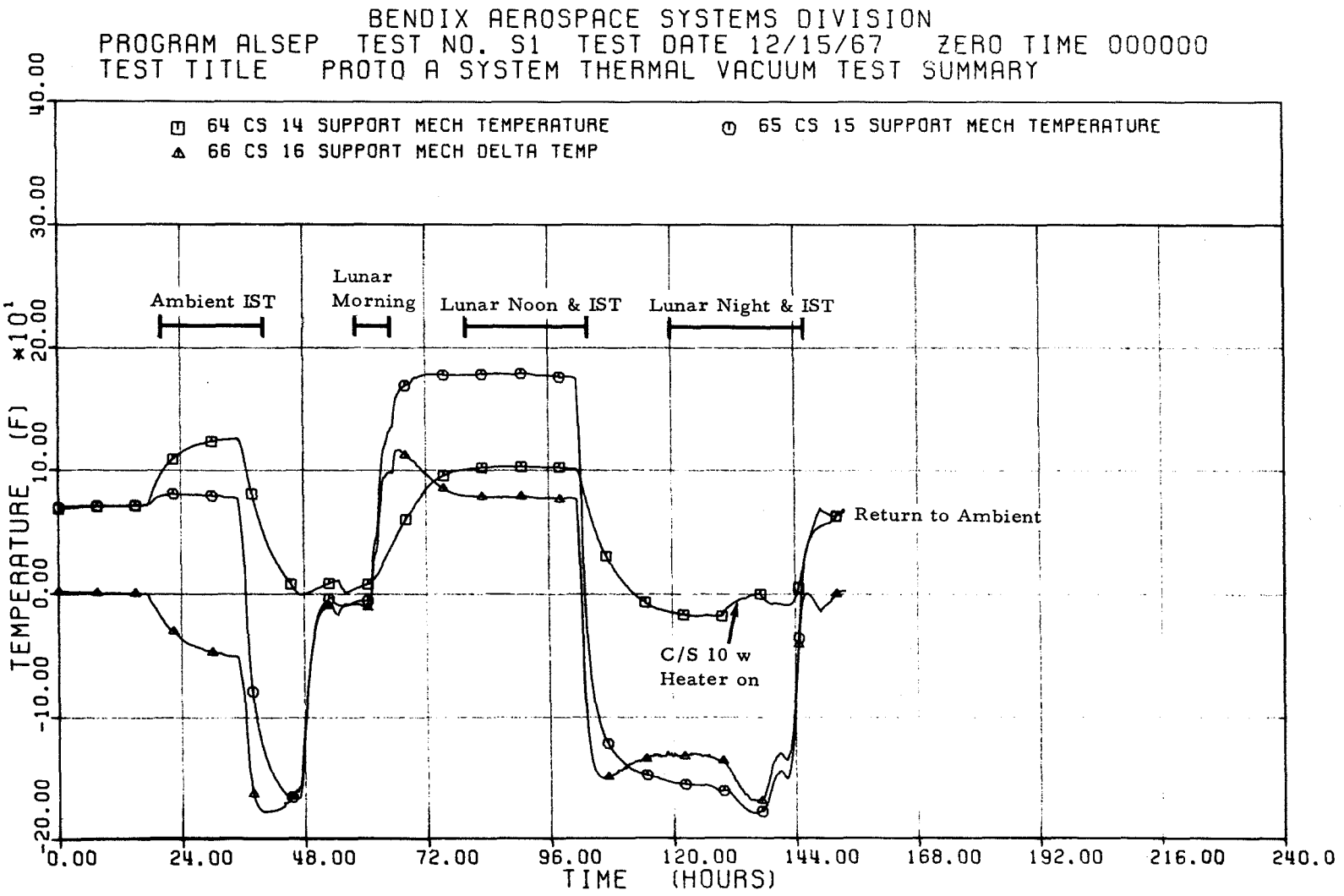
BENDIX AEROSPACE SYSTEMS DIVISION
PROGRAM ALSEP TEST NO. S1 TEST DATE 12/15/67 ZERO TIME 000000
TEST TITLE PROTO A SYSTEM THERMAL VACUUM TEST SUMMARY
64 CS 14 SUPPORT MECH TEMPERATURE
65 CS 15 SUPPORT MECH TEMPERATURE
66 CS 16 SUPPORT MECH DELTA TEMP
Ambient IST
Lunar Morning
Lunar Noon & IST
Lunar Night & IST
Return to Ambient
C/S 10 w Heater on
TEMPERATURE (F) *10¹
40.00
30.00
20.00
10.00
0.00
-10.00
-20.00
0.00
24.00
48.00
72.00
96.00
120.00
144.00
168.00
192.00
216.00
240.0
TIME (HOURS)

Figure 34

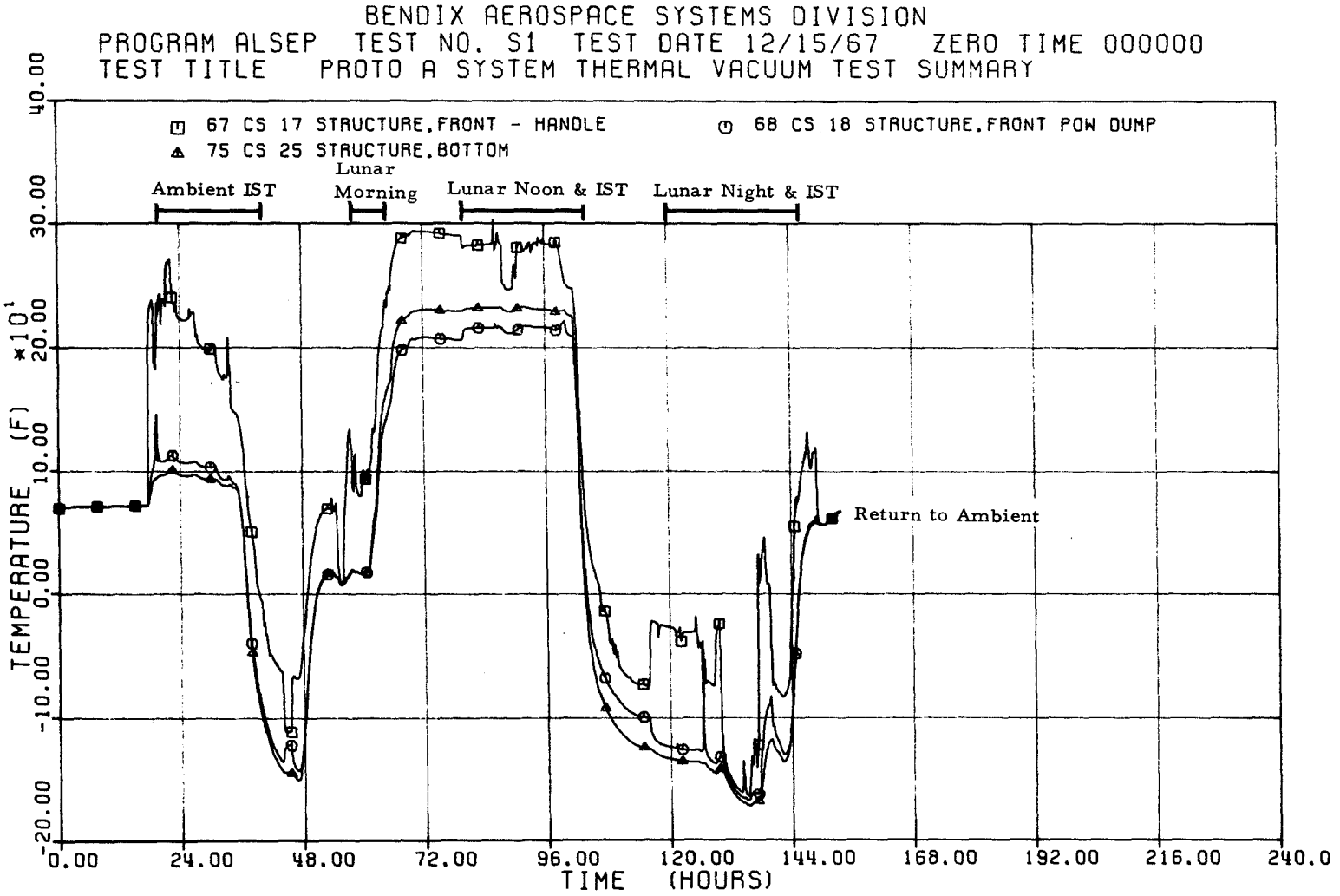
BENDIX AEROSPACE SYSTEMS DIVISION
PROGRAM ALSEP TEST NO. S1 TEST DATE 12/15/67 ZERO TIME 000000
TEST TITLE PROTO A SYSTEM THERMAL VACUUM TEST SUMMARY
67 CS 17 STRUCTURE.FRONT - HANDLE
68 CS 18 STRUCTURE.FRONT POW DUMP
75 CS 25 STRUCTURE.BOTTOM
Ambient IST
Lunar Morning
Lunar Noon & IST
Lunar Night & IST
Return to Ambient
TEMPERATURE (F) *10¹
40.00
30.00
20.00
10.00
0.00
-10.00
-20.00
0.00
24.00
48.00
72.00
96.00
120.00
144.00
168.00
192.00
216.00
240.0
TIME (HOURS)

Figure 35

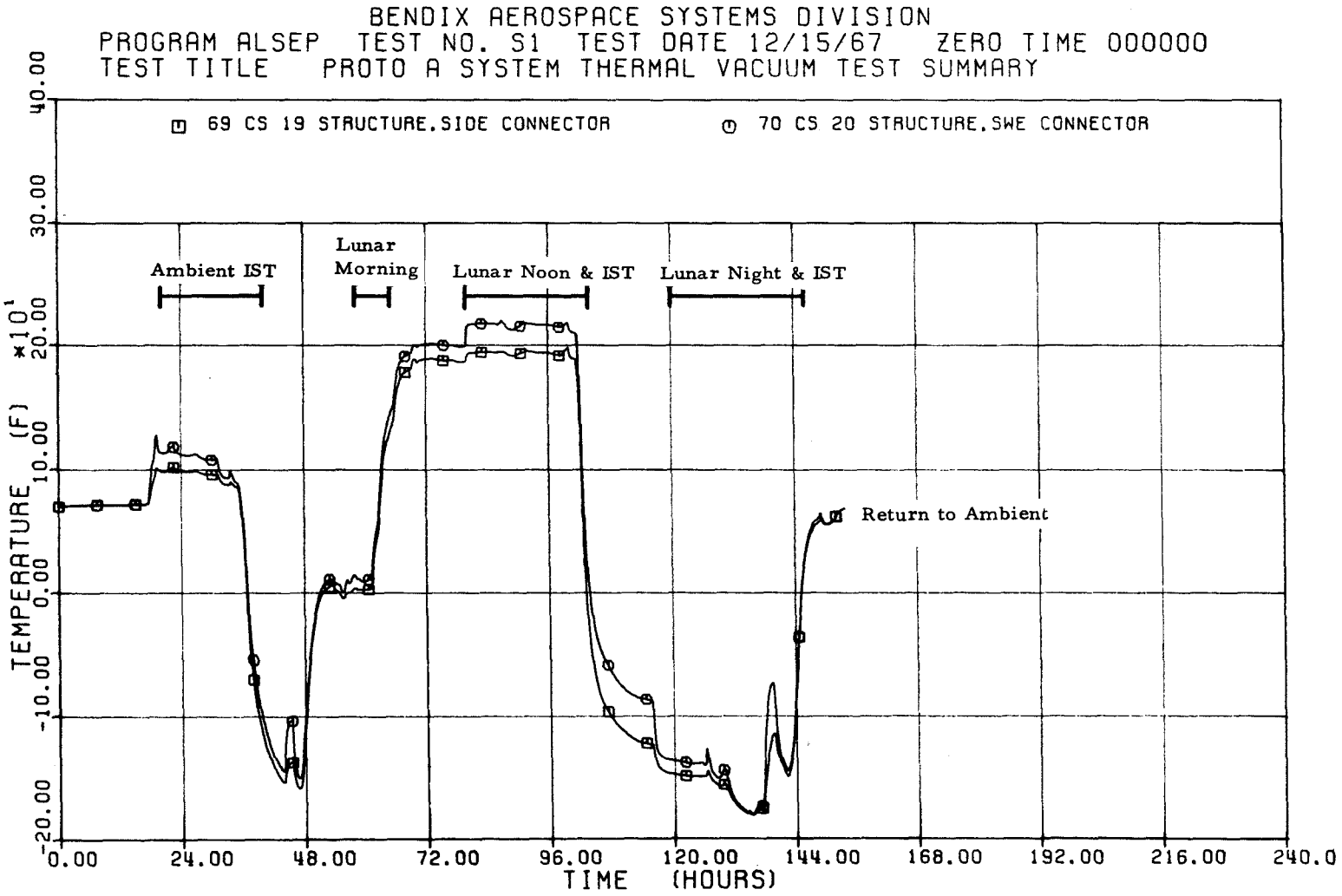
BENDIX AEROSPACE SYSTEMS DIVISION
PROGRAM ALSEP TEST NO. S1 TEST DATE 12/15/67 ZERO TIME 000000
TEST TITLE PROTO A SYSTEM THERMAL VACUUM TEST SUMMARY
69 CS 19 STRUCTURE.SIDE CONNECTOR
70 CS 20 STRUCTURE.SWE CONNECTOR
Ambient IST
Lunar Morning
Lunar Noon & IST
Lunar Night & IST
Return to Ambient
TEMPERATURE (F) *10¹
40.00
30.00
20.00
10.00
0.00
-10.00
-20.00
0.00
24.00
48.00
72.00
96.00
120.00
144.00
168.00
192.00
216.00
240.0
TIME (HOURS)

Figure 36

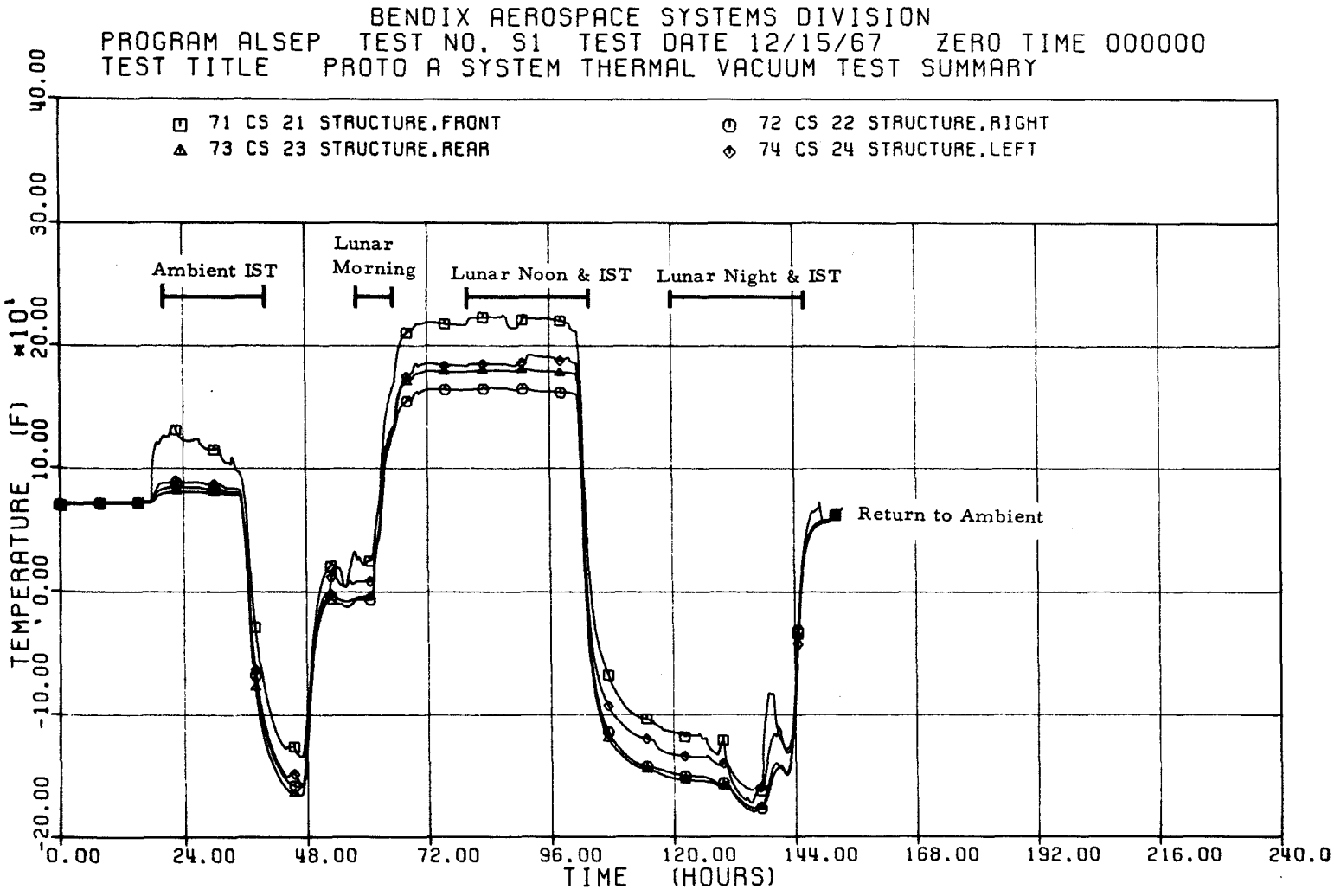
BENDIX AEROSPACE SYSTEMS DIVISION
PROGRAM ALSEP TEST NO. S1 TEST DATE 12/15/67 ZERO TIME 000000
TEST TITLE PROTO A SYSTEM THERMAL VACUUM TEST SUMMARY
71 CS 21 STRUCTURE.FRONT
72 CS 22 STRUCTURE.RIGHT
73 CS 23 STRUCTURE.REAR
74 CS 24 STRUCTURE.LEFT
Ambient IST
Lunar Morning
Lunar Noon & IST
Lunar Night & IST
Return to Ambient
TEMPERATURE (F) ×10¹
40.00
30.00
20.00
10.00
0.00
-10.00
-20.00
0.00
24.00
48.00
72.00
96.00
120.00
144.00
168.00
192.00
216.00
240.0
TIME (HOURS)

Figure 37

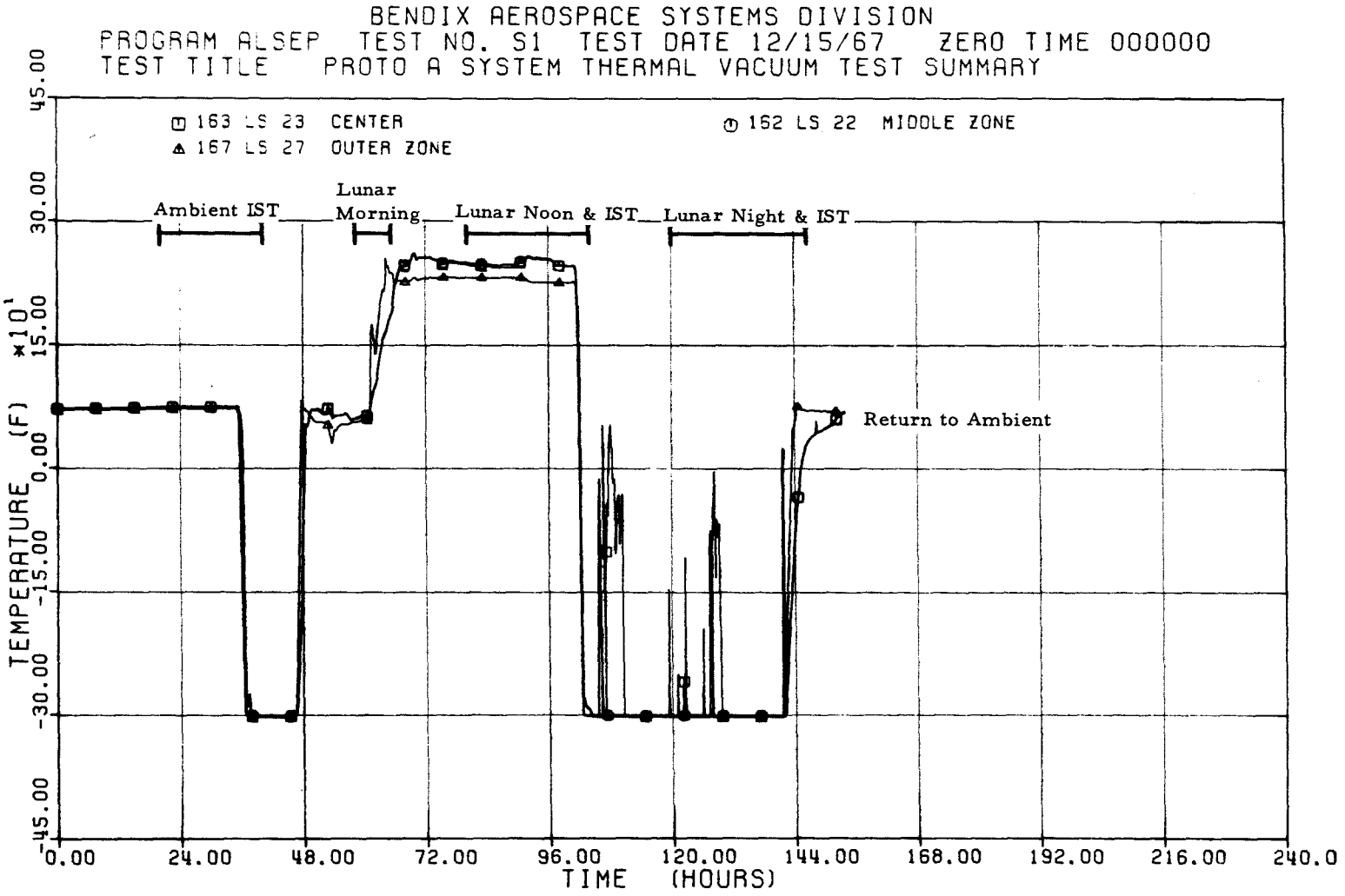
BENDIX AEROSPACE SYSTEMS DIVISION
PROGRAM ALSEP TEST NO. S1 TEST DATE 12/15/67 ZERO TIME 000000
TEST TITLE PROTO A SYSTEM THERMAL VACUUM TEST SUMMARY
163 LS 23 CENTER
167 LS 27 OUTER ZONE
162 LS 22 MIDDLE ZONE
Ambient IST
Lunar Morning
Lunar Noon & IST
Lunar Night & IST
Return to Ambient
TEMPERATURE (F) *10¹
45.00
30.00
15.00
0.00
-15.00
-30.00
-45.00
0.00
24.00
48.00
72.00
96.00
120.00
144.00
168.00
192.00
216.00
240.0
TIME (HOURS)

Figure 38

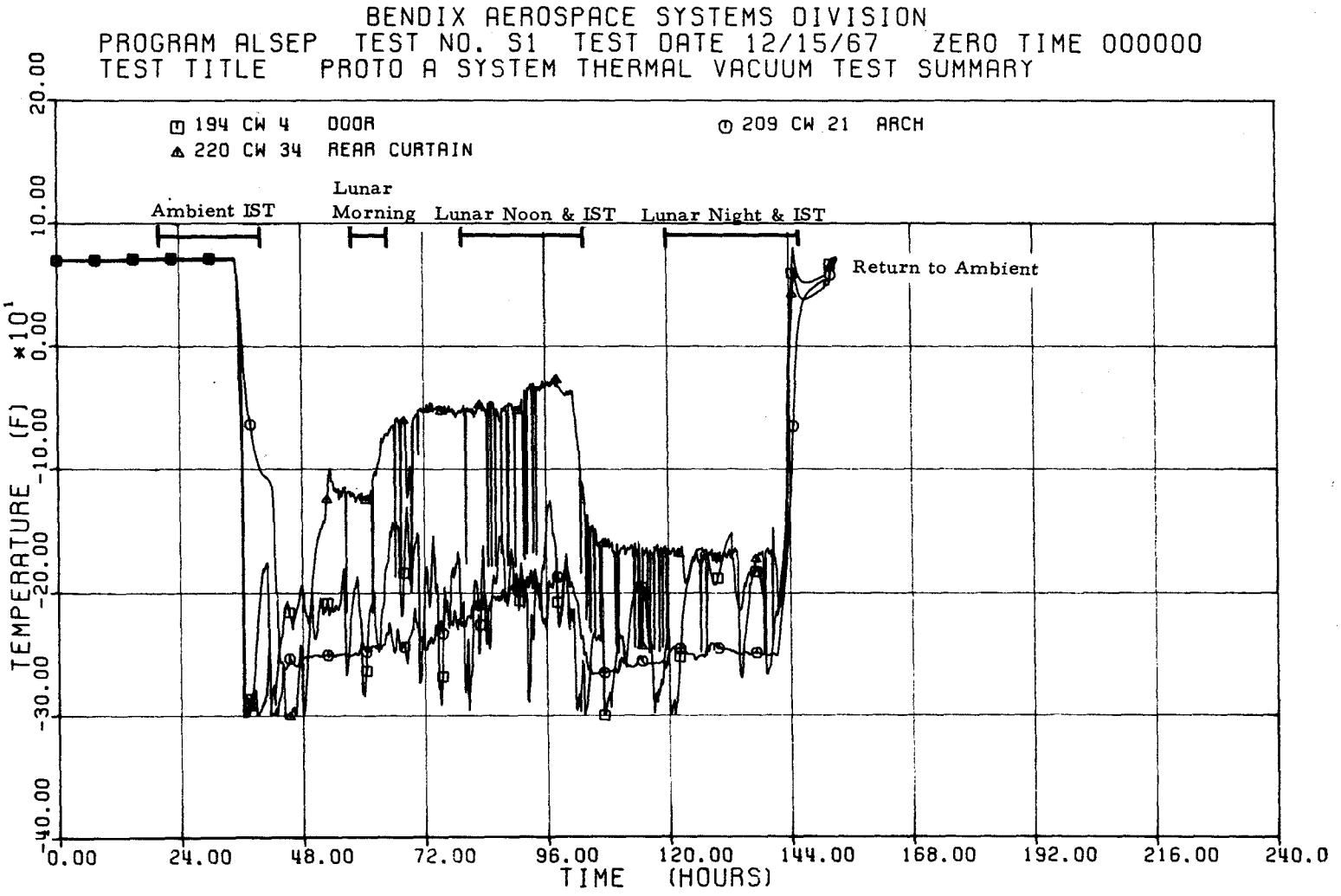
BENDIX AEROSPACE SYSTEMS DIVISION
PROGRAM ALSEP TEST NO. S1 TEST DATE 12/15/67 ZERO TIME 000000
TEST TITLE PROTO A SYSTEM THERMAL VACUUM TEST SUMMARY
194 CW 4 DOOR
220 CW 34 REAR CURTAIN
209 CW 21 ARCH
Ambient IST
Lunar Morning
Lunar Noon & IST
Lunar Night & IST
Return to Ambient
TEMPERATURE (F) *10¹
20.00
10.00
0.00
-10.00
-20.00
-30.00
-40.00
0.00
24.00
48.00
72.00
96.00
120.00
144.00
168.00
192.00
216.00
240.0
TIME (HOURS)

TABLE 8

PROTOTYPE "A" TEST TELEMETRY DATA

Thermal Analyzer Node No.	Description	Temperatures (°F) HK#	AT#	Noon	Night
37	PCU Power Oscillator #1	64	36	122	-1
37	PCU Power Oscillator #2	76	37	114	-1
37	PCU Regulator #1	77	38	157	38
37	PCU Regulator #2	78	39	124	7
38	PDU Power Distribution - Internal	63	35	129	11
38	PDU Power Distribution - Base	62	34	108	-14
39	Analog Multiplex Converter-Internal	34	28	113	-8
39	Analog Multiplex Converter - Base	33	27	102	-23
41	Comm. Receiver - Local Osc. Crystal A	16	21	-	-
41	Comm. Receiver - Local Osc. Crystal B	17	22	111	-9
42	Digital Data Processor - Internal	47	30	108	-17
42	Digital Data Processor - Base	46	29	102	-20
43	Command Decoder - Base	48	31	99	-23
43	Command Decoder - Internal	49	32	103	-20
43	Command Demodulator - VCO	61	33	105	-17
47	Transmitter A - Heat Sink	19	24	130	6
47	Transmitter A - Crystal	18	23	111	0
48	Transmitter B - Heat Sink	32	26	24	-
48	Transmitter B - Crystal	31	25	-	-10
105, 106	Thermal Plate	4	3	100	-17
103, 104	Thermal Plate	28	4	101	-20
107-108	Thermal Plate	43	5	103	-20
114	Thermal Plate	58	6	101	-20
109	Thermal Plate	71	7	105	-17
49	Primary Structure - Front	88	11	32	-122
50	Primary Structure - Left Side	59	8	160	-142
52	Primary Structure - Right Side	87	9	203	-125
53	Primary Structure - Bottom	15	10	223	-137
54	Thermal Bag - Inside	60	12	103	-16
55	Thermal Bag - Outside	72	13	177	-97
31	Sunshield - Top	27	1	35	-228
34	Sunshield - Bottom	42	2	37	-225

REFERENCES

1. Hearin, L., "Thermal Analysis of ALSEP Prototype "A" Central Station With Comparison to Test Results", Bendix ATM-751.

2. Bendix Thermal Analyzer Computer Program

3. Oppenheim, A. K., "Radiation Analysis by the Network Method", American Society of Mechanical Engineers, Transactions, Vol. 78, No. 4 (May 1956), pp. 725-735.

4. Ziering, M. D. and Sarofin, A. F., "The Electrical Network Analog to Radiative Transfer: Allowance for Specular Reflection", American Society of Mechanical Engineers, Transactions, Journal of Heat Transfer, August 1966, pp. 341-342.

5. Kreith, F., "Radiation Heat Transfer for Spacecraft and Solar Power Plant Design", International Textbook Co., Scranton, Pa., 1962.

6. Toups, K. A., "A General Computer Program for the Determination of Radiant-Interchange Configuration and Form Factors - CONFAC II", North American Aviation, Inc., Space and Information Systems Division, Report No. SID 65-1043-2, October 1965.

7. "Configuration Factors for Thermal Radiation", Engineering Report LB-30247, Douglas Aircraft Co., Inc., Long Beach, Calif., Oct. 1959.

8. "ALSEP Prototype "A" Thermal Vacuum Test Summary Analysis", Bendix ATM-752, May 1968.

9. Simms, R. J., "Lunar Subsurface Model", Bendix IM 9712-767.

APPENDIX 1

PHYSICAL CHARACTERISTICS AND FUNCTIONS OF CENTRAL STATION COMPONENTS

The overall objective of the Central Station is to dissipate electronics heat to space with minimum lunar noon/lunar night radiator plate temperature swing and while maintaining electronics operating temperatures within allowable limits.

In order to realize this objective, components were designed with the following considerations as guidelines:

1. Radiate heat to space with lowest feasible radiator and electronics temperatures during lunar noon.

2. Maintain electronics operating temperatures above minimum allowables during lunar night.

3. Minimize heat transfer (thermal and reflected solar) between lunar surface and C/S.

4. Minimize heat transfer (or heat leak) along cables which pass from outside the C/S into the electronics compartment.

5. Dissipate as much electronics heat as feasible at the radiator plate.

6. Prevent direct impingement of solar radiation on radiator baseplate or on any section of electronics compartment.

Brief descriptions of physical characteristics and functions of various C/S components are presented below.

1.0 Radiator Baseplate

This item, constructed of 0.131 inch aluminum, directly removes most of the electronics heat dissipation and then radiates this heat directly and indirectly from the C/S to space. Though the plate has an upper surface

area of over 4 ft^2, only 2 ft^2 radiate the heat away since insulation masks cover the remaining area. Bare regions of the upper plate surface are coated with a white paint which has a high thermal emissivity of about 0.9 and a solar absorptivity of approximately 0.2. The bottom surface is aluminized and has a low thermal emissivity of around 0.05, which minimizes heat leak between the plate, structure, and thermal bag. The performance of the radiator governs the performance of the entire C/S. A good portion of the heat dissipated by the plate is radiated to space via the specular reflector.

2.0 Specular Reflector

The specular reflector serves primarily to minimize indirect radiation from the moon to the radiator plate via the side curtains and sunshield awnings while also increasing the effectiveness of heat dissipation from the radiator to space. It is constructed of aluminized mylar, which exhibits the radiation properties listed in Table 5 and which can be folded during the "stored" configuration.

3.0 Thermal Bag

This component is most important in isolating C/S electronics from solar and thermal radiation in the lunar environment. It consists of alternate layers of aluminized mylar and glass fiber separators (about 40 of each), with a total thickness of about 0.6 inch. Thermal conductivity for the bag ranges from around 9.4×10^{-4} Btu/fthr°F at lunar noon to about 1.8×10^{-4} Btu/fthr°F at lunar night.

4.0 Sunshield and Side Curtains

The primary function of these items is to prevent direct solar heating of the radiator baseplate during the lunar day. The sunshield is constructed from aluminum honeycomb so it can also serve as a mounting pallet for ALSEP experiments in the "stored" configuration. White paint coats the upper surface while the underside is insulated with layers of crinkled aluminized mylar. All side curtains consist of alternate layers of aluminized mylar and silk separators (about 10 of each), with the external surface being coated with silicon monoxide (SiO). Radiation properties for these surfaces are listed in Table 5, and conduction properties are presented in Section 14 of Appendix 2.

5.0 Extenders

Four extenders, which act like helical springs, support the sunshield, side curtains, and reflector in the deployed configuration of the C/S. The extender material is 0.006 inch thick stainless steel.

6.0 Insulation Masks

Insulation masks cover six inch wide sections on two sides of the radiator baseplate and serve to reduce the effective radiation area of the plate. This in turn forces the radiator and electronics to operate at elevated temperatures when dissipating the electronics heat. The masks are needed to maintain electronics operating temperatures above minimum allowables during lunar night. Each mask contains about 30 layers of aluminized mylar and has radiation and conduction properties listed in Table 5 and in Section 14 (Appendix 2).

7.0 Radiator Plate Isolator Supports

The primary structure supports the radiator with four thermal "isolator" supports. Since the structure operates at higher and lower temperatures than the plate during lunar noon and night, respectively, it is necessary to isolate the plate from structure temperature effects in order to minimize "temperature swing". Consequently, the support was designed to provide a high-resistance heat flow path. The support consists primarily of an aluminum housing, stainless steel spring, and fiberglass "standoff" post as shown in Figure 2.1 in Appendix 2. The fiberglass post has a thermal conductivity of approximately 0.17 Btu/ft-hr^{o}F.

8.0 Primary Structure

The primary structure serves to house and support the C/S components. External surfaces (except the bottom) are coated with high emissivity/low solar absorptivity white paint which maintains the structure at lowest possible temperatures during the lunar day. Internal surfaces and the bottom are aluminized to minimize heat transfer from the structure to the thermal bag and lunar surface. Radiation properties are listed in Table 5.

9.0 Manganin Cable Inserts

Manganin, which has about 1/15 the thermal conductivity of copper, was inserted into most cables entering the electronics compartment from outside the C/S in order to minimize heat leak to or from the electronics.

APPENDIX 2

ANALYSIS AND CALCULATION DETAILS FOR EVALUATION OF RESISTANCE PATHS

This appendix presents specific methods used to evaluate various resistance paths and sample calculations for the vacuum chamber test condition. Objectives are to 1) elaborate on approximation techniques, 2) state assumptions, 3) outline step-by-step procedures for the more complicated calculations, and 4) present parameters which contribute to final resistance values.

Note that for radiation resistance calculations, the resistance reciprocal or conductance is the objective since this quantity is input to the Thermal Analyzer computer program. The following paths are covered:

Section	Description
1	Electronics to Radiator Baseplate
2	Structure to Radiator via Posts
3	Structure Insulation to Radiator
4	Electronics and Radiator to Thermal Bag
5	Structure to Thermal Bag
6	Structure Node Connections
7	Structure to Sunshield
8	Structure to Lunar Surface and Space
9	Side Curtains to Lunar Surface and Space
10	Sunshield to Space
11	Enclosure behind Reflectors

Section	Description
12	Radiosity Node Network
13	Cable Heat Leak from Structure to Environment
14	Aluminized Mylar Insulation Resistance

NOMENCLATURE

The following general nomenclature is used in this appendix. Units are as noted in calculations.

Symbol	Description
A	Area for either Conduction or Radiation Heat Transfer
F_{m-n}	Form Factor from Surface m to Surface n
$\mathfrak{F}_{m-n}$	Radiant Interchange Factor (Script "F") from Surface m to Surface n
h_c	Contact Conductance
K	Thermal Conductivity
L	Length of Conduction Heat Transfer Path
q	Heat Transfer Rate
R_{m-n}	Resistance between Surfaces m and n
T	Temperature
ϵ	Thermal Emissivity
α_s	Solar Absorptivity
ρ	Reflectance
σ	Stefan-Boltzman Constant = 0.1713×10^{-8} Btu/ft^{2}hr$^\circ$R^4

1.0 CONDUCTION FROM ELECTRONICS TO RADIATOR BASEPLATE (PATHS 1-27)

Electronic components were fastened to the radiator baseplate with stainless steel machine screws and with a layer of "thermal grease" to insure good heat conduction from the components to the plate. Consequently, the resistence network between each component and the radiator is as shown below:

1.1 Thermal Model

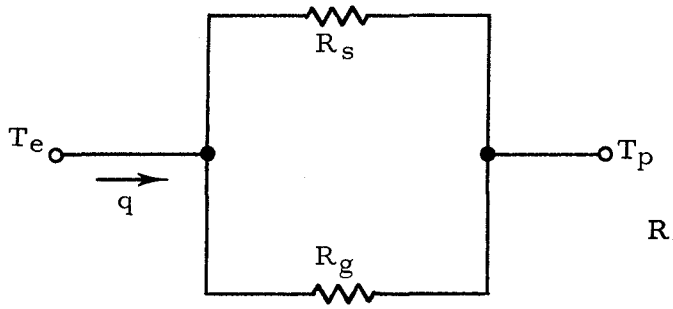

$$q = \frac{T_e - T_p}{R_{Tot}}$$

$$R_{Tot} = \frac{R_s R_g}{R_s + R_g}$$

q = heat transfer rate

T_e = electronic component temperature

T_p = radiator baseplate temperature

R_s = screw resistance

R_g = thermal grease resistance

1.2 Resistance Evaluation

Since the thickness of grease between a component and the plate is extremely difficult to measure, a thermal conductance (Cg) of 20 Btu/ft^{2}hr ^{o}F was assumed. As test and predicted temperatures for the plate and components

agreed satisfactorily, this value appears adequate. Therefore,

$$R_g = \frac{1}{20A_{c-p}}$$

A_{c-p} is the component area adjacent to a particular plate node. For the screws, an effective length (L_s) was found as follows:

$$L_s = \frac{K_g}{C_g} = \frac{0.2419}{20} = 0.01214 \text{ ft.}$$

where K_g is the manufacturer's value of thermal conductivity in Btu/ft hr ^oF. Most screws are type MS 24693-C47 stainless steel, which have a 0.164 inch diameter and a 9.4 Btu/ft hr ^oF conductivity.

Thus $$R_s = \frac{L_s}{nK_sA_s} = \frac{8.82}{n}$$

A_s = screw cross sectional area = .0001466 ft^2

n = number of screws fastening component to plate

1.3 Example

A sample calculation is presented for the resistance paths 1 and 2 between the P.C.U. (Node 37) and the adjacent two plate nodes (101 & 105).

$A_{g\ (37\text{-}101)} = 0.1549\ ft^2$ $\qquad n_{37\text{-}101} = 4$

$A_{g\ (37\text{-}105)} = 0.0834\ ft^2$ $\qquad n_{37\text{-}105} = 2$

$$R_{g\ (37\text{-}101)} = \frac{1}{(20)(.1549)} = 0.323 \text{ hr } ^oF/\text{Btu}$$

$$R_{s\ (37\text{-}101)} = \frac{8.82}{4} = 2.205 \text{ hr } ^oF/\text{Btu}$$

$$R_{Tot\ (37-101)} = \frac{(.323)\ (2.205)}{.323 + 2.205} = 0.281 \text{ hr } ^{o}F/Btu$$

$$R_{g\ (37-105)} = \frac{1}{(20)\ (.0834)} = 0.600 \text{ hr } ^{o}F/Btu$$

$$R_{s(37-105)} = \frac{8.82}{2} = 4.41 \text{ hr } ^{o}F/Btu$$

$$R_{Tot\ (37-105)} = \frac{(0.600)\ (4.41)}{0.600 + 4.41} = 0.528 \text{ hr } ^{o}F/Btu$$

2.0 CONDUCTION THROUGH RADIATOR PLATE SUPPORT POSTS (PATHS 61-64)

Four posts support the thermal plate and provide the only heat conduction paths between the primary structure and radiator plate. The posts are made of a low thermal conductivity material which minimizes heat flow between the structure and plate and which are supported in housings fastened to the structure as illustrated in Figure 2.1.

Since it is important to isolate the radiator plate from structure influence, a somewhat detailed analysis was performed to evaluate the support resistances. In order to account for most heat flow paths, a rather complex resistance network, shown in Figure 2.2, results. Each resistance has been evaluated and the type of heat transfer designated. Node locations for various parts of the post and post housing are specified in Figure 2.1.

2.1 Network Reduction

In order to incorporate the "post" resistance into the thermal analyzer without adding unnecessary nodes and paths, it was desirable to reduce the complex network to a simple one. All resistances in Figure 2.2 were evaluated, with careful attention given to those paths considered critical (Paths 1, 3, 4, 10, 18, & 19). Procedures used to reduce and evaluate the network will now be presented along with sample calculations.

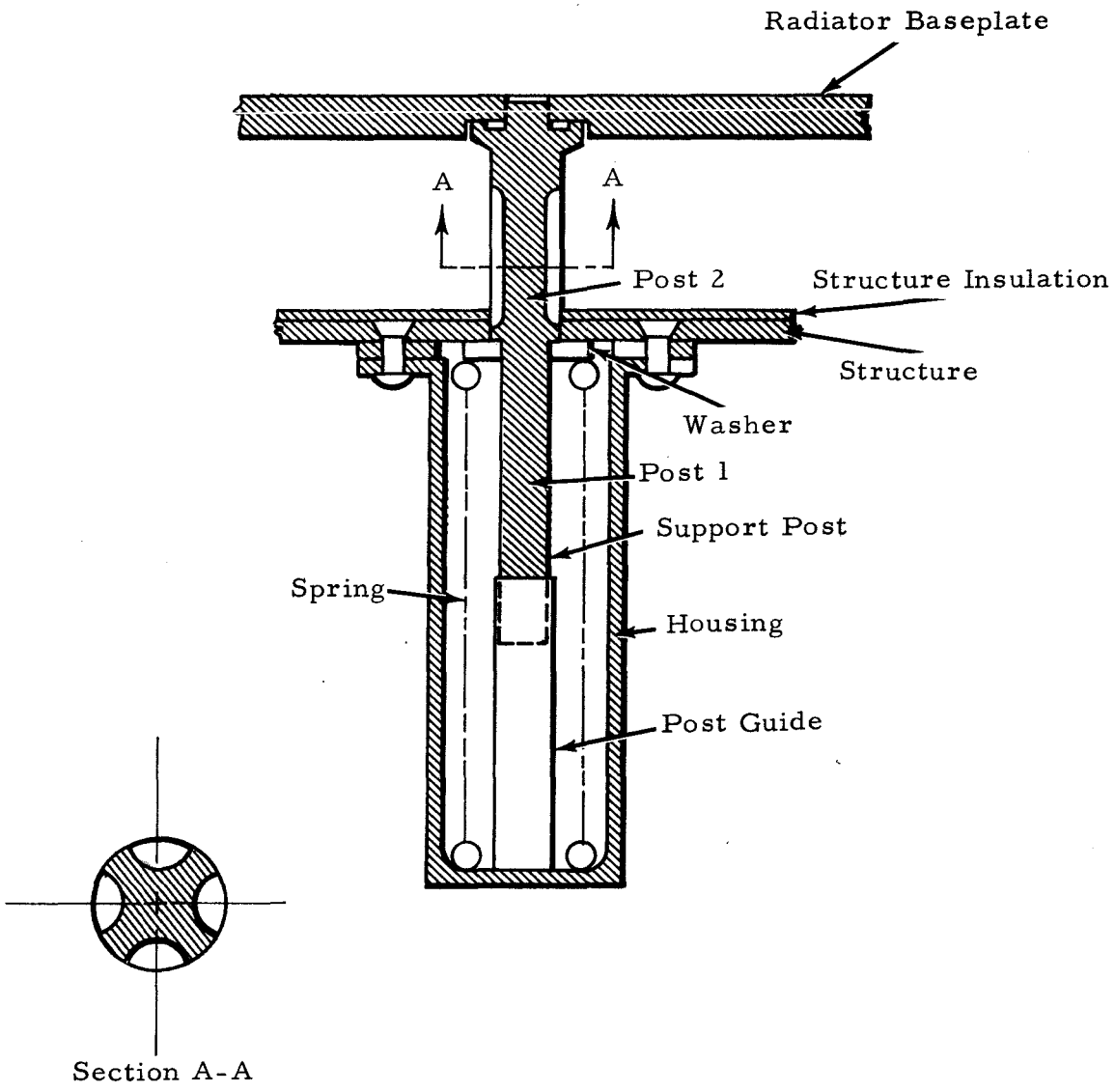

Figure 2.1 Radiator Baseplate Support Mechanism (Deployed Configuration)

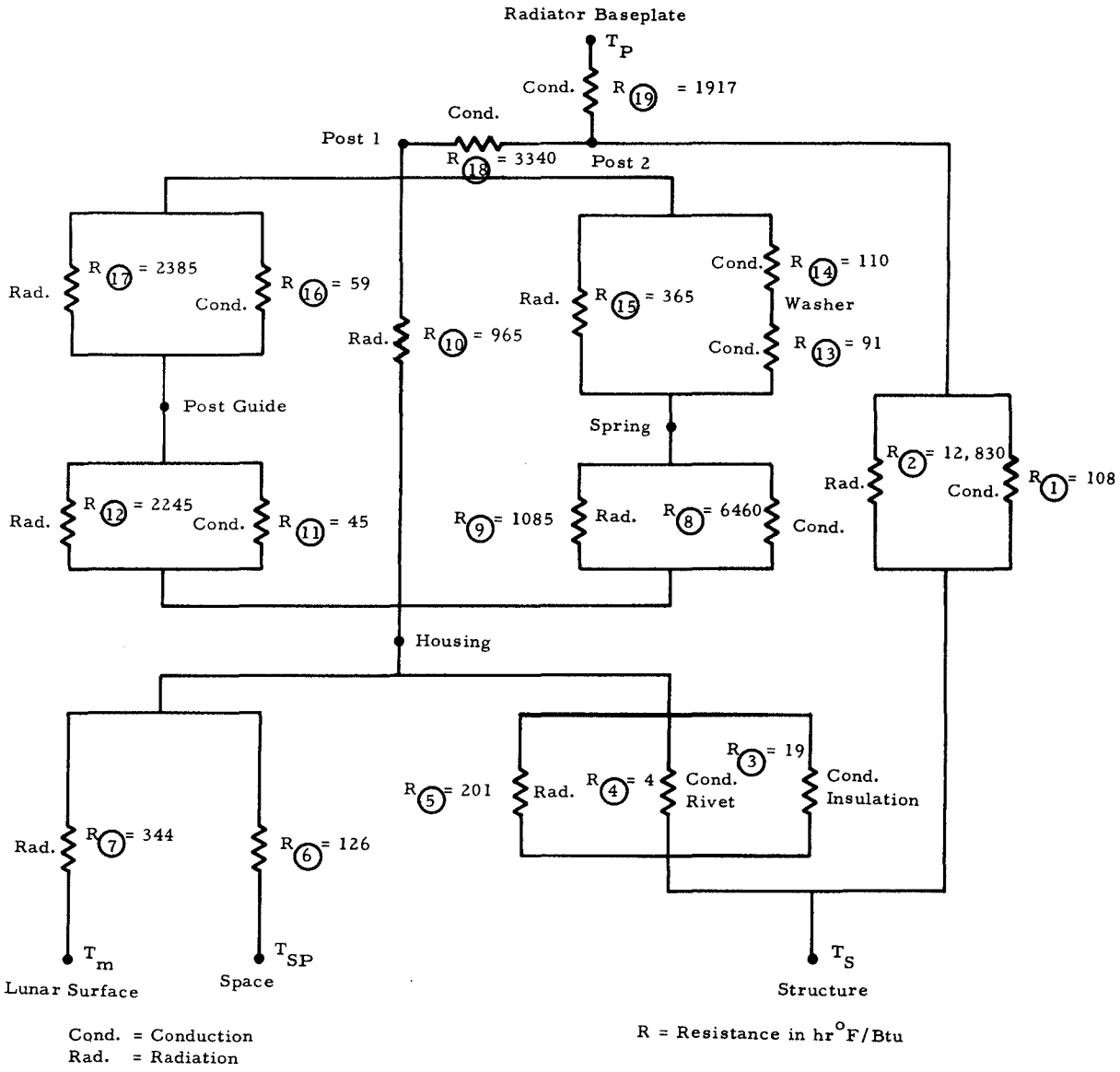

Figure 2.2 Resistance Network for Thermal Support Posts

The Figure 2.2 network can be reduced to the following:

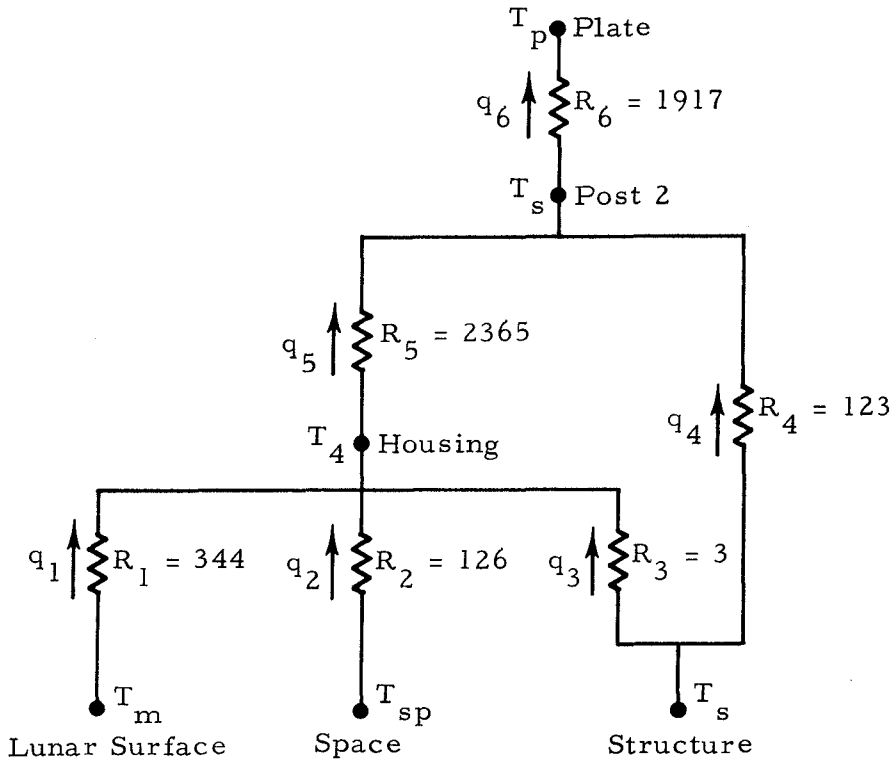

R = resistance in hr ^{o}F/Btu

$R_1 = R_{(7)}$ $R_2 = R_{(6)}$ $\frac{1}{R_3} = \frac{1}{R_{(3)}} + \frac{1}{R_{(4)}} + \frac{1}{R_{(5)}}$

$\frac{1}{R_4} = \frac{1}{R_{(1)}} + \frac{1}{R_{(2)}}$ $R_6 = R_{(19)}$

$R_5 = R_5^{11111} + R_{(18)}$

$\frac{1}{R_5^{11111}} = \frac{1}{R_5^{1} + R_5^{11}} + \frac{1}{R_{(10)}} + \frac{1}{R_5^{111} + R_5^{1111}}$

$$\frac{1}{R_5^{1}} = \frac{1}{R_{(11)}} + \frac{1}{R_{(12)}} \qquad \frac{1}{R_5^{11}} = \frac{1}{R_{(16)}} + \frac{1}{R_{(17)}}$$

$$\frac{1}{R_5^{111}} = \frac{1}{R_{(13)} + R_{(14)}} + \frac{1}{R_{(15)}} \qquad \frac{1}{R_5^{1111}} = \frac{1}{R_{(8)}} + \frac{1}{R_{(9)}}$$

T_p = radiator plate temperature

T_m = lunar surface temperature

T_{sp} = space temperature

T_s = primary structure temperature

To further reduce the network, the following equation can be written:

$$q_5 = q_1 + q_2 + q_3 = \frac{T_{el} - T_4}{R_{el}} = \frac{T_m - T_4}{R_1} + \frac{T_{sp} - T_4}{R_2} + \frac{T_s - T_4}{R_3} \qquad (2.1)$$

The following <u>definitions</u> are made:

T_{el} = an "equivalent" temperature

$$\frac{1}{R_{el}} = \frac{1}{R_1} + \frac{1}{R_2} + \frac{1}{R_3} \qquad (2.2)$$

Equation 2.1 can be rearranged to give

$$T_{el} = R_{el}\left(\frac{T_m}{R_1} + \frac{T_{sp}}{R_2} + \frac{T_s}{R_3}\right) + T_4\left[1 - R_{el}\left(\frac{1}{R_1} + \frac{1}{R_2} + \frac{1}{R_3}\right)\right]$$

Substitution of Equation 2.2 produces

$$T_{el} = R_{el}\left(\frac{T_m}{R_1} + \frac{T_{sp}}{R_2} + \frac{T_s}{R_3}\right) \qquad (2.3)$$

Since T_m, T_{sp}, and T_s are of the same order of magnitude and since R_3 is 40 to 100 times smaller than R_2 and R_1, Equations 2.2 and 2.3 can be reduced to

$$R_{e1} = R_3$$

$$T_{e1} = \frac{R_{e1}}{R_3} T_s = T_s$$

Therefore, the effect of space and lunar surface are negligible, and the network becomes

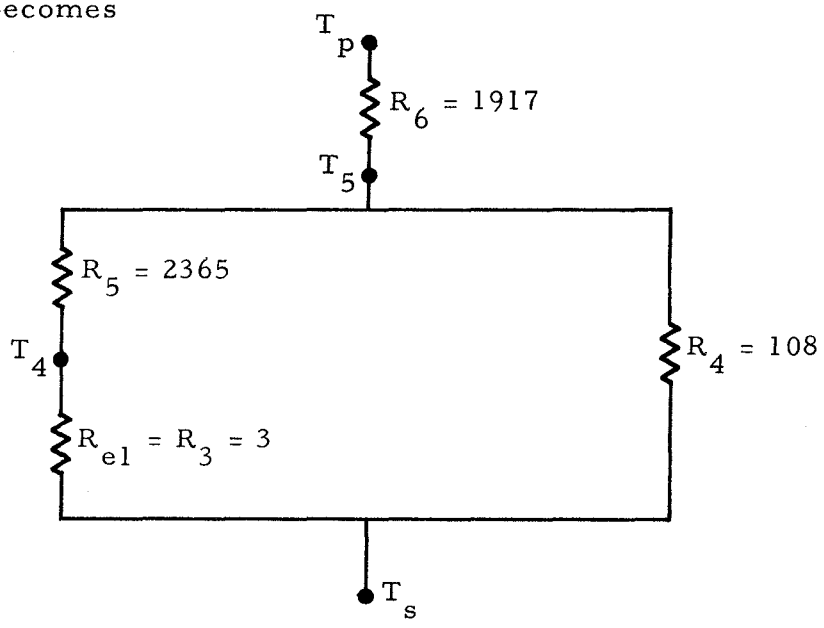

A further simplification yields

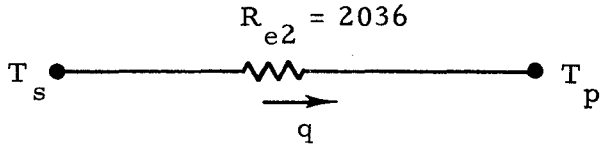

$$R_{e2} = \frac{(R_{e1} + R_5)\ (R_4)}{R_{e1} + R_5 + R_4} + R_6$$

2.2 Resistance Path Calculations

Calculations are presented for a few of the more critical paths.

2.2.1 Resistance between Structure and Post 2 Node ($R_{①}$)

This path involves heat conduction across the structure-post contact and into the post.

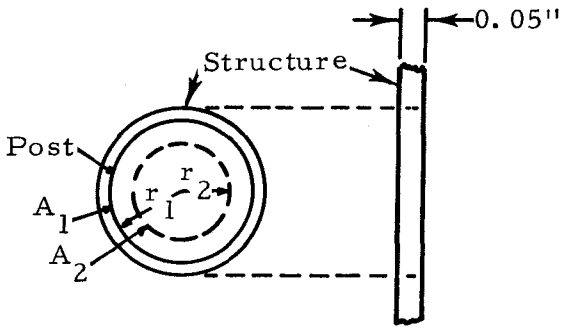

$r_1 = 0.095$ inches

A_1 = contract area between structure and post

$$A_1 = \pi\left(\frac{.19}{12}\right)\left(\frac{.04}{12}\right) + \frac{1}{3}\pi\left(\frac{.19}{12}\right)\left(\frac{.01}{12}\right) = 0.0259/144 \text{ ft}^2$$

Note that .01 inches of the contact length involves the section of post with cutouts.

It is assumed that no temperature gradient exists across the post diameter and therefore that heat flows from the structure to a radius which divides the post cross-sectional area in half.

$$\text{Thus,} \quad \pi r_2^2 = \frac{1}{2}\,\frac{\pi}{4}\left(\frac{.19}{12}\right)^2 \qquad r_2 = \frac{.0671}{12} \text{ ft}$$

$$A_2 = 2\pi\left(\frac{.0671}{12}\right)\left(\frac{.04}{12}\right) + \frac{1}{3}(2\pi)\left(\frac{.0671}{12}\right)\left(\frac{.01}{12}\right)$$

$$= 0.0183/144 \text{ ft}^2$$

The resistance network for $R_{①}$ is

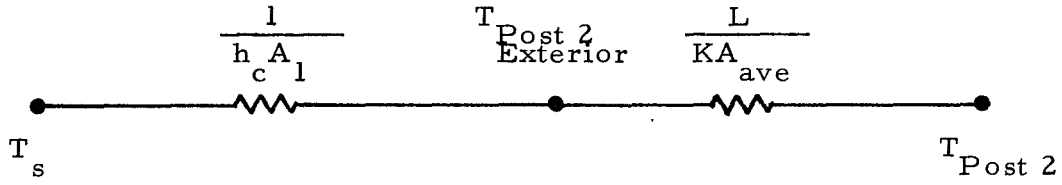

h_c = contact conductance between structure and post = 300 Btu/ft^2 hr ^{o}F (assumed)

L = $r_2 - r_1$ = .0279/12 ft

K = post thermal conductivity = 0.17 Btu/ft hr ^{o}F

The value for conductivity was obtained from the Material Selector for types G-7 to G-11 laminated thermosetting materials (glass cloth base).

$$R_{①} = \frac{1}{h_c A_1} + \frac{L}{KA_{ave}} = 18.5 + 89.2 = 107.7 \text{ hr } ^{o}\text{F/Btu}$$

2.2.2 Resistance between Post 1 and Post 2 Locations ($R_{⑱}$)

This resistance path involves simple conduction

$$R_{⑱} = \frac{L}{KA}$$

$$A \approx \frac{\pi}{4} \quad (0.127)^2/144 = 0.0127/144 \text{ ft}^2$$

L = 0.41/12 ft

K = 0.17 Btu/ft hr ^{o}F

$R_{⑱}$ = 2280 hr ^{o}F/Btu

2.2.3 Resistance between Post 2 and Radiator Plate (R_{19})

Since all conduction from the structure to radiator must pass between the Post 2 location and the plate, this is the most critical resistance. Figure 2.1 contains a sketch detail of the post and shows that the post was broken into two segments for analysis purposes. The resistance network is

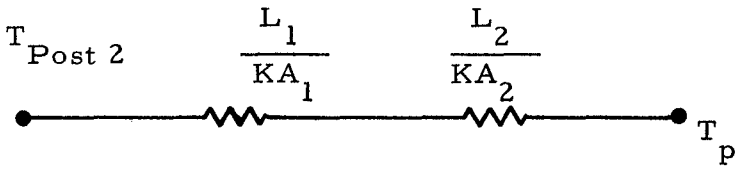

A_1 is the cross sectional area of that section of post with cutouts.

$A_1 = 0.0181/144 \text{ ft}^2$

$A_2 = \frac{\pi}{4} (.19)^2/144 = 0.0284/144 \text{ ft}^2$

$L_1 = L_2 = 0.3/12 \text{ ft}$

$K = 0.17 \text{ Btu/ft hr } ^\circ\text{F}$

$R_{19} = \frac{L_1}{KA_1} + \frac{L_2}{KA_2} = 1917 \text{ hr } ^\circ\text{F/Btu}$

3.0 RADIATION BETWEEN STRUCTURE AND RADIATOR (PATHS 69-83)

This radiation actually occurs between the radiator baseplate and the insulation resting on top of the structure. Resistance paths were determined between each structure side and the adjacent radiator nodes. Because of the relative unimportance of these resistances (they are very large) the form factors were determined by approximate hand methods rather than with the CONFAC II program. Typical resistance calculations for radiation between node 56 (the insulation on structure node 49) and the adjacent radiator nodes (105, 106, 107, and 108) will be presented.

The form factor between node 56 and the entire adjacent radiator plate (nodes 105-108) was calculated and then proportioned for the individual plate nodes. Sections 3.1 and 3.2 illustrate the techniques involved.

3.1 Form Factor Between Node 56 and Adjacent Plate

The surfaces involved are illustrated below

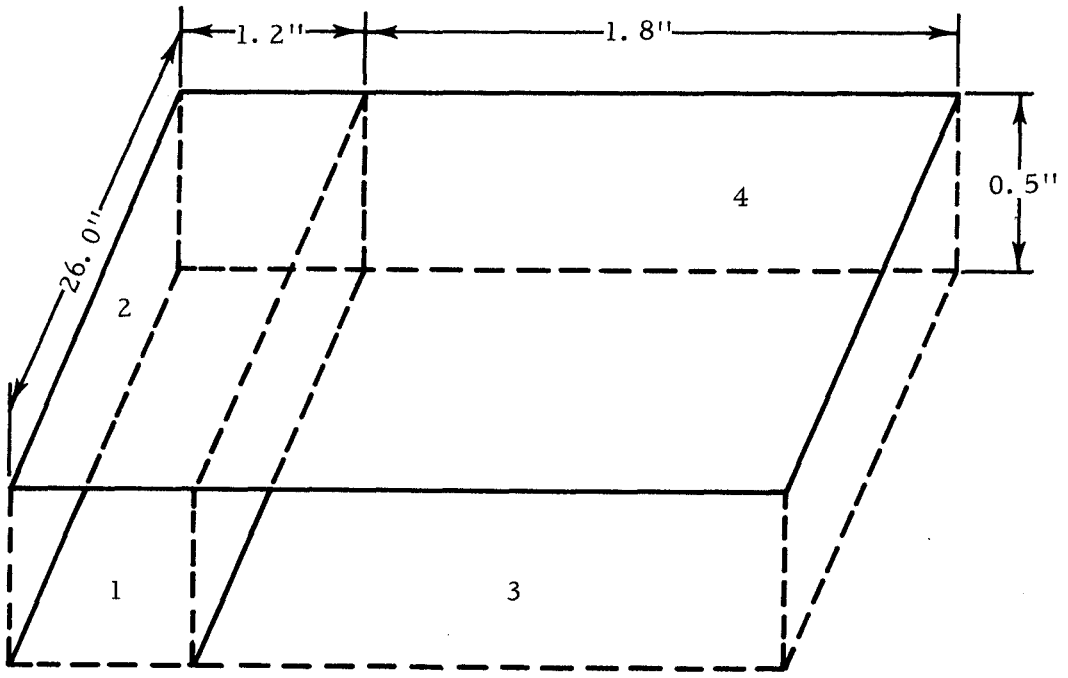

Surfaces 1, 2, 3, and 4 represent the following nodes

Surface 1 = Node 56

Surface 3 = "Dummy" Node

Surface 2 + 4 = Nodes 105 + 106 + 107+ 108

A_1 = (1.2) (26) = 31.2 in^2

A_3 = (1.8) (26) = 46.8 in^2

A_{1+3} = 78 in^2

From view factor geometry, the following equation can be developed.

$$A_1 F_{1-(2+4)} = \frac{1}{2} \left[A_{1+3} F_{(1+3)-(2+4)} + A_1 F_{1-2} - A_3 F_{3-4}\right]$$

A = surface area

F = form factor

Subscripts refer to the surfaces

The following form factor values were obtained from Figure 11 in Reference 7.

$F_{(1+3)-(2+4)} = 0.82$ $F_{1-2} = 0.64$ $F_{3-4} = 0.73$

$$F_{1-(2+4)} = \frac{1}{(2)(31.2)} \left[(78)(0.82) + (31.2)(0.64) - (46.8)(0.73)\right] = 0.80$$

Since some radiation from node 56 will be intercepted by electronics and cabling and eventually reach the radiator, assume $F_{1-(2+4)} = 0.9$. This is conservative and allows for inaccuracies in the analysis.

Therefore, $F_{56-(105+106+107+108)} = 0.90$.

3.2 Form Factors Between Node 56 and Individual Plate Nodes

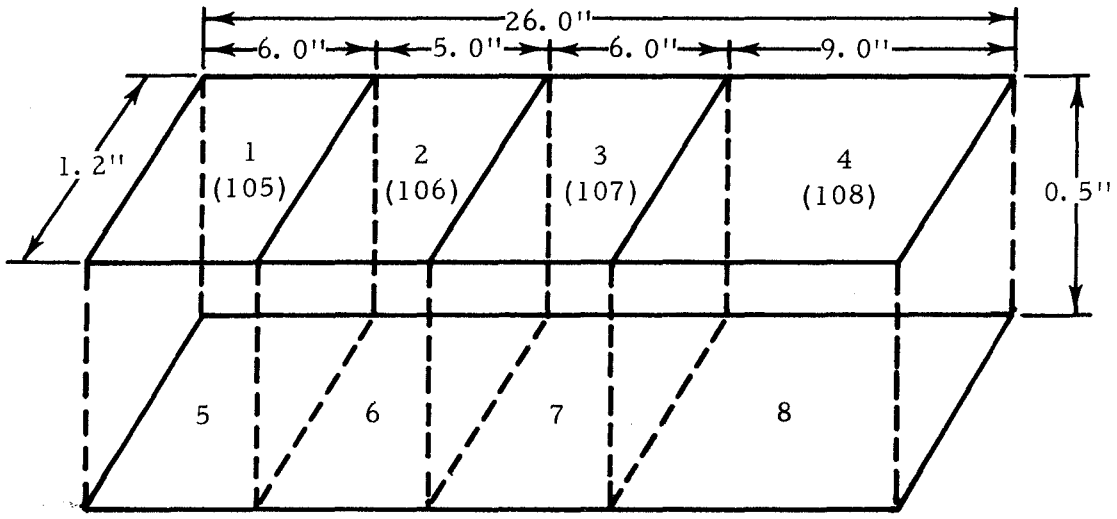

Surfaces 1, 2, 3, and 4 represent nodes 105, 106, 107, and 108, respectively.

Surfaces 5 + 6 + 7 + 8 = node 56

Note that only part of the nodes 105 to 108 are involved in the above model. No convenient hand techniques are available to calculate factors between node 56 and each complete plate node. Form factors determined here will represent a proportion of the total 0.9 factor. All factors, except those evaluated in equations presented here, were obtained from Reference 7 (Figure 11).

$A_1 = A_3 = A_5 = A_7 = (6)\ (1.2) = 7.2\ in^2$

$A_2 = A_6 = (5)\ (1.2) = 6.0\ in^2$

$A_4 = A_8 = (9)\ (1.2) = 10.8\ in^2$

$A_{1+2} = 13.2\ in^2 \qquad A_{3+4} = 18.0\ in^2$

$A_{1+2+3} = A_{5+6+7} = 20.4\ in^2$

$A_{1+2+3+4} = A_{5+6+7+8} = 31.2\ in^2$

$A_{2+3+4} = A_{6+7+8} = 24.0\ in^2$

$F_{(1+2+3+4) - (5+6+7+8)} = 0.64 \quad F_{1-5} = 0.63 \quad F_{(2+3+4) - (6+7+8)} = 0.65$

From form factor geometry,

$$A_1 F_{1 - (5+6+7+8)} = \frac{1}{2} \left[A_{1+2+3+4} F_{(1+2+3+4) - (5+6+7+8)} + A_1 F_{1-5} - A_{2+3+4} F_{(2+3+4) - (6+7+8)} \right]$$

$$F_{1 - (5+6+7+8)} = \frac{1}{(2)(7.2)} \left[(31.2)(.64) + (7.2)(.63) - (24.)(.65) \right] = 0.618$$

Performing a similar calculation for $F_{4 - (5+6+7+8)}$, we get

$$A_4 F_{4 - (5+6+7+8)} = \frac{1}{2} \left[A_{1+2+3+4} F_{(1+2+3+4) - (5+6+7+8)} + A_4 F_{4-8} - A_{1+2+3} F_{(1+2+3) - (5+6+7)} \right]$$

$F_{4-8} = 0.63 \qquad F_{(1+2+3) - (5+6+7)} = 0.65$

$$F_{4 - (5+6+7+8)} = \frac{1}{(2)(10.8)} \left[(31.2)(.64) + (10.8)(.63) - (20.4)(.65) \right]$$

$$= 0.626$$

The following equation holds for $F_{2 - (5+6+7+8)}$:

$$F_{2 - (5+6+7+8)} = F_{2 - (6+7+8)} + F_{2 - (5+6)} - F_{2 - 6}$$

$F_{2 - (6+7+8)}$ and $F_{2 - (5+6)}$ are found as follows:

$$A_2 F_{2 - (6+7+8)} = \frac{1}{2} \left[A_{2+3+4} F_{(2+3+4) - (6+7+8)} + A_2 F_{2-6} - A_{3+4} F_{(3+4) - (7+8)} \right]$$

$F_{(2+3+4) - (6+7+8)} = .65 \quad F_{2-6} = .62 \quad F_{(3+4) - (7+8)} = .65$

$$F_{2-(6+7+8)} = \frac{1}{(2)(6.0)}\left[(24)(.65) + (6)(.62) - (18)(.65)\right]$$

$$= .635$$

$$A_2F_{2-(5+6)} = \frac{1}{2}\left[A_{1+2}F_{(1+2)-(5+6)} + A_2F_{2-6} - A_1F_{1-5}\right]$$

$$F_{(1+2)-(5+6)} = 0.63 \quad F_{2-6} = 0.62 \quad F_{1-5} = 0.63$$

$$F_{2-(5+6)} = \frac{1}{(2)(6.0)}\left[(13.2)(.63) + (6.0)(0.62) - (7.2)(0.63)\right]$$

$$= 0.625$$

$$\text{Thus } F_{2-(5+6+7+8)} = 0.635 + 0.625 - 0.620$$

$$= 0.640$$

Node 56 will be substituted for surface 5+6+7+8 in the following calculations. The following relation is now useful:

$$F_{56-1} = F_{(5+6+7+8)-1} = \frac{A_1}{A_{5+6+7+8}} F_{1-(5+6+7+8)}$$

$$= \frac{7.2}{31.2}(0.618) = 0.143$$

Similarly,

$$F_{56-2} = \frac{6.0}{31.2}(0.640) = 0.123$$

$$F_{56-4} = \frac{10.8}{31.2}(0.626) = 0.217$$

F_{56-3} is obtained with the following relationship:

$$F_{56-3} = F_{56-(1+2+3+4)} - F_{56-1} - F_{56-2} - F_{56-4}$$

Since $F_{56 - (1+2+3+4)} = F_{(1+2+3+4) - (5+6+7+8)} = 0.64$,

$F_{56 - 3} = 0.640 - 0.143 - 0.123 - 0.217 = 0.157$

Because $F_{56 - 1}$, $F_{56 - 2}$, $F_{56 - 3}$, and $F_{56 - 4}$ are based on a 0.64 total form factor between the structure and plate nodes 105 to 108 instead of the real value of 0.90 obtained in section 3.1, a correction factor is introduced.

$$\text{Correction factor} = \frac{0.90}{0.64} = 1.405$$

$F_{56 - 105} = (0.143)(1.405) = 0.201$

$F_{56 - 106} = (0.123)(1.405) = 0.173$

$F_{56 - 107} = (0.157)(1.405) = 0.221$

$F_{56 - 108} = (0.217)(1.405) = 0.305$

These form factors were input along with surface emissivities and areas into the interchange factor ($\mathfrak{F}$) computer program described in Reference 5. Emissivities and areas were as follows:

$A_{56} = (1.2)(26) = 31.20 \text{ in}^2 = 0.2165 \text{ ft}^2$

$A_{105} = A_{107} = (6.0)(3) = 18 \text{ in}^2 = 0.1249 \text{ ft}^2$

$A_{106} = (5)(3) = 15 \text{ in}^2 = 0.1041 \text{ ft}^2$

$A_{108} = (9)(3) = 27 \text{ in}^2 = 0.1874 \text{ ft}^2$

$\epsilon_{56} = 0.1$

$\epsilon_{105} = \epsilon_{106} = \epsilon_{107} = \epsilon_{108} = 0.05$

Radiation resistance paths were then determined as follows:

Path	Nodes	$\mathfrak{F}_{56-n}$	A_{56} (ft^2)	$\frac{1}{R} = A_{56}\,\mathfrak{F}_{56-n}$
69	56 - 105	.001391	.2165	.000301
70	56 - 106	.001197	.2165	.000259
71	56 - 107	.001529	.2165	.000331
72	56 - 108	.002110	.2165	.000457

Actually, the resistance reciprocals are listed above since this is the way radiation resistance data are input to the thermal analyzer.

Also, radiation interchange factors between the radiator plate nodes were determined, but the resultant resistances were so large that these paths were neglected.

The above procedures were repeated to obtain all resistance paths between the primary structure and the radiator plate. These resistances are listed in Appendix 3 as paths 69 to 83.

4.0 THERMAL BAG TO ELECTRONICS AND RADIATOR PLATE (PATHS 86-111)

Radiation between the thermal bag, electronics, and radiator plate is complex because of the presence of irregularly-orientated surfaces, cables, and wires. Since all involved components are at roughly similar temperatures, the resistances are relatively unimportant. Consequently, the following gross assumptions were made.

1. The electronics and plate form a single plane surface equal in area to the radiator plate and parallel to the thermal bag internal surface (node 54).

2. The form factor from the thermal bag to all electronic and plate surfaces combined is 0.5. The interference of cables is the reason for assuming this low value.

3. Form factors from the bag to each electronic and plate surface is a percentage of the 0.5 value equal to the ratio of surface area to total plane surface area. For example,

$$F_{54\text{-}37} = \frac{A_{37}}{A_{Plate}} \quad (0.5)$$

4. Reflected radiant energy is ignored; i.e., all radiation is direct. The analysis technique in Section 5.1.2.2 therefore applies.

5. $\epsilon = 0.1$ for electronics

   $\epsilon = 1.0$ for thermal bag

   $\epsilon = 0.05$ for radiator plate

The general resistance equation is

$$R_{54\text{-}n} = \frac{1 - \epsilon_{54}}{A_{54}\,\epsilon_{54}} + \frac{1}{A_{54}F_{54\text{-}n}} + \frac{1 - \epsilon_{n}}{A_{n}\,\epsilon_{n}}$$

An electronic components radiation area was assumed equal to the component area adjacent to the radiator plate. The radiation area for a plate node was the area not covered by electronics.

4.1 Examples

4.1.1 Resistance Path 86

This path involves the bag and PCU (node 27)

$$A_{37} = 0.2392 \text{ ft}^2$$

$$A_{54} = 4.13 \text{ ft}^2$$

$$F_{54\text{-}37} = \frac{0.2392}{4.13} (0.5) = 0.02896$$

$$R_{54\text{-}37} = \frac{1.0 - 1.0}{(4.13)(1.0)} + \frac{1}{(4.13)(.02896)} + \frac{1.0 - 0.1}{(.2392)(0.1)} = 45.993 \text{ ft}^{-2}$$

The value input to the thermal analyzer was $\frac{1}{R_{54\text{-}37}} = 0.02172 \text{ ft}^2$

4.1.2 Resistance Path 98

The bag and plate node 101 are involved. The total surface area of node 101 is 0.2413 ft^2, but that portion which radiates to the bag is 0.0831 ft^2.

$$F_{54\text{-}101} = \frac{.0831}{4.13} (0.5) = 0.01005$$

$$R_{54\text{-}101} = \frac{1.0 - 1.0}{(4.13)(1.0)} + \frac{1}{(4.13)(.01005)} + \frac{1.0 - 0.05}{(.0831)(.05)} = 252.736 \text{ ft}^2$$

$$\frac{1}{R_{54\text{-}101}} = 0.00395 \text{ ft}^2$$

5.0 RADIATION FROM PRIMARY STRUCTURE TO THERMAL BAG EXTERIOR (PATHS 112-116)

Two major assumptions were made:

1. Form factors from structure (Nodes 49-53) to bag (node 55) equal 1.0.

2. Nearly all heat exchange is between the structure and bag.

Consequently, the equation from Section 5.1.2.2 is applicable.

$$R_{n-55} = \frac{1}{A_n} \left[\frac{1}{\epsilon_n} + \frac{A_n}{A_{55}} \left(\frac{1}{\epsilon_{55}} - 1 \right) \right]$$

$$\epsilon_{49} = \epsilon_{50} = \epsilon_{51} = \epsilon_{52} = \epsilon_{53} = 0.1$$

$$\epsilon_{55} = 0.5$$

Subscript n refers to structure nodes

Sketches below give the general configurations used to obtain resistances.

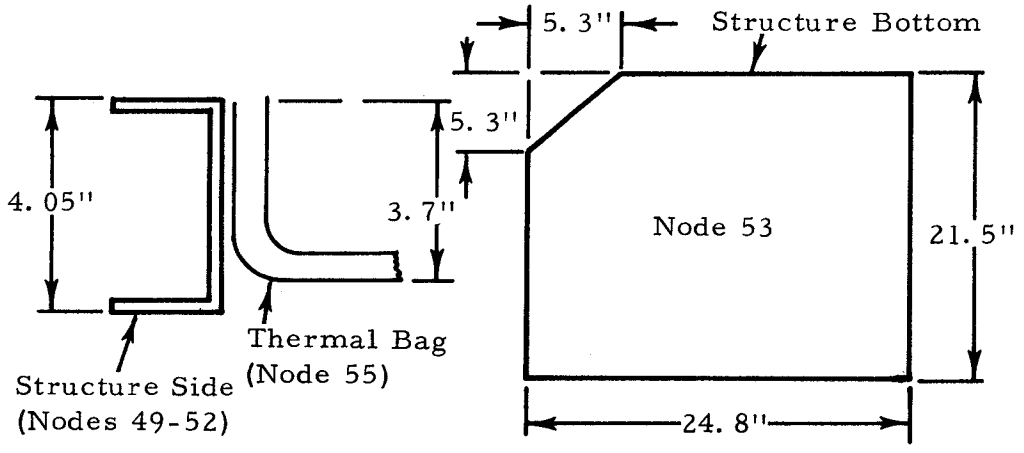

A_{53} and A_{55} were assigned equal areas for the resistance path $R_{53\text{-}55}$.

Overall dimensions are easily obtained from drawings.

5.1 Resistance Path 114

A sample evaluation, involving resistance $R_{51\text{-}55}$, is presented below:

$$A_{51} = (24.8 - 5.3)\,(4.05)/144 = 0.548 \text{ ft}^2$$

$$A_{55} = (24.8 - 5.3)\,(3.7)/144 = 0.501 \text{ ft}^2$$

$$R_{51\text{-}55} = \frac{1}{.548}\left[\frac{1}{.1} + \frac{.548}{.501}\left(\frac{1}{.5} - 1\right)\right] = 20.25 \text{ ft}^{-2}$$

$$\frac{1}{R_{51\text{-}55}} = 0.0494 \text{ ft}^2$$

6.0 CONDUCTION RESISTANCE BETWEEN STRUCTURE NODES

6.1 Conduction Around Structure Sides (Paths 118-121)

Sketches of the two types of channels used in the structure are shown below:

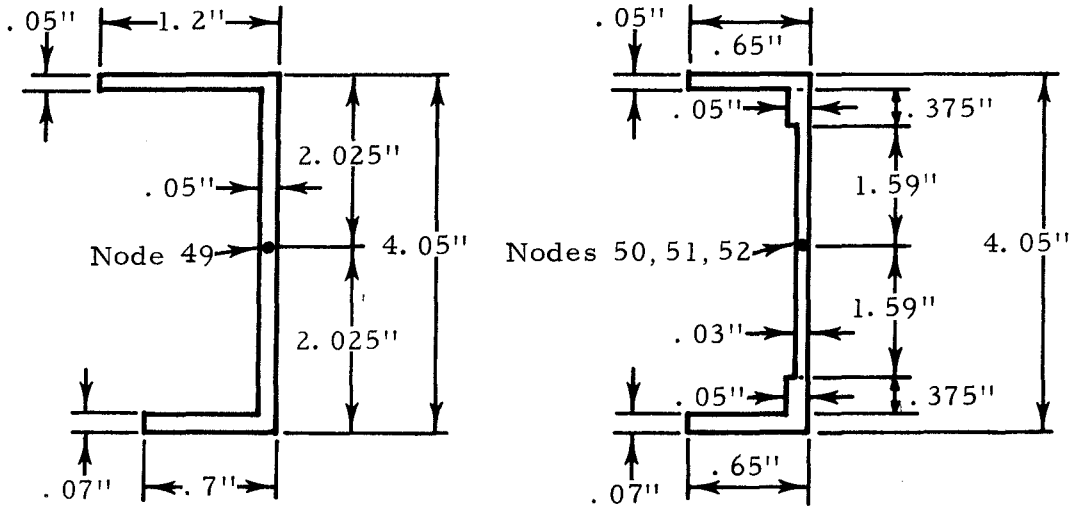

Lengths of the sides can be obtained from the sketch in Section 5.0 of the appendix.

The cross-sectional heat conduction areas are calculated below:

$$A_{49} = \left[(1.2)\,(.05) + (.7)\,(.07) + (4.05-.05-.07)\,(.05)\right] / 144 = 0.00212 \text{ ft}^2$$

$$A_{50} = A_{51} = A_{52} = \left[(.65)\,(.05) + (2)\,(.375)\,(.05) + (3.18)\,(.03) + (.65)\,(.07)\right]/144$$
$$= 0.00146 \text{ ft}^2$$

Each node is centered in a side, so that the resistance path length L consists of half the length of two adjacent sides. For example,

$$L_{49-50} = \frac{L_{49}}{2} + \frac{L_{50}}{2}$$

The equation of Section 5.2.1 is used with no contact resistances:

$$R_{m-n} = \frac{L_m}{K_m A_m} + \frac{L_n}{K_n A_n} = R_m + R_n$$

For a specific example (Path 118),

$$R_{49-50} = \frac{L_{49}/2}{K_{49} A_{49}} + \frac{L_{50}/2}{K_{50} A_{50}} = \frac{(24.8)/(2)(12)}{(99)(.00212)} + \frac{(23.7)/(2)(12)}{(99)(.00146)}$$

$$= 4.93 + 6.83 = 11.76 \text{ hr } ^{o}\text{F/Btu}$$

6.2 Conduction from Structure Sides to Bottom (Paths 149-152)

The resistance equation, from Section 5.2.1, is

$$R_{n-53} = \frac{L_n}{K_n A_n} + \frac{1}{h_c A_c} + \frac{L_{53}}{K_{53} A_{53}}$$

The techniques used to evaluate this resistance are best illustrated by an example involving path 152 and R_{52-53}. L_n is the distance from a structure side node to the center of the bottom flange. For example, it is easily seen from the previous sketches that

$$L_{52} = \frac{(1.59 + .375 + .65/2)}{12} = 0.191 \text{ ft}$$

Since the area varies along the length L_n, A_n represents an effective area which can be determined by the equation below (valid for constant K):

$$A_n = \frac{L_n}{\frac{L_1}{A_1} + \frac{L_2}{A_2} + \ldots + \frac{L_m}{A_m}}$$

For node 52,

$$L_1 = \frac{1.59}{12} = .1325 \text{ ft} \qquad A_1 = \frac{(23.4)(.03)}{144} = .00487 \text{ ft}^2$$

$$L_2 = \frac{.375}{12} = .0312 \text{ ft} \qquad A_2 = \frac{(23.4)(.05)}{144} = .00812 \text{ ft}^2$$

$$L_3 = \frac{.325}{12} = .0271 \text{ ft} \qquad A_2 = \frac{(23.4)(.07)}{144} = .01137 \text{ ft}^2$$

$$A_{52} = \frac{.191}{\frac{.1325}{.00487} + \frac{.0312}{.00812} + \frac{.0271}{.01137}} = .00571 \text{ ft}^2$$

Thus $\dfrac{L_{52}}{K_{52} A_{52}} = \dfrac{.191}{(99)(.00571)} = .34 \text{ hr } ^{\circ}\text{F/Btu}$

Assume that there is no contact resistance; i.e., $h_c = \infty$.

To obtain a reasonable evaluation of the term $\dfrac{L_{53}}{K_{53} A_{53}}$ requires some assumptions. Below is an outline of the structure bottom (represented by node 53):

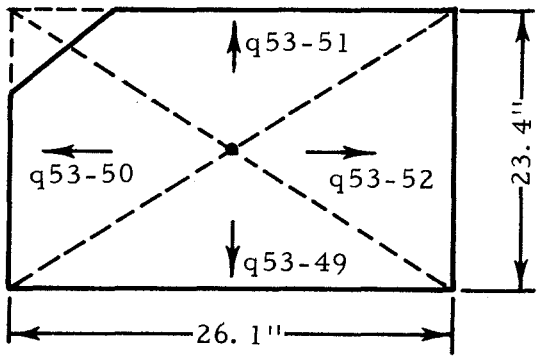

It would be convenient to locate node 53 at the center of the bottom, but the resulting resistance would be excessively high. This is because all heat flow across the bottom is not concentrated at the center but is somewhat evenly distributed over the surface. Consequently, all heat does not have to travel the entire distance from the bottom center to the sides, and it is assumed that node 53 is located halfway between the bottom center and each side. Also, we assume constant heat flow along a triangular path with varying area as illustrated in the sketches above and below.

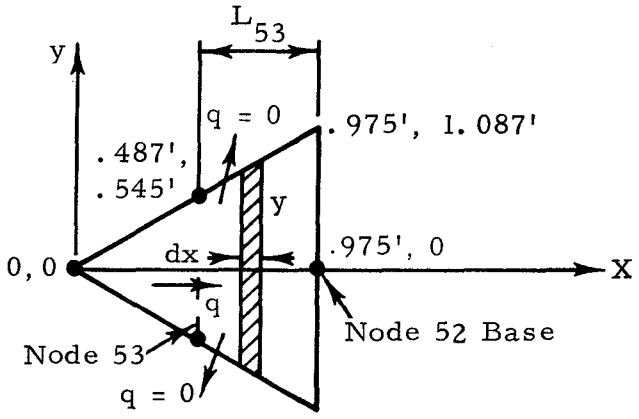

The resistance $\frac{L_{53}}{K_{53}\ A_{53}}$ is typical and will be calculated as an example. Heat flow across the element dx can be represented by

$$q = -K_{53}\ A_{53}\ \frac{dT}{dx}$$

$$y = \frac{13.05}{11.7}\ x = 1.12x$$

$$A = 2y\delta = 2.24\,\delta\,x$$

δ = plate thickness = 0.02 in.

Thus

$$q = -2.24\,Kx\,\delta\frac{dT}{dx} = \text{constant}$$

$$\int_{.487}^{.973}\frac{dx}{x} = -\frac{2.24K\delta}{q}\Delta T$$

Note that $x = .487'$ is the midway point between the bottom center and the bottom of side node 52.

$$\log_e x\Big]_{.487}^{.973} = -\frac{2.24K\delta}{q}\quad \Delta T = \log_e .973 - \log_e .487 = 0.692$$

$$q = -\frac{2.24K\delta}{.692}\qquad \Delta T = \frac{\Delta T}{R_{53}}$$

$$R_{53} = \frac{L_{53}}{A_{53}K_{53}} = \frac{q}{\Delta T} = \frac{(.692)\,(12)}{(2.24)\,(99)\,(.02)} = 1.87\ \text{hr}\ ^{o}\text{F/Btu}$$

The total resistance $R_{52\text{-}53}$ for path 152 is

$$R_{52\text{-}53} = \frac{L_{52}}{K_{52}A_{52}} + \frac{L_{53}}{K_{53}A_{53}} = 0.34 + 1.87 = 2.21\ \text{hr}\ ^{o}\text{F/Btu}$$

Remaining resistance paths are evaluated in the same manner.

7.0 CONDUCTION FROM STRUCTURE SIDES TO SUNSHIELD (PATHS 122-125)

Four posts of equal resistance provide heat flow paths between the structure and sunshield (node 31). Resistance path 126, which connects nodes 49 and 31, will be evaluated here as an example. Only the post material will be considered as all contact resistances are assumed zero.

Each post is a spring-like, hollow-tube device made of 0.006" stainless steel with bottom and top diameters of 5/8" and 1/4", respectively. A one-quarter overlap of the sides is assumed.

Average wall thickness = (0.25) (.012) + (0.75) (.006) = .0075 in.

Average diameter = 7/16 = 0.4375 in.

$$R_{49-31} = \frac{L}{KA} \qquad K = 9.4 \text{ Btu/ft hr } ^{\circ}F$$

$$A = \frac{\pi}{4}\left[(.4375)^2 - (.4225)^2\right] / 144 = 7.1 \times 10^{-5} \text{ ft}^2$$

$$L = 25 \text{ in.} = 2.085 \text{ ft}$$

$$R_{49-31} = \frac{2.085}{(9.4)\,(7.1\times10^{-5})} = 3125 \text{ hr } ^{\circ}F/\text{Btu}$$

Use $R_{49-31} = R_{50-31} = R_{51-31} = R_{52-31} = 3000$ hr $^{\circ}$F/Btu

8.0 RADIATION FROM STRUCTURE TO MOON AND SPACE (PATHS 126-146)

Radiation from the structure sides is complicated by the channel-type construction and the side curtain "overhang" on two sides (nodes 50 and 52). Also, brackets, wiring, and connectors complicate heat transfer from the front side (node 49). Figure 8.1 shows the model used to obtain form factors. Note that side curtain overhang was neglected and node 49 was treated as a flat plat instead of a channel, except that the bottom flange (49D) was considered in the moon factor. Letters after the node numbers refer to a part of the node. For example, 51A, 51B, 51C, and 51D refer, respectively, to the external vertical channel section, the top flange underside, the bottom flange topside, and the bottom flange underside.

8.1 Models for Obtaining Interchange Factors ($\mathcal{F}$'s)

Form factors between all surfaces, moon, and space were obtained with the CONFAC II program. Side curtain overhang was considered in the evaluation of the interchange factors and final resistance values. Curtain overhang essentially isolates the top flange and part of the vertical surface of nodes 50 and 52 from any radiant heat exchange with the moon and space, as illustrated in the sketches below.

Node 50

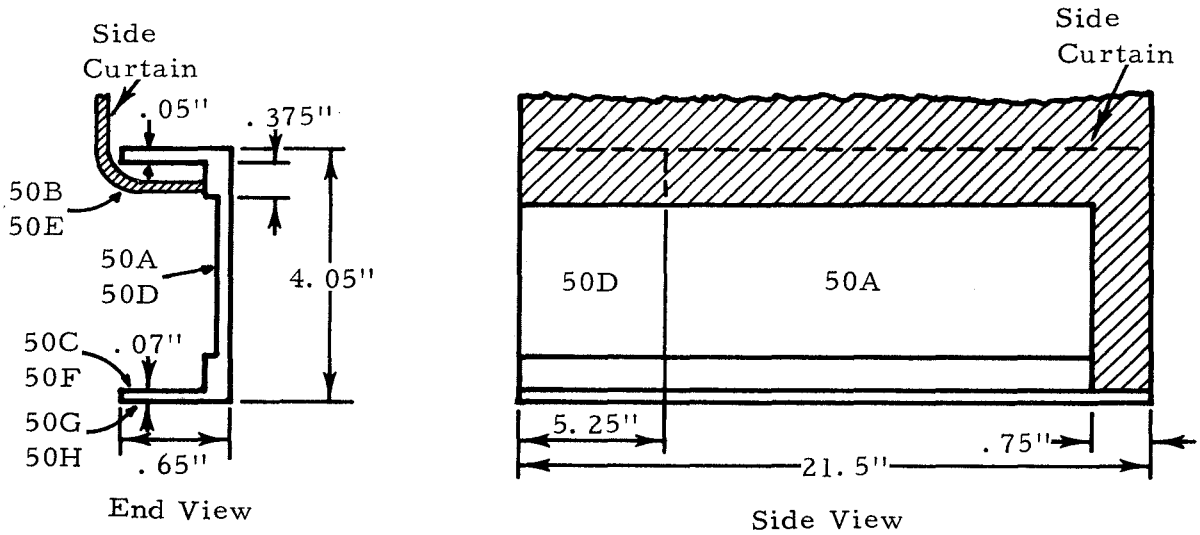

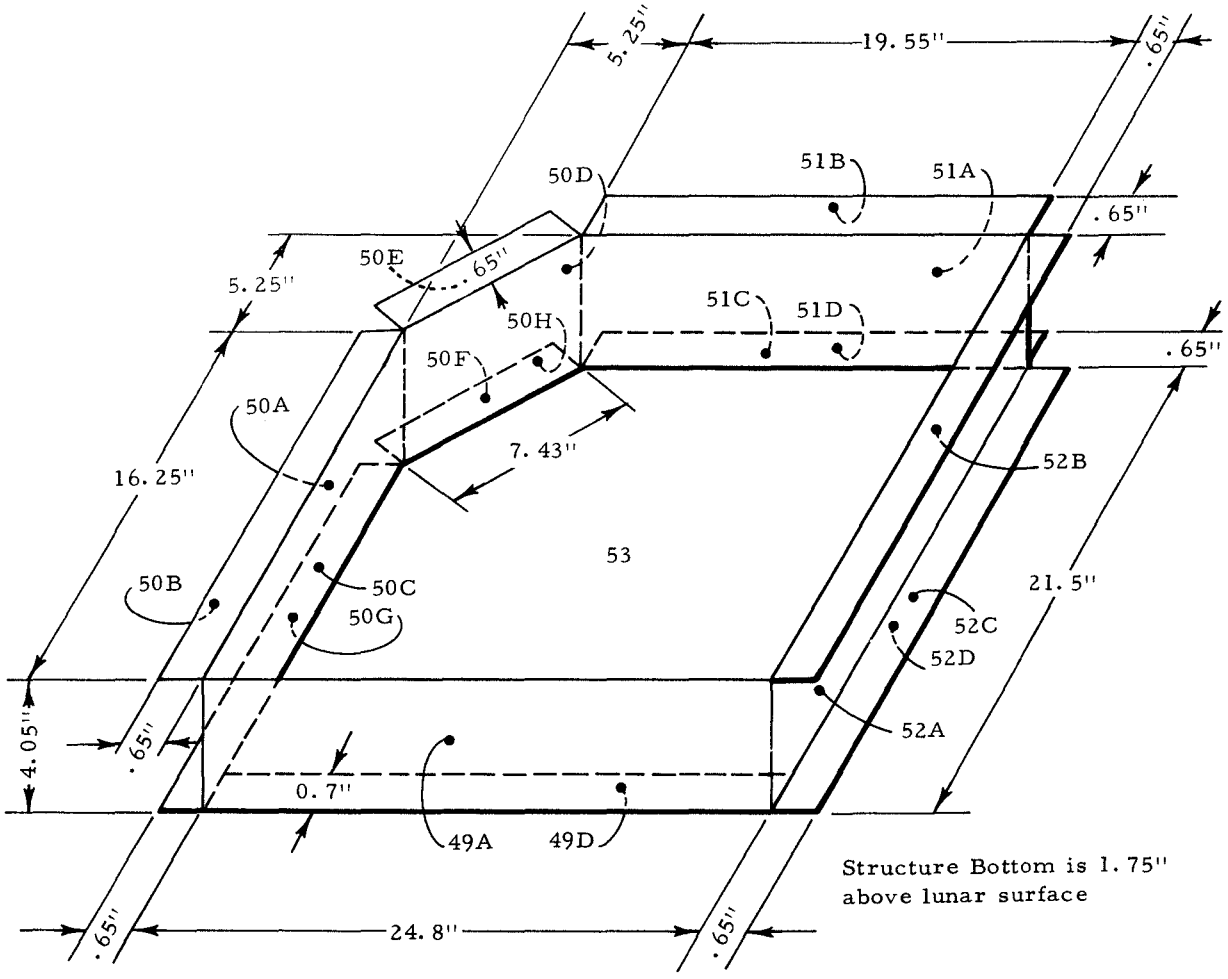

Figure 8.1 Primary Structure Model for Form Factors to Moon and Space

$\epsilon_{50A} = \epsilon_{50c} = \epsilon_{50D} = \epsilon_{50F} = 0.9 \qquad \epsilon_{50B} = \epsilon_{50E} = 0.5$

$\epsilon_{50G} = \epsilon_{50H} = 0.1$

$A_{50A} = (4.05 - .375 - .07 - .05)\ (16.25 - .75)/144 = .385\ ft^2$

$A_{50c} = A_{50G} = (16.25 - .75)\ (.65)/144 = .07\ ft^2$

$A_{50D} = (\frac{5.25}{.707})\ \ (4.05 - .375 - .07 - .05)/144 = .184\ ft^2$

$A_{50F} = A_{50H} = (\frac{5.25}{.707})\ (.65)/144 = .034\ ft^2$

Node 52

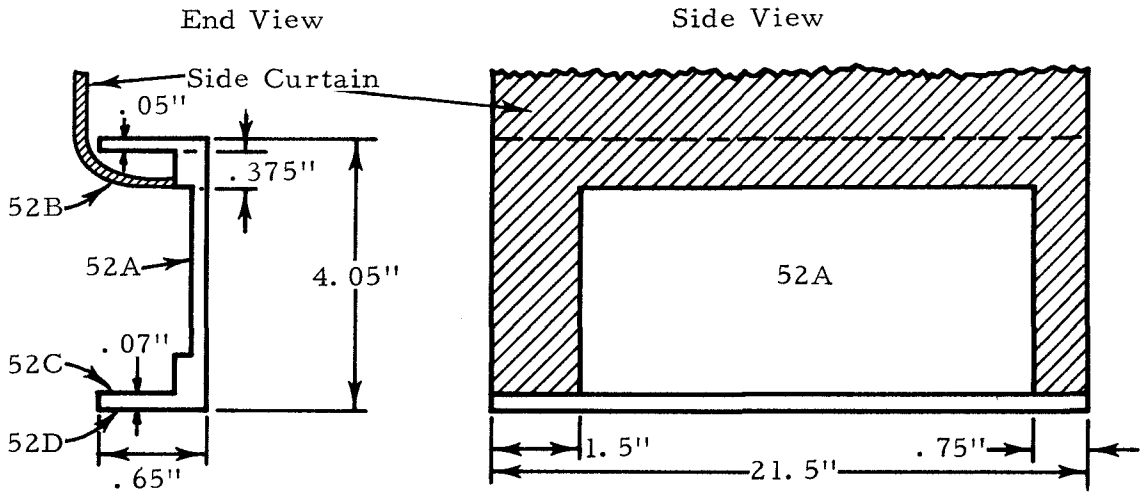

$\epsilon_{52A} = \epsilon_{52C} = 0.9 \qquad \epsilon_{52B} = 0.5 \qquad \epsilon_{52D} = 0.1$

$A_{52A} = (21.5 - .75 - 1.5)\ (4.05 - .375 - .05 - .07)/144 = .477\ ft^2$

$A_{52C} = A_{52D} = (21.5 - .75 - 1.5)\ (.65)\ /144 = .087\ ft^2$

When obtaining $\mathcal{F}$'s with the computer program, each side curtain section blocking a top flange was assumed to be the flange. Because of the relatively low emissivity and consequent small $\mathcal{F}$, these top flanges were neglected in the final resistance equations for nodes 50 and 52 as illustrated in the following equations.

8.2 Resistance Calculations

Sample calculations are presented for two structure sides, one with and one without side curtain overhang. Unless otherwise specified, $\mathcal{F}$'s were obtained with the ABSORP computer program.

8.2.1 Structure with Side Curtain Overhang

Calculations are presented for radiation resistances between node 50, moon, and space. Node 50 consists of sections 50A through 50H, as shown on previous figures. An energy balance between node 50 and the lunar surface (node 99) can be written as follows:

$$q_{50-99} = \Big[\mathcal{F}_{50A-99} A_{50A} + \cancelto{0}{\mathcal{F}_{50B-99}} A_{50B} + \mathcal{F}_{50c-99} A_{50c} + \mathcal{F}_{50D-99} A_{50D} + \cancelto{0}{\mathcal{F}_{50E-99}} A_{50E} + \mathcal{F}_{50F-99} A_{50F} + \mathcal{F}_{50G-99} A_{50G} + \mathcal{F}_{50H-99} A_{50H} \Big]$$

$$\sigma (T_{50}^4 - T_{99}^4) = \mathcal{F}_{50-99} A_{50} \sigma (T_{50}^4 - T_{99}^4)$$

$$= \frac{1}{R_{50-99}} \sigma (T_{50}^4 - T_{99}^4)$$

All node 50 sections are assumed equal in temperature. $\mathcal{F}_{50B-99}$ and $\mathcal{F}_{50E-99}$ represent the curtains and are assumed negligible.

$$\frac{1}{R_{50-99}} = (.36899)(.385) + (.01931)(.070) + (.35967)(.184) + (.01768)(.034) + (.1)(1)(.070) + (.1)(1)(.034)$$

$$= .22059 \text{ ft}^2$$

In the above equation, the form factors from surfaces 50G and 50H to the moon were assumed equal to 1, which gave

$$\mathcal{F}_{50G-99} A_{50G} = F_{50G-99} \epsilon_{50G} A_{50G} = (1)(.1)(.070) = .0070$$

$$\mathcal{F}_{50H-99} A_{50H} = F_{50H-99} \epsilon_{50H} A_{50H} = (1)(.1)(.034) = .0034$$

Similarly, the resistance between node 50 and space (node 100) is obtained as follows:

$$q_{50-100} = \Big[\mathcal{F}_{50A-100} A_{50A} + \cancelto{0}{\mathcal{F}_{50B-100} A_{50B}} + \mathcal{F}_{50C-100} A_{50C} + \mathcal{F}_{50D-100} A_{50D} + \cancelto{0}{\mathcal{F}_{50E-100} A_{50E}} + \mathcal{F}_{50F-100} A_{50F} + \cancelto{0}{\mathcal{F}_{50G-100} A_{50G}} + \cancelto{0}{\mathcal{F}_{50H-100} A_{50H}} \Big]$$

$$\sigma (T_{50}^4 - T_{100}^4) = \mathcal{F}_{50-100} A_{50} \sigma (T_{50}^4 - T_{100}^4) = \frac{1}{R_{50-100}} \sigma (T_{50}^4 - T_{100}^4)$$

$\mathcal{F}_{50B-100}$ and $\mathcal{F}_{50E-100}$ represent the curtains and are assumed negligible. $\mathcal{F}_{50G-100}$ and $\mathcal{F}_{50H-100}$ are zero since $F_{50G-100} = F_{50H-100} = 0$.

$$\frac{1}{R_{50-100}} = (.40933)(.385) + (.45774)(.070) + (.44987)(.184) + (.48722)(.034) = .28897$$

Two paths, $\frac{1}{R_{50-99}}$ and $\frac{1}{R_{50-100}}$, have to be adjusted to account for the non-uniform space and lunar noon surface temperature distributions. This is duscussed in sections 8.2.3 and 8.2.4.

8.2.2 Structure with No Side Curtain Overhang

Evaluation of resistance paths between node 51, moon, and space is presented. An energy balance between the node and lunar surface gives

$$q_{51-99} = \left[\mathcal{F}_{51A-99} A_{51A} + \mathcal{F}_{51B-99} A_{51B} + \mathcal{F}_{51C-99} A_{51C} + \mathcal{F}_{51D-99} A_{51D} \right]$$

$$\sigma (T_{51}^4 - T_{99}^4) = \mathcal{F}_{51-99} A_{51} \sigma (T_{51}^4 - T_{99}^4) = \frac{1}{R_{51-99}} \sigma (T_{51}^4 - T_{99}^4)$$

$$\frac{1}{R_{51-99}} = (.35980)(.545) + (.42504)(.0875) + (.01910)(.0875)$$
$$+ (.1)(1)(.0875) = .24370$$

where

$$\mathcal{F}_{51D-99} A_{51D} = F_{51D-99} \epsilon_{51D} A_{51D} = (1)(.1)(.0875) = .00875$$

An energy balance between node 51 and space gives

$$q_{51-100} = \left[\mathcal{F}_{51A-100} A_{51A} + \mathcal{F}_{51B-100} A_{51B} + \mathcal{F}_{51C-100} A_{51C} + \mathcal{F}_{51D-100} A_{51D} \right]$$

(0)

$$\sigma (T_{51}^4 - T_{100}^4) = \mathcal{F}_{51-100} A_{51} \sigma (T_{51}^4 - T_{100}^4) = \frac{1}{R_{51-100}}$$

$$\sigma (T_{51}^4 - T_{100}^4)$$

$$\frac{1}{R_{51-100}} = (.41762)(.545) + (.04685)(.0875) + (.45279)(.0875) = .27132$$

Again, these values will be adjusted, as explained in the following sections, to account for uneven moon and space temperature distributions.

8.2.3 Effect of Moon Temperature Distribution on Resistance Paths

Figure 23 showed a wide variation in lunar surface temperature for the noon condition. Since temperatures closest to the structure exert the greatest influence, the moon surface was divided into 13 isothermal nodes depicted in Figure 15. The large nodes exert relatively little influence on primary structure temperature since they receive only about 15% of the heat flux from the structure. Average temperature for each node is listed in Table 1 and has been corrected for the "non-black" properties of the lunar surface simulator as explained in Section 5.3.

The effect of varying moon temperature was accounted for by determining resistance paths from each structure node to all applicable moon nodes. Approximate techniques were employed to obtain form factors and resistances since more exact, time-consuming calculations would not improve analysis accuracy. If we assume form factors from bottom structure flanges to node 152 equal to one, then

$$\frac{1}{R_{m-152}} = F_{m-152} \epsilon_m A_m = (1.0)(0.1) A_m$$

where m refers to the surface which "sees" node 152. Consequently, the resistances calculated in sections 8.2.1 and 8.2.2 are adjusted as follows:

$$\frac{1}{R_{50-152}} = F_{50G-152} A_{50G} \epsilon_{50G} + F_{50H-152} A_{50H} \epsilon_{50H}$$
$$= (1)(.070)(.1) + (1)(.034)(.1)$$
$$= \underline{0.01040 \text{ ft}^2}$$

$$\frac{1}{R_{50-(143+144+145)}} = \frac{1}{R_{50-99}} - \frac{1}{R_{50-152}} = 0.22059 - 0.01040$$
$$= \underline{0.21019}$$

$$\frac{1}{R_{51-152}} = F_{51D-152} A_{51D} \epsilon_{51D} = (1)(.0875)(.1)$$
$$= \underline{0.00875 \text{ ft}^2}$$

$$\frac{1}{R_{51-(146+147+148)}} = \frac{1}{R_{51-99}} - \frac{1}{R_{51-152}} = 0.24370 - 0.00875$$
$$= \underline{0.23495}$$

It is now necessary to obtain individual resistances from structure nodes to the remaining moon nodes 140-151. The following model was used in determining individual form factors for all structure sides.

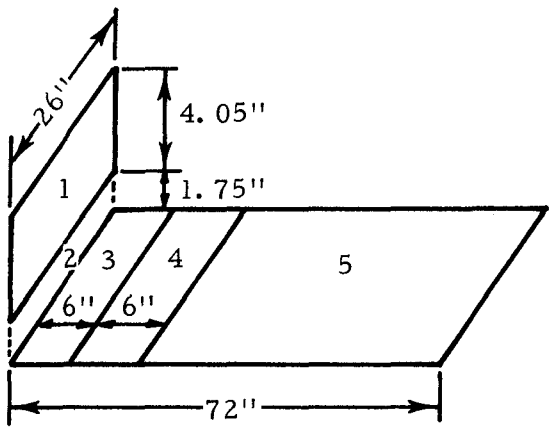

$A_1 = 105.3 \text{ in.}^2$

$A_2 = 45.5 \text{ in.}^2$

$A_{1+2} = 150.8 \text{ in.}^2$

Surface 1 = structure node

Surface 2 = gap between structure and moon

Surfaces 3, 4, 5 = moon nodes

From Figure 12, reference 7,

$$F_{(1+2)-(3+4+5)} = 0.39 \qquad F_{2-(3+4+5)} = 0.46$$

From form factor geometry,

$$A_{(1+2)} F_{(1+2)-(3+4+5)} = A_1 F_{1-(3+4+5)} + A_2 F_{2-(3+4+5)}$$

$$F_{1-(3+4+5)} = \frac{(150.8)(.39) - (45.5)(.46)}{105.3}$$

$$= \underline{0.361},$$ the form factor from the structure node to entire moon.

Form factors from the structure node to individual moon nodes are found in a similar manner.

$$F_{(1+2)-3} = 0.28 \qquad F_{2-3} = 0.41$$

$$A_{1+2} F_{(1+2)-3} = A_1 F_{1-3} + A_2 F_{2-3}$$

$$F_{1-3} = \frac{(150.8)\,(.28) - (45.5)(.41)}{105.3}$$

$$= \underline{.225}$$

$$F_{(1+2)\,-\,(3+4)} = 0.34 \qquad F_{2\,-\,(3+4)} = 0.44$$

$$F_{(1+2)\,-4} = F_{(1+2)\,-\,(3+4)} - F_{(1+2)\,-3}$$

$$= 0.34 - 0.28 = 0.06$$

$$F_{2-4} = F_{2-\,(3+4)} - F_{2-3}$$

$$= 0.44 - 0.41 = 0.03$$

$$A_{1+2}\, F_{(1+2)-4} = A_1\, F_{1-4} + A_2\, F_{2-4}$$

$$F_{1-4} = \frac{(150.8)\,(.06) - (45.5)\,(.03)}{105.3}$$

$$= \underline{.073}$$

$$F_{1-5} = F_{1-(3+4+5)} - F_{1-3} - F_{1-4}$$

$$= 0.361 - 0.225 - 0.073$$

$$= \underline{0.063}$$

These form factors were used in the following manner to obtain resistances to individual moon nodes.

$$\frac{1}{R_{m-3}} = \frac{0.225}{0.361} \quad \frac{1}{R_{m-(3+4+5)}} = \frac{0.624}{R_{m-(3+4+5)}}$$

$$\frac{1}{R_{m-4}} = \frac{0.073}{0.361} \quad \frac{1}{R_{m-(3+4+5)}} = \frac{0.202}{R_{m-(3+4+5)}}$$

$$\frac{1}{R_{m-5}} = \frac{0.063}{0.361} \quad \frac{1}{R_{m-(3+4+5)}} = \frac{0.174}{R_{m-(3+4+5)}}$$

For the examples presented in Sections 8.2.1 and 8.2.2, the resistances used in the thermal analyzer for noon condition are as follows:

Path	Nodes	$\frac{1}{R_{m-n}}$
131	50-143	(.624) (.21019) = .13116
132	50-144	(.202) (.21019) = .04246
133	50-145	(.174) (.21019) = .03657
134	50-152	.01040 (as determined previously)
136	51-146	(.624) (.23495) = .14661
137	51-147	(.202) (.23495) = .04756
138	51-148	(.174) (.23495) = .04088
139	51-152	.00875 (as determined previously)

8.2.4 Effect of Space Temperature Distribution on Resistance Paths

Figure 24 showed the temperature distribution over the vacuum chamber arch, door, and curtain; Figure 16 gave the nodal division

of the simulated space which applied to both noon and night conditions; and Table 1 lists the average temperature of each node. Each primary structure node was assumed to see only one of the 3 space nodes (97, 98, or 100) as designated below:

Resistance Path	Nodes	$\frac{1}{R_{m-n}}$
130 (Noon)	49-100	.16681
131 (Night)	"	"
135 (Noon)	50-97	.28897
133 (Night)	"	"
140 (Noon)	51-100	.27132
135 (Night)	"	"
145 (Noon)	52-98	.24825
137 (Night)	"	"

8.2.5 Assumption for Primary Structure Front

A somewhat gross assumption was made concerning node 49, the structure front surface. Because of all the brackets, cables, connectors, etc. which reduce radiation effectiveness from this surface, only one-half of section 49A was used in calculating resistance paths to moon and space.

9.0 RADIATION FROM SIDE CURTAINS TO MOON & SPACE (PATHS 166-174)

Form factors were obtained by supplying coordinates, shown in Figure 9.1, to the CONFAC II program. Coordinatesare X, Y, Z from top to bottom. Although not shown, coordinates for the lunar surface were input along with the node data. The method of section 5.1.2.1 was then used to obtain resistances, with $\epsilon_{27} = \epsilon_{28} = \epsilon_{29} = \epsilon_{30} = 0.5$.

PATH	NODES	F_{m-n}	$\mathfrak{F}_{m-n}$	A (ft^2)	$\frac{1}{R}$ (ft^2)
166	27-99	0.26212	0.13106	5.4767	0.71778
167	27-100	0.73788	0.36894	5.4767	2.02057
168	28-99	0.39180	0.19590	3.8241	0.74914
169	28-100	0.60820	0.30410	3.8241	1.16291
170*	29-30	0.03833	0.00958	1.3498	0.01293
171	29-99	0.38243	0.19121	1.3498	0.25810
172	29-100	0.57924	0.28962	1.3498	0.39093
173	30-99	0.38176	0.19088	0.6533	0.12470
174	30-100	0.53904	0.26952	0.6533	0.17608

* This path involves the only two side curtain external nodes which "see" each other. The resistance was calculated with a special equation for two "grey" surfaces seeing each other plus moon and space.

$$\frac{1}{R_{29-30}} = \frac{1}{\mathfrak{F}_{29-30} A_{29}} \left(\frac{1-\rho_{29}\ \rho_{30}\ F_{29-30} F_{30-29}}{\epsilon_{29}\ \epsilon_{30}\ F_{29-30}} \right) \frac{1}{A_{29}}$$

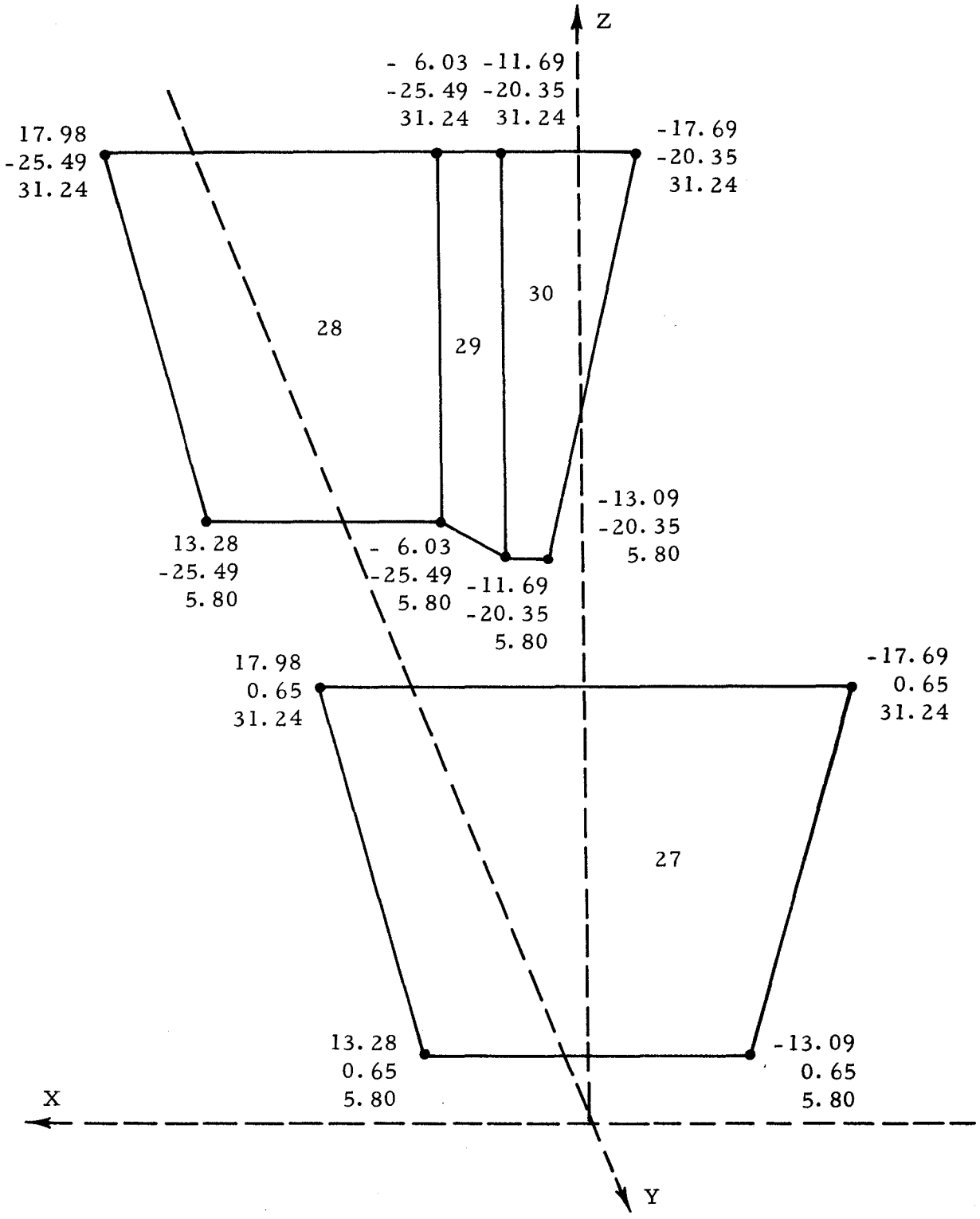

Figure 9.1 Form Factor Model for Side Curtains (Nodes 27-30)

where $F_{30-29} = \left(\frac{A_{29}}{A_{30}}\right)\left(F_{29-30}\right) = .07920$

$\rho_{29} = \rho_{30} = 0.5$ (surface reflectance)

10.0 RADIATION FROM SUNSHIELD TO SPACE (PATHS 175-179)

Even though space was divided into three nodes (97, 98, 100), only the honeycombed portion (node 31) of the sunshield was assumed to radiate to all space nodes. This was done only for correlation purposes and not because sunshield temperatures affect C/S performance. The following sections describe resistance calculations for each sunshield portion and show plan views of the nodes.

10.1 Node 31 to Space (Paths 175, 176, & 179)

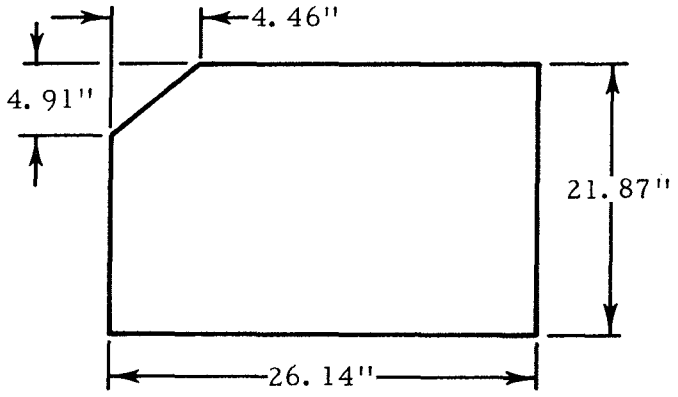

$A_{31} = \left[(26.14)(21.87) - (.5)(4.91)(4.46)\right] / 144 = 3.894 \text{ ft}^2 \quad \epsilon_{31} = 0.9$

Approximate form factors to the three space nodes can be found as follows: Reference 7 gives the equation for factors between a point source and a disk:

$$F_{31-n} = \left(\frac{D}{2}\right)\left[\frac{1+R^2+D^2}{\sqrt{(1+R^2+D^2)^2 - 4R^2}} - 1\right]$$

where D = a/b R = r/b

a, r, and b are defined in the sketch below where the sunshield is an assumed point source and the ends of the vacuum chamber are regarded as disks.

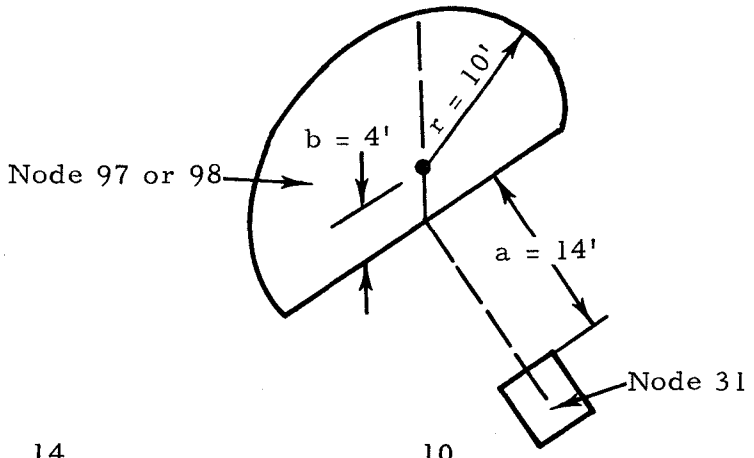

$$D = \frac{14}{4} = 3.5 \qquad R = \frac{10}{4} = 2.5$$

$$F_{31-97} = F_{31-98} = 0.06$$

With the assumption that $F_{31-97} + F_{31-98} + F_{31-100} = 1.0$, the method of Section 5.1.2.1, where $\frac{1}{R_{m-n}} = F_{m-n} A_m \epsilon_m$, may be used to determine resistance.

PATH	NODES	$1/R_{m-n}$ (ft^2)
175	31-97	(0.9) (0.06) (3.894) = 0.2105
176	31-100	(0.9) (0.88) (3.894) = 3.0840
179	31-98	(0.9) (0.06) (3.894) = 0.2105

10.2 Node 32 to Space (Path 177)

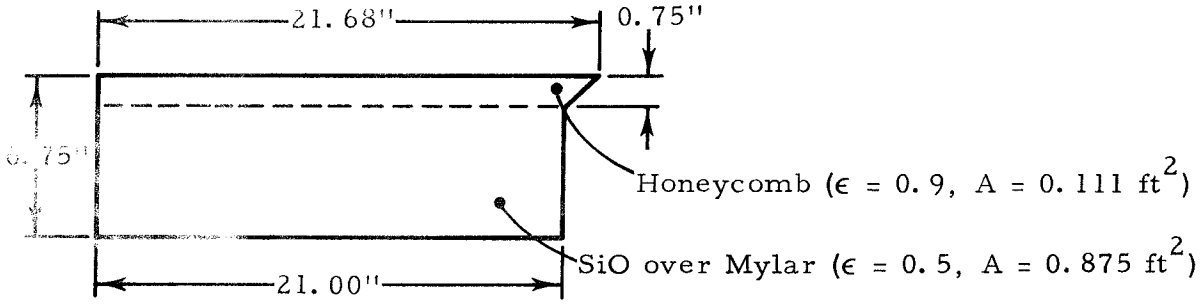

Assume that $F_{32-100} = 1.0$

Calculate an effective emissivity as follows:

$$A_{32}\ \epsilon_{32} = A_1\ \epsilon_1 + A_2\ \epsilon_2$$

$$\epsilon_{32} = \frac{1}{0.986}\left[(0.5)\ (0.875) + (0.9)\ (0.111)\right] = 0.54$$

The section 5.1.2.1 technique can now be employed.

$$\frac{1}{R_{32-100}} = F_{32-100}\ \epsilon_{32}\ A_{32} = (1)\ (.54)\ (0.986)$$

$$= 0.5325\ ft^2$$

10.3 Node 33 to Space (Path 178)

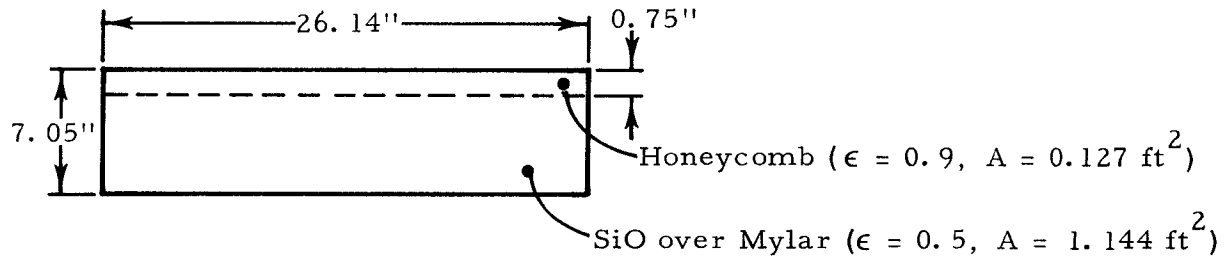

$F_{33-100} = 1.0$

$$\epsilon_{33} = \frac{1}{A_{33}} \left[A_1 \epsilon_1 + A_2 \epsilon_2 \right] = 0.54$$

$$\frac{1}{R_{33-100}} = F_{33-100} \epsilon_{33} A_{33} = (1)(.54)(1.271)$$
$$= 0.6862 \text{ ft}^2$$

11.0 RADIATION BEHIND REFLECTORS (PATHS 180-194)

Form factors for the enclosure formed by the reflector backsides, sunshield, and side curtains were obtained with the CONFAC II program. Since the geometrics involved are simple and the technique similar to that in Section 9.0, program input coordinates are not shown here. Interchange factors were then supplied by the ABSORP computer program. All surfaces are diffuse with 0.1 emissivities, except the "gap" had an assumed value of 0.95. The gap (node 132) refers to a void between the reflector (node 118) edge and side curtain. Form factors, areas, $\mathfrak{F}$'s, and resistance reciprocals are listed below.

PATH	NODES	F_{m-n}	$\mathfrak{F}_{m-n}$	$A_{m(ft^2)}$	$1/R_{m-n\ (ft^2)}$
180	35-34	0.26561	0.02027	1.932	0.03916
181	34-36	0.13965	0.00992	3.895	0.03864
182	117-34	0.28973	0.02026	5.025	0.12346
183	118-34	0.28859	0.02067	4.483	0.09266
184	34-132	0.01382	0.01249	3.895	0.04865
185	35-36	0.10325	0.00978	1.932	0.01889

PATH	NODES	F_{m-n}	$\mathfrak{F}_{m-n}$	$A_{m(ft^2)}$	$1/R_{m-n(ft^2)}$
186	35-117	0.31654	0.02615	1.932	0.05052
187	35-118	0.31093	0.02400	1.932	0.04637
188	35-132	0.00367	0.01172	1.932	0.02264
189	117-36	0.13150	0.00990	5.025	0.04975
190	118-36	0.09753	0.00988	4.483	0.04429
191	36-132	0.05340	0.01554	2.000	0.03108
192	117-118	0.44063	0.02457	5.025	0.12346
193	117-132	0.01749	0.01274	5.025	0.06402
194	118-132	0.00154	0.01183	4.483	0.05303

12.0 RADIOSITY NODE NETWORK (PATHS 200-299)

Radiosity resistance paths were determined as follows:

1. Form factors from all "real" C/S surfaces to all other real surfaces, reflector images, moon, and space were obtained with CONFAC II. All blocking effects were considered. Cutouts in the insulation masks were neglected, while the gap between the reflector node 118 and the side curtain was considered.

2. For resistance calculations, surface areas of actual insulation masks and reflectors were used. Cutout areas from the masks were added to the uninsulated radiator plate areas.

3. Techniques in Section 5.1.1 were employed to obtain the various resistance values and their reciprocals.
   a. Surface Resistance

$$\frac{1}{R_m} = A_m \left(\frac{\epsilon_m}{1-\epsilon_m}\right)$$

$\epsilon_m = 0.1$ for all diffuse surfaces

$\epsilon_m = 0.05$ for specular reflector

b. Resistance Between Diffuse Radiosity Nodes.

$$\frac{1}{R_m} = A_m \left(F_{m-n} + \rho_s F_{m-n\,(i)} \right)$$

F_{m-n} = form factor between real surfaces m and n

$F_{m-n(i)}$ = form factor from real surface m to surface n image in specular reflector

ρ_s = specular reflectivity of reflector = 0.9

c. Resistance between a Diffuse and a Diffuse-Specular Node

$$\frac{1}{R_{m-n}} = A_m F_{m-n} (1 - \rho_s)$$

13.0 CABLE HEAT LEAK BETWEEN STRUCTURE AND DEPLOYED EXPERIMENTS (PATH 422)

A method is presented to approximate cable resistance between the primary structure (node 49) and deployed experiments. Cables are treated as fins, and it is assumed that at some location (node 60) cables are at an "equivalent" temperature which is a function of lunar surface and space environmental effects described in the following sections. A "cable" resistance path is composed of three sections: (1) wire and insulation which constitute the various cables, (2) cable connectors on the primary structure, and (3) brackets fastened to the structure, which support the connectors.

Figure 13.1 shows a typical external cabling connection and cable feed-through into the C/S.

13.1 Cable Resistance

Cable resistance refers to the total resistance of all cables between experiments and the primary structure. Even though the following analysis techniques are developed for a single cable, they are applicable to every cable. A combined resistance is easily determined by treating the cables as parallel heat flow paths.

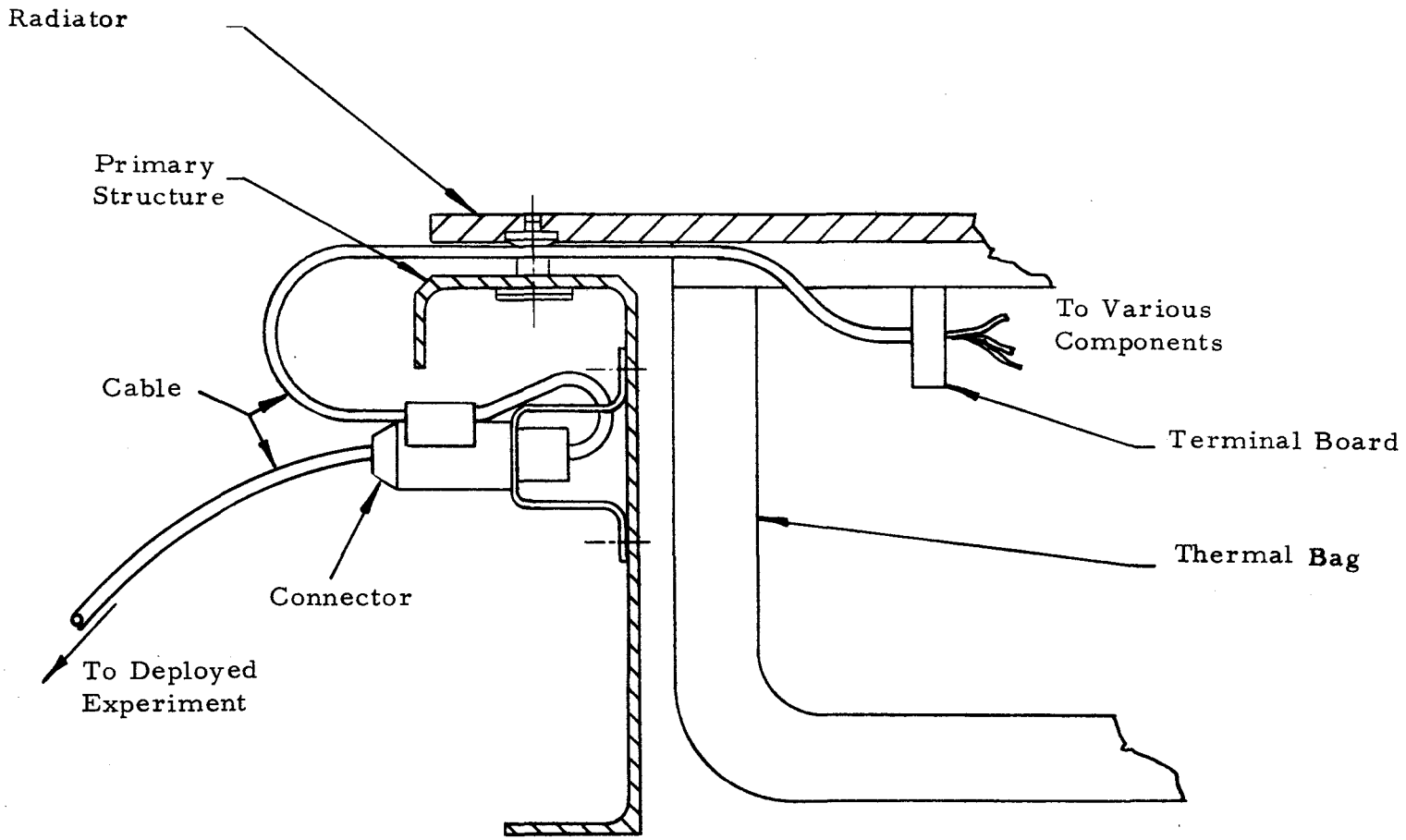

NOTE: Manganin inserts extend from connector to terminal board.

Figure 13.1 Typical Cable Feed-Through and Extension to Deployed Experiment

13.1.1 Thermal Model for Environmental Influence

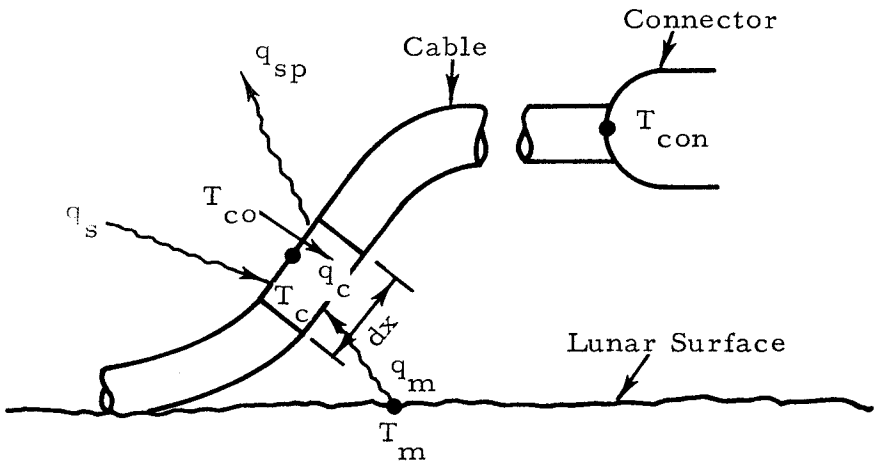

Besides evaluating an "equivalent" temperature, an "effective" conduction resistance will be formed which accounts for radiative environmental effects as well as wire resistance.

13.1.2 Energy Balance at External Insulation Surface

A cable is assumed to have a 0.005 inch layer of insulation about the copper wire. All heat transfer from the moon to the cable is assumed radiant.

$$q_s + q_m = q_{sp} + q_c$$

$$q_s = A_s Q_s \alpha_s = h_m A (T_s - T_m) = \text{solar heating}$$

q_c = Net heat flow into cable

q_m = Radiation from lunar surface

q_{sp} = Radiation to space

$$q_{sp} = A_{co2}\, \mathfrak{F}_{co2 - sp}\, \sigma (T_{co}^{4} - T_{sp}^{4}) = h_{sp} A (T_{co} - T_{sp})$$

$$q_{m} = A_{col}\, \mathfrak{F}_{col - m}\, \sigma (T_{m}^{4} - T_{co}^{4}) = h_{m} A (T_{m} - T_{co})$$

A_s = area receiving solar radiation, ft^2

A_{col} = radiation area - cable to moon, ft^2

A_{co2} = radiation area - cable to space, ft^2

A = total external cable area = $A_{col} + A_{co2}$, ft^2

$\mathfrak{F}_{col-m}$ = radiation interchange factor - cable to moon

$\mathfrak{F}_{co2-sp}$ = radiation interchange factor - cable to space

h_m = equivalent radiation coefficient - cable to moon, $Btu/ft^2\ hr\ ^oF$

h_{sp} = equivalent radiation coefficient - cable to space, $Btu/ft^2\ hr\ ^oF$

Q_s = solar radiation = 442 $Btu/ft^2\ hr$

T_s = equivalent solar temperature, ^oF

T_m = lunar surface temperature, ^oF

T_{sp} = space temperature, ^oF

T_c = wire temperature, ^oF

T_{co} = cable external surface temperature, ^oF

α_s = solar absorptivity

σ = Stefan-Boltzman constant = 0.1713×10^{-8} Btu/ft^2 hr $^oR^4$

13.1.3 Equivalent External Temperature (T_e) and Heat Transfer Coefficients (h_m & h_{sp})

$$h_m = \frac{\mathcal{F}_{col-m}\ \sigma\ (T_m^4 - T_{co}^4)\ A_{col}}{(T_m - T_{co})\ A}$$

$$h_{sp} = \frac{\mathcal{F}_{co2-sp}\ \sigma\ (T_{co}^4 - T_{sp}^4) A_{co2}}{(T_{co} - T_{sp})\ A}$$

Since $A_s\ Q_s\ \alpha_s = h_m\ A\ (T_s - T_m)$,

$$T_s = T_m + \frac{A_s\ Q_s\ \alpha_s}{h_m A}$$

From the energy balance, one can write

$$q_c = h_m A\ (T_s - T_m) + h_m A\ (T_m - T_{co}) - h_{sp} A\ (T_{co} - T_{sp})$$

$$= h_m A\ (T_s - T_{co}) - h_{sp} A\ (T_{co} - T_{sp})$$

Let $h_{sp} A\ (T_{co} - T_{sp}) = h_m A\ (T_{co}^1 - T_{sp})$

$$T_{co}^1 = T_{sp} + \frac{h_{sp}}{h_m}\ (T_{co} - T_{sp})$$

$$q_c = h_m A\ (T_s - T_{co} - T_{co}^1 + T_{sp}) = h_m A\ (T_e - T_{co})$$

where $$T_e = T_s - T_{co}^1 + T_{sp}$$

13.1.4 Evaluation of Coefficients

Assuming the following:

$$F_{col-m} = F_{co2-sp} = 0.5$$

$$\epsilon_{co} = 0.9 \qquad \alpha_s = 0.3$$

$$A_{col} = A_{co2} = A_s = \frac{A}{2}$$

Cable insulation transmissivity = 0

$$\mathcal{F}_{col-m} = F_{col-m}\ \epsilon_{co} = (0.9)(0.5) = 0.45$$

$$\mathcal{F}_{co2-sp} = F_{co2-sp}\ \epsilon_{co} = (0.9)(0.5) = 0.45$$

$$T_s = T_m + \frac{(442)(0.3)(0.5)}{h_m} = T_m + \frac{66.2}{h_m} \text{ for lunar noon}$$

13.1.4.1 Noon Condition

Assume $T_m = 250^\circ F$ $\qquad T_{co} = 220^\circ F$

$$T_{sp} = \frac{-203 - 213 - 248}{3} = -221^\circ F$$

$h_m = .518$ Btu/ft^2 hr $^\circ$F, $\qquad h_{sp} = 0.184$ Btu/ft^2 hr $^\circ$F

$T_s = 378^\circ F$ $\qquad T'_{co} - T_{sp} = 157^\circ F$ $\qquad T_e = 221^\circ F$

$$q_c = .518A\,(221 - T_{co})$$

13.1.4.2 Night Condition

Assume $T_m = -300\ ^\circ F$

$$T_{sp} = \frac{-231 - 239 - 260}{3} = -243\ ^\circ F$$

$$T_{co} = -240\ ^\circ F$$

$h_m = .0108$ Btu/ft^2 hr $^\circ$F, $h_{sp} = .0161$ Btu/ft^2 hr $^\circ$F

$T_s = -300\ ^\circ F$, $T'_{co} - T_{sp} = 4\ ^\circ F$, $T_e = -304\ ^\circ F$

13.1.5 Evaluation of Resistance Path

13.1.5.1 Thermal Model

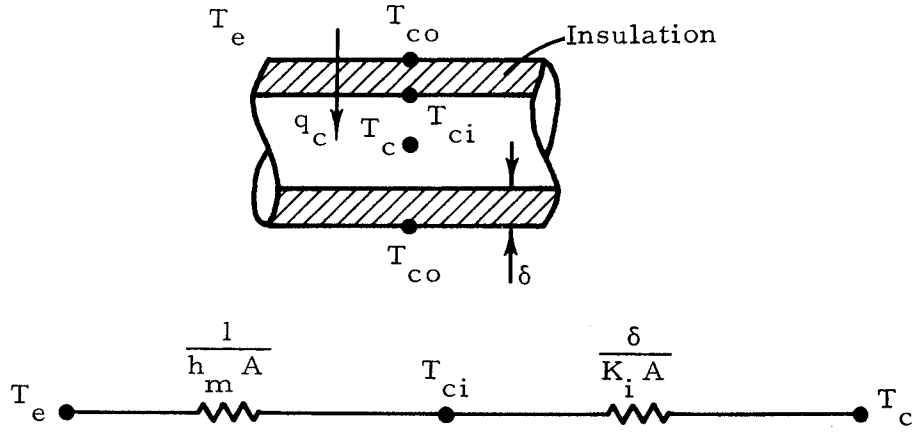

Assume the two areas are equal

δ = insulation thickness = 0.005" = .000417 ft

K_i = insulation conductivity = 0.17 Btu/ft hr $^\circ$F

Assume $T_{ci} = T_c$

13.1.5.2 Energy Balance

$$q_c = h_m A (T_e - T_{co}) = \frac{K_i A}{\delta} (T_{co} - T_c) = H (T_e - T_c)$$

$$H = \text{environmental conductance} = \frac{A}{\frac{\delta}{K_i} + \frac{1}{h_m}}$$

13.1.5.3 Cable Resistance (R_C)

Assume the cable is a fin

$$q_{con} = K_c A_c m (T_e - T_o) \tanh m L$$

q_{con} = heat flow at primary structure connector

K_c = copper conductivity = 220 Btu/ft hr ^{o}F

A_c = copper cross-sectional area

L = cable length between T_e and T_{con}

$$m = \sqrt{\frac{hC}{K_c A_c}} \qquad A = Cdx$$

$$h = \frac{H}{Cdx}$$

C = wire circumference

$$\text{Thus: } R = \frac{1}{K_c A_c \, m \tanh m L}$$

For conservatism, assume L long enough that tanh mL = 1.0. When evaluating R for the various cables, m always had a value of 3 or more. Since a value of 2.65 for mL results in tanh mL = 0.99, a length L = 0.9 ft = 11 inches or more is required. Consequently, the assumption of tanh mL = 1.0 appears justified.

Cables from the following deployed packages to the structure (node 49) were considered in the evaluation of a combined cable resistance:

Component	No. of Wires	Wire Gage	C(ft)	$A_c(ft^2 \times 10^5)$
Radioisotope Thermoelectric Generator	12	24	0.0916	2.64
Radioisotope Thermoelectric Generator	17	28	0.0916	1.48
Sunshield Dust Detector & Thermistors	17	24	0.0704	3.74
Passive Seismometer	38	28	0.1250	8.24
Magnetometer	15	24	0.1458	3.31
Solar Wind	9	24	0.1040	1.98
Suprathermal Ion Detector	18	24	0.179	3.97

C values are actually the overall cable circumference, including insulation, divided by two. The division by two accounts for the double row of wires in the cables which means only about half of each wire is exposed to environmental influence.

The cables can be treated as resistances in parallel, which gives

$$\frac{1}{R_C} = \frac{1}{R_1} + \frac{1}{R_2} + \ldots + \frac{1}{R_n}$$

Since tanh mL = 1.0,

$$\frac{1}{R_C} = K_c \left[(A_c m)_1 + (A_c m)_2 + \ldots + (A_c m)_n \right]$$

13.1.5.3.1 Noon Condition

$$H = \frac{A}{\frac{.000417}{.17} + \frac{1}{.518}} \approx 0.518A$$

$$h = \frac{0.518A}{A} = 0.518 \text{ Btu/ft}^2\text{hr}^\circ\text{F}$$

$$m = \sqrt{\frac{hC}{K_c A_c}} = 0.0485\sqrt{\frac{C}{A_c}} \text{ ft.}^{-1}$$

$$\frac{1}{R_n} = (K_c A_c m)_n = (220)\ (A_c)\ (.0485)\sqrt{\frac{C}{A_c}}$$

$$\frac{1}{R_n} = 10.65\ \sqrt{CA_c}$$

Supplying values of C and A_c gives the total resistance:

$$\frac{1}{R_C} = 10.65\ (.001555 + .001165 + .001623 + .003210 + .002197 + .001435 + .002666) = 10.65\ (.013851) = .1475$$

$$R_C = 6.8 \text{ hr}^\circ\text{F/Btu}$$

13.1.5.3.2 Night Condition

$$H = \frac{A}{\frac{.000417}{.17} + \frac{1}{.0108}} \approx .0108A \qquad h = 0.0108 \text{ Btu/ft}^2 \text{ hr}^\circ\text{F}$$

$$m = .00701\ \sqrt{\frac{C}{A_c}} \text{ ft}^{-1}$$

$$\frac{1}{R_n} = (220)\ A_c\ (.00701)\ \sqrt{\frac{C}{A_c}}$$

$$\frac{1}{R_n} = 1.54\ \sqrt{CA_c}$$

$$\frac{1}{R_C} = 1.54 \quad (.013851) = .02133$$

$$R_C = 46.9 \text{ hr } ^{o}F/\text{Btu}$$

13.2 Bracket Resistance (R_B)

A thermal circuit for bracket resistance is presented below:

T_{49} = temperature of structure node 49

T_B = bracket temperature at junction with connector

h_c = contact conductance between bracket and structure

= 40 Btu/ft^2 hr ^{o}F (assumed)

A_c = contact area = (4) (0.3) (0.3) / 144 = .0025 ft^2

L_B = bracket heat flow length = 1.2/12 = 0.1 ft

K_B = bracket thermal conductivity = 99 Btu/ft hr ^{o}F

A_B = bracket heat flow area = (4) (0.3) (0.03)/144 = .00025 ft^2

$$R_n = \frac{1}{A_c h_c} + \frac{L_B}{A_B K_B} = 10 + 4 = 14 \text{ hr } ^{o}F/\text{Btu}$$

Since there are six connectors with associated brackets,

$$\frac{1}{R_B} = \frac{6}{R_n}$$

$$R_B = \frac{14}{6} = 2.3 \text{ hr } ^{o}F/\text{Btu}$$

13.3 Connector Resistance (R_{con})

A resistance circuit for connectors is shown below

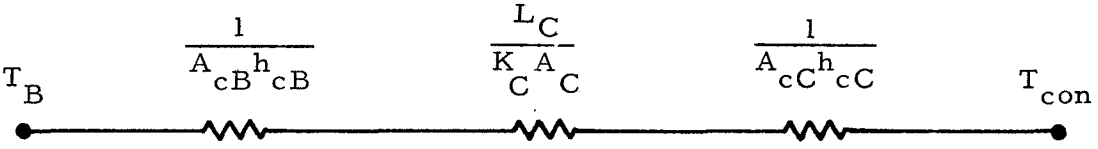

T_{con} = connector temperature at junction with cable

h_{cB} = contact conductance between bracket and connector = 200 Btu/ft^2 hr $^\circ$F (assumed)

A_{cB} = contact area = (2)(0.3)(0.3)/144 = .00125 ft^2

L_C = connector heat flow length = 1.2/12 = 0.1 ft

K_C = 0.2 Btu/ft hr $^\circ$F (assumed)

A_C = connector heat flow area = (2)(0.35)(1.0)/144 = .00486 ft^2

h_{cC} = contact conductance between connector and cable = 1000 Btu/ft^2 hr $^\circ$F (assumed)

A_{cC} = contact area = .0025 ft^2 (assumed)

$$R_n = \frac{1}{A_{cB}h_{cB}} + \frac{L_C}{K_C A_C} + \frac{1}{A_{cC}h_{cC}} = 4 + 103 + 0 = 107 \text{ hr } ^\circ\text{F/Btu}$$

Since there are six connections,

$$R_{con} = \frac{R_n}{6} = \frac{107}{6} = 17.8 \text{ hr } ^\circ\text{F/Btu}$$

13.4 Total Cable Resistance (Path 422)

13.4.1 Noon Condition

$$R_{49-60} = R_C + R_B + R_{con} = 6.8 + 2.3 + 17.8 = 26.9 \text{ hr}^\circ\text{F/Btu}$$

13.4.2 Night Condition

$$R_{49-60} = R_C + R_B + R_{con} = 46.9 + 2.3 + 17.8 = 67.0 \text{ hr}^\circ\text{F/Btu}$$

The cable from the antenna goes directly to the Diplexer Filter (node 46) without any connection on the structure. Its resistance (path 413) was determined with the techniques previously outlined in this section.

14.0 ALUMINIZED MYLAR CONDUCTION RESISTANCE

Because of uncertainty of thickness and thermal conductivity of the installed sections of mylar, reasonable conductance ($\frac{K}{L}$) values were used which gave good correlation between test and predicted temperatures. The following table summarizes parameters used to determine aluminized mylar conduction resistances.

PATH	NODES	Description	K/L Btu/ft^2 hr °F	A(ft^2)	$R = \frac{L}{KA}$ (hr°F/Btu)
53	105-115	Insulation Masks	0.0048	0.235	885.
54	106-115	" "	"	0.210	990.
55	107-115	" "	"	0.258	807.
56	108-115	" "	"	0.362	575.
57	112-116	" "	"	0.319	652.
58	113-116	" "	"	0.316	658.
59	114-116	" "	"	0.356	585.

PATH	NODES	Description	K/L Btu/ft^2 hr °F	A(ft^2)	$R = \frac{L}{KA}$ (hr°F/Btu)
65	49-56	Structure Insul.	0.0040	0.192	1304
66	50-57	" "	"	0.126	1985
67	51-58	" "	"	0.106	2370
68	52-59	" "	"	0.085	2930
153	27-35	Side Curtain Insul.	1.200	1.932	0.431
154	27-121	" " "	"	1.796	0.464
155	27-122	" " "	"	1.752	0.476
156	28-36	" " "	"	1.737	0.480
157	28-119	" " "	"	1.796	0.464
158	28-126	" " "	"	0.294	2.835
159	29-36	" " "	"	0.262	3.180
160	29-125	" " "	"	1.088	0.765
161	30-124	" " "	"	0.654	1.274
162	31-34	Sunshield Insulation	0.120	3.895	2.140
163	32-123	Side Curtain Insul.	1.200	0.986	0.845
164	33-120	Side Curtain Insul.	"	1.271	0.656

APPENDIX 3

RADIATION AND CONDUCTION RESISTANCE INPUT VALUES FOR THERMAL ANALYZER

Conduction resistances have units of hr °F/btu, while radiation values are the reciprocal of resistance as defined in previous sections and have units of ft^2. The computer program uses conduction resistance in the following manner in calculating heat input to a node:

$$q_{1-2} = \frac{T_1 - T_2}{R_{1-2}}$$

where R_{1-2} is the resistance input to the program. For radiation the program uses the following relation:

$$q_{1-2} = \frac{1}{R_{1-2}} \sigma \, (T_1 + T_2) \, (T_1^2 + T_2^2) \, (T_1 - T_2)$$

where $\frac{1}{R_{1-2}}$ is the resistance-reciprocal input to the program.

The following table presents computer input values for all resistance paths used to obtain results in Tables 1 and 2.

Resistor No.	Nodes Conn.	Description	Type Heat Trans.	Resistor Input Test Moon	Resistor Input Real Moon
1	37-101	Electronics to Radiator	Conduction	.281	.281
2	37-105	" "	"	.528	.528
3	38-102	" "	"	.356	.356
4	38-106	" "	"	.649	.649
5	39-103	" "	"	.424	.424
6	39-107	" "	"	.590	.590
7	40-104	" "	"	.226	.226
8	40-108	" "	"	.338	.338
9	41-101	" "	"	18.52	18.52
10	41-102	" "	"	21.73	21.73
11	41-109	" "	"	.208	.208
12	41-110	" "	"	4.32	4.32
13	42-102	" "	"	6.88	6.88
14	42-103	" "	"	.915	.915
15	42-110	" "	"	.339	.339
16	43-104	" "	"	.782	.782
17	43-111	" "	"	.307	.307
18	44-109	" "	"	2.09	2.09
19	44-112	" "	"	11.07	11.07
20	45-109	" "	"	.863	.863
21	45-112	" "	"	.905	.905
22	46-110	" "	"	1.493	1.493
23	46-110	" "	Radiation	.0051	.0051
24	46-111	" "	Radiation	.00017	.00017
25	47-112	" "	Conduction	17.87	17.87
26	47-113	" "	"	.369	.369
27	48-113	" "	"	.362	.362
31	101-102	Radiator Node Connections	Conduction	.811	.811
32	101-105	"	"	.895	.895
33	101-109	"	"	.940	.940
34	102-103	"	"	.892	.892
35	102-106	"	"	1.102	1.102
36	102-109	"	"	1.93	1.93
37	102-110	"	"	4.48	4.48
38	103-104	"	"	1.233	1.233

Resistor No.	Nodes Conn.	Description	Type Heat Trans.	Resistor Input Test Moon	Resistor Input Real Moon
39	103-107	Radiator Node Connections	Conduction	.895	.895
40	103-110	"	"	.880	.880
41	104-108	"	"	.600	.600
42	104-111	"	"	.580	.580
43	105-106	"	"	.835	.835
44	106-107	"	"	.835	.835
45	107-108	"	"	1.153	1.153
46	109-110	"	"	1.395	1.395
47	109-112	"	"	.535	.535
48	110-111	"	"	1.363	1.363
49	110-113	"	"	.718	.718
50	111-114	"	"	.600	.600
51	112-113	"	"	1.093	1.093
52	113-114	"	"	1.294	1.294
53	105-115	Insulation Masks	Conduction	885	885
54	106-115	" "	"	990	990
55	107-115	" "	"	807	807
56	108-115	" "	"	575	575
57	112-116	" "	"	652	652
58	113-116	" "	"	658	658
59	114-116	" "	"	585	585
61	49-105	Radiator Support Posts	Conduction	2036	2036
62	49-109	" " "	"	2036	2036
63	51-114	" " "	"	2036	2036
64	51-113	" " "	"	2036	2036
65	49-56	Structure Insulation	Conduction	1304	1304
66	50-57	" "	"	1985	1985
67	51-58	" "	"	2370	2370
68	52-59	" "	"	2930	2930
69	56-105	Structure to Radiator	Radiation	.000301	.000301
70	56-106	" "	"	.000259	.000259
71	56-107	" "	"	.000331	.000331
72	56-108	" "	"	.000457	.000457
73	57-101	" "	"	.000119	.000119
74	57-105	" "	"	.000133	.000133
75	57-109	" "	"	.000119	.000119
76	57-112	" "	"	.000145	.000145

ATM-796

Resistor No	Nodes Conn.	Description	Type Heat Trans	Resistor Input Test Moon	Resistor Input Real Moon
77	58-112	Structure to Radiator	Radiation	.000098	.000098
78	58-113	" "	"	.000163	.000163
79	58-114		"	.000193	.000193
80	59-104	" "	"	.000119	.000119
81	59-108	" "	"	.000133	.000133
82	59-111	" "	"	.000119	.000119
83	59-114	" "	"	.000133	.000133
86	37-54	Electronics to Thermal Bag	Radiation	.02172	.02172
87	38-54	" "	"	.01724	.01724
88	39-54	" "	"	.01594	.01594
89	40-54	" "	"	.03048	.03048
90	41-54	" "	"	.02025	.02025
91	42-54	" "	"	.01700	.01700
92	43-54	" "	"	.01807	.01807
93	44-54	" "	"	.00117	.00117
94	45-54	" "	"	.00877	.00877
95	46-54	" "	"	.01067	.01067
96	47-54	" "	"	.00954	.00954
97	48-54	" "	"	.00954	.00954
98	101-54	Radiator to Thermal Bag	Radiation	.00395	.00395
99	102-54	" "	"	.00323	.00323
100	103-54	" "	"	.00432	.00432
101	104-54	" "	"	.00515	.00515
102	105-54	" "	"	.00812	.00812
103	106-54	" "	"	.00668	.00668
104	107-54	" "	"	.00859	.00859
105	108-54	" "	"	.01154	.01154
106	109-54	" "	"	.00499	.00499
107	110-54	" "	"	.00315	.00315
108	111-54	" "	"	.01002	.01002
109	112-54	" "	"	.01025	.01025
110	113-54	" "	"	.00522	.00522
111	114-54	" "	"	.01807	.01807
112	49-55	Structure to Thermal Bag	Radiation	.0629	.0629
113	50-55	" "	"	.0600	.0600

Resistor No.	Nodes Conn.	Description	Type Heat Trans.	Resistor Input Test Moon	Resistor Input Real Moon
114	51-55	Structure to Thermal Bag	Radiation	.0494	.0494
115	52-55	"	"	.0545	.0545
116	53-55	"	"	.3280	.3280
117	54-55	Thermal Bag Insulation	Conduction	10.55*	10.55*
117	54-55	"	"	51.70**	51.70**
118	49-50	Structure Node Connections	"	11.76	11.76
119	50-51	"	"	12.43	12.43
120	51-52	"	"	11.79	11.79
121	52-49	"	"	11.12	11.12
122	49-31	Structure to Sunshield	Conduction	3000	3000
123	50-31	"	"	3000	3000
124	51-31	"	"	3000	3000
125	52-31	"	"	3000	3000
126	49-140	Structure to Moon and Space	Radiation	.09174*	NA
127	49-141	"	"	.02970*	NA
128	49-142	"	"	.02558*	NA
129	49-152	"	"	.01200*	NA
130	49-100	"	"	.16680*	NA
130	49-99	"	"	.15900**	.16880
131	50-143	"	"	.13120*	NA
131	49-100	"	"	.16680**	.15703
132	50-144	"	"	.04246*	NA
132	50-99	"	"	.22060**	.24442
133	50-145	"	"	.03657*	NA
133	50-97	"	"	.28900**	.27331
134	50-152	"	"	.01040*	NA
134	51-99	"	"	.24370**	.26171
135	50-97	"	"	.28900*	NA
135	51-100	"	"	.27130**	.25331
136	51-146	"	"	.14660*	NA
136	52-99	"	"	.17130**	.20316
137	51-147	"	"	.04746*	NA
137	52-98	"	"	.24820**	.22519

Resistor No.	Nodes Conn.	Description	Type Heat Trans.	Resistor Input Test Moon	Resistor Input Real Moon
138	51-148	Structure to Moon and Space	Radiation	.04088*	NA
138	53-99	"	"	.36500**	NA
138	53-88	"	"	NA	.36500
139	51-152	"	"	.00875*	NA
140	51-100	"	"	.27130*	NA
141	52-149	"	"	.10210*	NA
142	52-150	"	"	.03306*	NA
143	52-151	"	"	.02847*	NA
144	52-152	"	"	.00870*	NA
145	52-98	"	"	.24820*	NA
146	53-152	"	"	.36500*	NA
147	53-99	"	Conduction	33.3	NA
147	53-88	"	"	NA	33.3
149	49-53	Structure Sides to Bottom	"	2.26	2.26
150	50-53	"	"	2.76	2.76
151	51-53	"	"	2.21	2.21
152	52-53	"	"	2.73	2.73
153	27-35	Side Curtain and Sun-shield Insulation	"	.431	.431
154	27-121	"	"	.464	.464
155	27-122	"	"	.476	.476
156	28-36	"	"	.480	.480
157	28-119	"	"	.464	.464
158	28-126	"	"	2.835	2.835
159	29-36	"	"	3.180	3.180
160	29-125	"	"	.765	.765
161	30-124	"	"	1.274	1.274
162	31-34	"	"	2.140	2.140
163	32-123	"	"	.845	.845
164	33-120	"	"	.656	.656
166	27-99	Side Curtains to Moon and Space	Radiation	.7178	1.3642
167	27-98	"	"	2.0210	1.3742
168	28-99	"	"	.7491	.9526
169	28-97	"	"	1.1630	.9595
170	29-30	"	"	.0129	.0129

Resistor No.	Nodes Conn.	Description	Type Heat Trans.	Resistor Input Test Moon	Resistor Input Real Moon
171	29-99	Side Curtains to Moon and Space	Radiation	.2581	.3362
172	29-97	"	"	.3909	.3387
173	30-99	"	"	.1247	.1627
174	30-97	"	"	.1761	.1640
175	31-97	Sunshield to Space	"	.2105	.2105
176	31-100	"	"	3.0840	3.0840
177	32-100	"	"	.5325	.5325
178	33-100	"	"	.6862	.6862
179	31-98	"	"	.2105	.2105
180	34-35	Enclosure Behind Reflectors	"	.03916	.03916
181	34-36	"	"	.03864	.03864
182	34-117	"	"	.10180	.10180
183	34-118	"	"	.09266	.09266
184	34-132	"	"	.04865	.04865
185	35-36	"	"	.01889	.01889
186	35-117	"	"	.05052	.05052
187	35-118	"	"	.04637	.04637
188	35-132	"	"	.02264	.02264
189	36-117	"	"	.04975	.04975
190	36-118	"	"	.04429	.04429
191	36-132	"	"	.03108	.03108
192	117-118	"	"	.12350	.12350
193	117-132	"	"	.06402	.06402
194	118-132	"	"	.05303	.05303
200	127-15	Radiosity Network	"	.02328	.02328
201	127-17	"	"	.06331	.06331
202	127-19	"	"	.20780	.20780
203	127-20	"	"	.10090	.10090
204	127-21	"	"	.20780	.20780
205	127-99	"	"	.00852	.11731
206	127-100	"	"	.42530	.32957
207	15-17	"	"	.04027	.04027
208	15-19	"	"	.18830	.18830
209	15-20	"	"	.10090	.10090
210	15-21	"	"	.18830	.18830

Resistor No.	Nodes Conn.	Description	Type Heat Trans.	Resistor Input Test Moon	Resistor Input Real Moon
211	15-99	Radiosity Network	Radiation	.03920	.10377
212	15-100	"	"	.41690	.29154
213	19-17	"	"	.06021	.06021
214	19-20	"	"	.19760	.19760
215	19-21	"	"	.28120	.28120
216	19-99	"	"	.23890	.39738
217	19-100	"	"	.62090	.46244
218	21-17	"	"	.06021	.06021
219	21-20	"	"	.19760	.19760
220	21-99	"	"	.38670	.39738
221	21-100	"	"	.47310	.46244
222	20-17	"	"	.02602	.02602
223	20-99	"	"	.59230	.64676
224	20-100	"	"	.06029	.00000
225	17-99	"	"	.12410	.16978
226	17-100	"	"	.12510	.07937
227	129-16	"	"	.02559	.02559
228	129-18	"	"	.06437	.06437
229	129-22	"	"	.21500	.21500
230	129-23	"	"	.08336	.08336
231	129-24	"	"	.02922	.02922
232	129-25	"	"	.18890	.18890
233	129-26	"	"	.09912	.09912
234	129-99	"	"	.01352	.03479
235	129-100	"	"	.35980	.33859
236	16-18	"	"	.03514	.03514
237	16-22	"	"	.17800	.17800
238	16-23	"	"	.06470	.06470
239	16-24	"	"	.03650	.03650
240	16-25	"	"	.15680	.15680
241	16-26	"	"	.03114	.03114
242	16-99	"	"	.03587	.06509
243	16-100	"	"	.32860	.29939
244	22-18	"	"	.05824	.05824
245	22-23	"	"	.17510	.17510
246	22-24	"	"	.12520	.12520
247	22-25	"	"	.16910	.16910

Resistor No.	Nodes Conn.	Description	Type Heat Trans.	Resistor Input Test Moon	Resistor Input Real Moon
248	22-26	Radiosity Network	Radiation	.04534	.04534
249	22-99	"	"	.36350	.47692
250	22-100	"	"	.42860	.31519
251	24-18	"	"	.01658	.01658
252	24-23	"	"	.09785	.09785
253	24-99	"	"	.14520	.23490
254	24-100	"	"	.20300	.11330
255	25-18	"	"	.04946	.04946
256	25-23	"	"	.04346	.04346
257	25-26	"	"	.03369	.03369
258	25-99	"	"	.13980	.22109
259	25-100	"	"	.14270	.06148
260	26-18	"	"	.00811	.00811
261	26-23	"	"	.01136	.01136
262	26-99	"	"	.01595	.02658
263	26-100	"	"	.05464	.04401
264	23-18	"	"	.01839	.01839
265	23-99	"	"	.41880	.47594
266	23-100	"	"	.07412	.01697
267	18-99	"	"	.09417	.12921
268	18-100	"	"	.09685	.06176
269	127-128	"	"	.09968	.09968
270	15-115	"	"	.11210	.11210
271	19-119	"	"	.19960	.19960
272	21-121	"	"	.19960	.19960
273	20-120	"	"	.14120	.14120
274	17-117	"	"	.26040	.26040
275	129-130	"	"	10.410	10.410
276	16-116	"	"	.10050	.10050
277	22-122	"	"	.19470	.19470
278	24-124	"	"	.07263	.07263
279	25-125	"	"	.12080	.12080
280	26-126	"	"	.03264	.03264
281	23-123	"	"	.10960	.10960
282	18-118	"	"	.22380	.22380
283	128-101	Radiosity Radiator to	Conduction	.10	.10
284	128-102	Radiator Nodes	"	.10	.10

Resistor No.	Nodes Conn.	Description	Type Heat Trans.	Resistor Input Test Moon	Resistor Input Real Moon
285	128-103	Radiosity Radiator to	Conduction	.10	.10
286	128-104	Radiator Nodes	"	.10	.10
287	130-109	"	"	.10	.10
288	130-110	"	"	.10	.10
289	130-111	"	"	.10	.10
290	129-131	Radiosity Network	Radiation	.01483	.01483
291	16-131	"	"	.01587	.01587
292	22-131	"	"	.00655	.00655
293	24-131	"	"	.00220	.00220
294	25-131	"	"	.19760	.19760
295	26-131	"	"	.04426	.04426
296	23-131	"	"	.00670	.00670
297	131-99	"	"	.04680	.09161
298	131-100	"	"	.04680	.00200
299	131-132	"	"	9.528	9.528
350	37-38	Cables	Conduction	107	107
351	37-39	"	"	262	262
352	37-43	"	"	2280	2280
353	37-49	"	"	5250	5250
354	37-49	"	"	67.3*	67.3*
354	37-49	"	"	136**	136**
357	38-49	"	"	12.3	12.3
358	38-40	"	"	630	630
359	38-41	"	"	329	329
360	38-42	"	"	85	85
361	38-43	"	"	66	66
362	38-44	"	"	1165	1165
363	38-45	"	"	733	733
364	38-47	"	"	773	773
365	38-48	"	"	813	813
366	38-49	"	"	902	902
367	38-49	"	"	172.4*	172.4*
367	38-49	"	"	316**	316**
368	38-102	"	"	396	396
369	38-103	"	"	289	289
370	38-106	"	"	305	305
371	38-107	"	"	1205	1205

Resistor No.	Nodes Conn.	Description	Type Heat Trans.	Resistor Input Test Moon	Resistor Input Real Moon
372	38-108	Cables	Conduction	1142	1142
373	38-109	"	"	1455	1455
374	38-111	"	"	1427	1427
375	38-114	"	"	1970	1970
381	39-40	"	"	254	254
382	39-41	"	"	321	321
383	39-42	"	"	57	57
384	39-43	"	"	1020	1020
385	39-47	"	"	829	829
386	39-48	"	"	868	868
387	39-49	"	"	775.2*	775.2*
387	39-49	"	"	1750**	1750**
388	39-103	"	"	1550	1550
389	39-106	"	"	1375	1375
390	39-108	"	"	2030	2030
391	39-109	"	"	3010	3010
392	39-114	"	"	4520	4520
395	40-42	"	"	238	238
396	40-43	"	"	135	135
397	40-49	"	"	312*	312*
397	40-49	"	"	468**	468**
399	41-43	"	"	1677	1677
400	41-46	"	"	48.7	48.7
403	42-43	"	"	218	218
404	42-47	"	"	1507	1507
405	42-48	"	"	1605	1605
406	42-49	"	"	854.7*	854.7*
406	42-49	"	"	1918**	1918**
407	43-44	"	"	1110	1110
408	43-49	"	"	757.6*	757.6*
408	43-49	"	"	1192**	1192**
409	44-49	"	"	3600*	3600*
409	44-49	"	"	4150**	4150**
410	45-46	"	"	25	25
411	45-47	"	"	55.5	55.5
412	45-48	"	"	55.5	55.5

Resistor No.	Nodes Conn.	Description	Type Heat Trans.	Resistor Input Test Moon	Resistor Input Real Moon
413	46-60	Cables	Conduction &	783*	783*
413	46-60	"	Radiation	5767**	5767**
416	103-104	"	Conduction	717	717
417	104-111	"	"	1208	1208
418	111-112	"	"	626	626
419	106-107	"	"	531	531
420	107-111	"	"	1230	1230
421	107-112	"	"	3440	3440
422	49-60	"	Conduction &	27*	27*
422	49-60	"	Radiation	67**	81**
500	88-76	Lunar Subsurface Nodes	Conduction	NA	.894
501	76-75	"	"	NA	1.788
502	76-87	"	"	NA	12.5
503	75-96	"	"	NA	2.012
504	75-86	"	"	NA	12.5
505	96-95	"	"	NA	2.459
506	96-85	"	"	NA	10.0
507	95-94	"	"	NA	2.905
508	95-84	"	"	NA	8.33
509	94-93	"	"	NA	3.576
510	94-83	"	"	NA	7.14
511	93-92	"	"	NA	4.917
512	93-82	"	"	NA	5.55
513	92-91	"	"	NA	7.375
514	92-81	"	"	NA	3.84
515	91-90	"	"	NA	11.622
516	91-80	"	"	NA	2.5
517	90-89	"	"	NA	27.715
518	90-79	"	"	NA	1.56
519	89-77	"	"	NA	.44702
520	89-78	"	"	NA	.5
521	88-99	"	"	NA	50.0

* Lunar Noon Only
** Lunar Night Only

APPENDIX 4*

RADIOSITY METHOD FOR RADIANT INTERCHANGE CALCULATIONS

Consider a surface, i, which has a total heat flux, H_i, impinging upon it and a total heat flux, J_i, leaving it. The quantity J_i will be termed "radiosity".

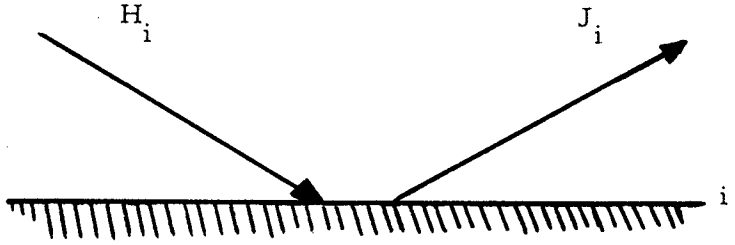

NOTE: Throughout this discussion, the term total heat flux is used to signify all of the heat flux traveling in a specified path and direction, while net heat flux is the difference between the total heat flux entering and that leaving a surface.

The net heat rate leaving surface i is then:

$$\dot{q}_{NET_i} = A_i (J_i - H_i) \qquad (1)$$

where A_i = area of surface i

For any surface:

$$\alpha + \rho + \tau = 1 \text{ (first law)}$$

where:

α = absorptance of the surface

ρ = reflectance of the surface

τ = transmittance of the surface

* Abstracted from Bendix Report BSR-2021, "Advanced Analytical Techniques for Thermal Control."

assume that for surface i:

$$\tau_i = 0 \text{ (opaque surface)}$$

then:

$$\alpha_i + \rho_i = 1$$

assume in addition that:

$$\alpha_i = \epsilon_i \text{ (gray body)} \tag{2}$$

then:

$$\epsilon_i + \rho_i = 1 \tag{3}$$

Now the total heat flux, J_i, leaving surface i consists of both emitted and reflected radiation. By the definition of emissivity and reflectivity, we can conclude that:

$$J_i = E_{b_i} \epsilon_i + \rho_i H_i \tag{4}$$

where E_{b_i} = emissive power of a black body at the temperature of surface i.

Combining equations 3 and 4, we have:

$$J_i = E_{b_i} \epsilon_i + (1 - \epsilon_i) H_i$$

or,

$$H_i = \frac{J_i - E_{b_i} \epsilon_i}{(1 - \epsilon_i)} \tag{5}$$

Combining equations 1 and 5, we get:

$$q_{NET_i} = A_i \left[J_i - \frac{(J_i - E_{b_i} \epsilon_i)}{(1 - \epsilon_i)} \right]$$

$$= \frac{A_i \epsilon_i}{(1 - \epsilon_i)} (E_{b_i} - J_i) \qquad (6)$$

The significance of equation 6 is that it expresses the net heat rate leaving surface i as a function only of its emissivity, ϵ_i, area, A_i, and the difference between its black body potential, E_{b_i}, and its radiosity, J_i.

In this way, the net heat rate leaving surface i is expressed independently of the total heat rate, H_i, entering it.

Consider now the case of radiant interchange between surface i and another surface, j.

The total heat rate leaving surface i is simply:

$$A_i J_i$$

Of this amount, the fraction

$$A_i J_i F_{ij}$$

impinges directly upon surface j, where F_{ij} is the geometric view factor from surface it to surface j.

Similarly, the total heat rate leaving surface j is:

$$A_j J_j$$

and the fraction:

$$A_j J_j F_{ji}$$

of this quantity impinges directly upon surface i.

The net heat rate from surface i to surface j is simply the difference between the heat rate leaving i and impinging upon j, and that leaving j and impinging upon i.

Then,

$$\dot{q}_{NET_{i_j}} = A_i J_i F_{ij} - A_j J_j F_{ji} \tag{7}$$

By the reciprocity theorem,

$$A_i F_{ij} = A_j F_{ji} \tag{8}$$

Combining equations 7 and 8, we get:

$$\dot{q}_{NET_{i_j}} = A_i F_{ij} (J_i - J_j) \tag{9}$$

Equation 9 suggests that the net heat rate from surface i to surface j can be expressed as the product of a constant ($A_i F_{ij}$) and the difference of the radiosities of surfaces i and j. Equation 6, on the other hand, indicates that the net heat rate leaving surface i is the product of a constant $\frac{A_i \epsilon_i}{1 - \epsilon_i}$ and the difference between its black body potential E_{b_i}, and its radiosity, J_i.

From the above, one can construct an analogous resistance-type electrical network in which voltage is equivalent to emissive power and current to heat rate. The equivalent network for the two-surface radiant interchange problem described above would appear as follows:

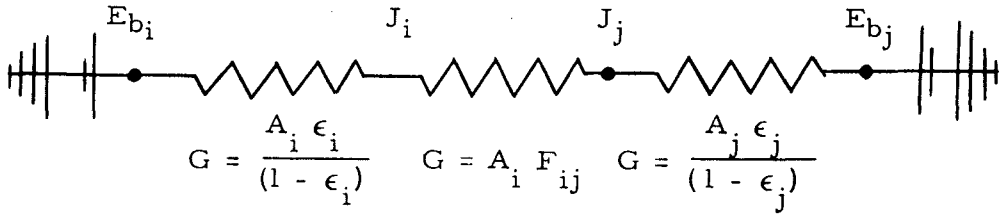

In this analogous network, one can see that the radiosities J_i and J_j act as floating potentials having values intermediate between E_{b_i} and E_{b_j}. From this analogy it is also clear that, if the emissivity of surface i were equal to 1.0, the value of the leftmost conductor would be infinity. As a result, the value of J_i would be identical to E_{b_i}. In physical terms, this means that all of the heat leaving a black body is due to emittance, and none to reflectance.

The analogy developed above for two nodes can be extended to any number of nodes by treating each pair of nodes having non-zero geometric view factors to each other in the same way as surfaces i and j were treated above. For example, the addition of two nodes k and l to the system would result in the following network:

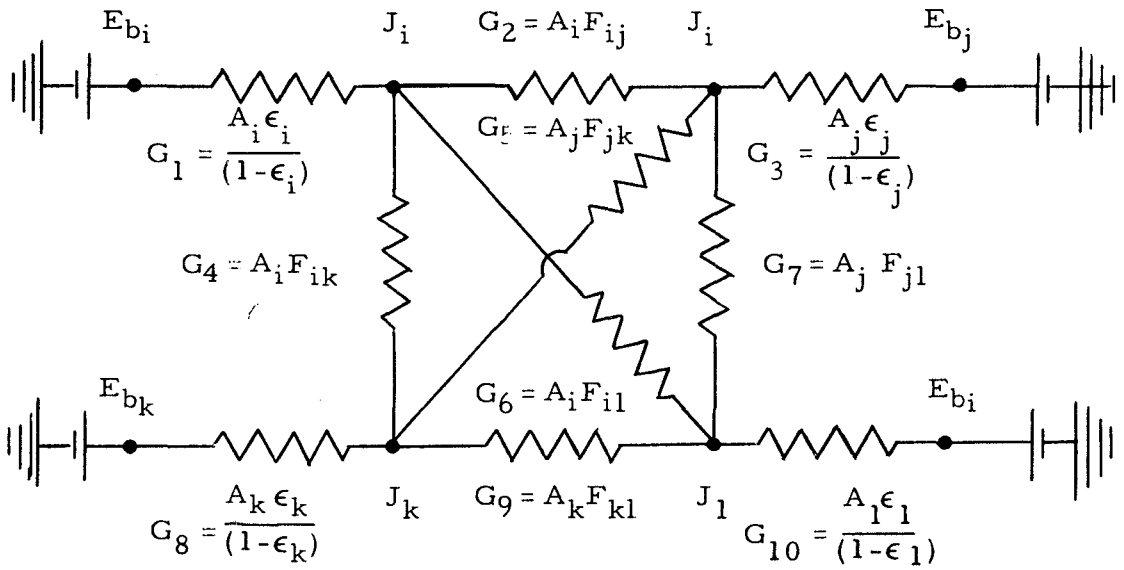

Such an extension is valid because the construction of the equivalent network for radiant interchange between two surfaces requires no assumptions regarding the existence of possible additional surfaces in the system (see derivations for equations 6 and 9 above).

If more than two surfaces are present, the total radiant heat interchange between any two surfaces can consist of one direct component and a number of indirect components. These indirect components are a result of reflection and reradiation via other surfaces in the system. As an example, the direct radiation from i to j in the four-surface network illustrated above flows through conductor No. 2, while the indirect components can flow through conductors 4, 5, 6, 7, and 9.